Cosmic Ray Characteristics Based on Induced Radioactivity in Lunar Samples and Meteorites

by

Sourendra Kumar Bhattacharya

Physical Research Laboratory
Ahmedabad 380009, India.

A Thesis
Submitted for the Ph. D. Degree
of the
Gujarat University

August 1979

C E R T I F I C A T E

I hereby declare that the work presented in this thesis is original and has not formed the basis for the award of any degree or diploma by any University or Institution.

S. K. Bhattacharya

S.K. Bhattacharya
(Author)

Certified by:

N Bhandari

Prof. N. Bhandari

August, 1979

To Dipti

TABLE OF CONTENTS

		Page
Statement	...	1
Acknowledgements	...	6
List of Figures	...	8
List of Tables	...	11
Chapter I Introduction	...	13
A. Study of ^{26}Al activity in Lunar rocks	...	18
B. Study of production profile of ^{26}Al and ^{53}Mn activity in Meteorites	...	19
C. Radioisotope studies in Dhajala	...	21
Chapter II Experimental Techniques	...	23
A. Sample description	...	23
1. Description of Lunar rocks studied	...	23
2. Sampling of rocks for nondestructive $\beta-\gamma$ counting	...	26
3. Sampling of meteorites for γ-counting	...	29
4. The fall and sampling of Dhajala	...	30
5. Coring of meteorites for ^{53}Mn and track profile	...	31

Page

B. Radiochemical methods ... 32

1. Radiochemical investigation of Dhajala ... 37

2. Neutron activation analysis of ^{53}Mn in meteorites ... 38

a. Pre-irradiation chemistry ... 38

b. Neutron irradiation ... 40

c. Post-irradiation chemistry ... 41

C. Counting techniques and track measurement ... 43

1. The β- γ coincidence spectrometer ... 44

2. The beta, X-ray and gamma counters ... 47

3. The Ge(Li) counting systems ... 50

4. Measurement of nuclear tracks ... 51

Chapter III Results ... 53

A. Analysis of β-γ coincidence counting data in Lunar rocks ... 53

B. Results of gamma counting in meteorites ... 61

C. Radionuclides in Dhajala ... 62

1. Results of gamma counting ... 62

2. Results of radiochemical analysis in Dhajala ... 66

D. Neutron activation analysis of ^{53}Mn in Meteorites ... 72

1. ^{53}Mn data from spot-samples ... 72

2. ^{53}Mn data from core-samples ... 80

3. Track data in core-samples ... 85

Page

a. St. Severin ... 85
b. Bansur ... 86
c. Udaipur ... 89
d. Madhipura ... 92

Chapter IV Discussions ... 95

A. ^{26}Al studies in Lunar rocks ... 95

1. The surface exposure age and erosion rate ... 96

2. ^{26}Al activities and SCR parameters ... 98

B. Production rates of radioisotopes in meteorites ... 106

1. ^{53}Mn activity profile in Marjalahti ... 109

2. Cosmic ray flux in meteorite orbits and the shape parameter α ... 113

3. Comparison between calculated and experimental values ... 115

4. Radionuclides in Dhajala ... 130

a. Short-lived activities and solar cycle effect ... 130

b. Long-lived isotopes and comparison with calculation ... 131

c. Excess activity of ^{22}Na and ^{54}Mn in Dhajala ... 134

d. Spatial variation of GCR fluxes ... 137

5. Measured depth-profile of ^{53}Mn activity in cores ... 141

Chapter V Conclusions ... 151

A. Average SCR parameters in the past ... 152

Page

B. GCR intensity deduced from meteorite studies ... 153

C. Activity profiles of ^{53}Mn in chondrites ... 155

D. Further scope ... 156

References ... 159

List of publications ... 174

Statement

The meteorites and the Lunar samples constitute two important classes of samples where the history of the cosmic radiations are preserved in relatively undisturbed form. These objects are continuously bombarded by galactic cosmic rays (GCR) and solar high energy particles (SCR) leading to the production of a number of stable and radioactive isotopes and ionisation tracks of heavy nuclei. The determination and analysis of these isotopes and tracks give information on a variety of subjects, such as the life history and origin of meteorites, the exposure history of Lunar rocks, and the intensity, energy spectrum, spatial distribution and possible time variations of the GCR and SCR particles.

In this thesis the primary concern is the study of radioactive species supplemented by analysis of nuclear tracks to get information on the history of SCR and GCR. The Lunar rocks were used as monitors for detecting possible changes in solar radiation over the time scale of a few million years and a large group of meteorites were studied for getting information on the nature of interaction of GCR and their temporal and spatial variations.

Chapter I gives a brief introduction to the objective and nature of the work carried out in addition to a summary of the salient features of contemporary cosmic rays. Specific details of the work include:

A. Measurement and analysis of radioisotope ^{26}Al activity in Lunar rocks to derive long-term parameters and

relative variation of solar cosmic rays.

B. Analytical calculation of production rates of low energy radioisotopes like ^{26}Al, ^{53}Mn, in meteorites and measurement of ^{26}Al, ^{53}Mn activities in a large number of meteorites.

C. Measurement of a suite of radioisotopes ranging in half-life from 5.6 days to 3.7 m.y. in a meteorite, Dhajala, which fell near Ahmedabad, Gujarat in January 1976 and was recovered within a day of the fall.

The measurement of ^{26}Al in Lunar rocks was carried out by a non-destructive beta-gamma coincidence spectrometer. This method, in contrast to destructive analysis, preserves the integrity of the samples and allows a fine depth resolution in deducing the activity profile. Several Lunar rocks were studied and the description of the samples and counting methods are given in chapter II. This chapter also includes the experimental techniques used for (1) non-destructive gamma counting of meteorite samples, (2) radiochemical separation of elements in the Dhajala meteorite and the counting of beta, X-ray and gamma emitters, (3) neutron activation analysis of ^{53}Mn in spot and core-samples of several meteorites and the counting of irradiated samples using the Ge(Li) detector systems.

The results of the various measurements are given in chapter III. In addition to measurement of radioisotope

activities, the samples from the Lunar rocks and the meteorites were studied for nuclear tracks. The track densities in the core-samples taken from four chondrites, St. Severin, Bansur, Udaipur and Madhipura are also presented in this chapter.

A meaningful discussion of the results of various investigations carried out in this work is possible only when they are supplemented by analytical calculation of production rates of the isotopes. These calculations are well established for the case of Lunar rocks and were followed for comparing the measured ^{26}Al activities with those expected on the basis of various SCR parameters, target chemistry and exposure histories of the rocks. The exposure age and the rate of erosion of the rocks on the Lunar surface are two particularly important inputs for deciding the best choice of SCR parameters on the basis of the observed activities. An independent estimation of these two is essential to avoid potential circularity in the derivation of SCR parameters. In this work, the exposure ages and erosion rates for the rocks were estimated from measurements of nuclear tracks and in one case by supplementary study of microcrater densities.

For meteorites there is as yet no consensus on the production rate calculations. A semi-empirical approach was developed by closely following the model applicable to the case of the Moon. A detailed discussion of the assumptions and the methods used for deriving the model is given in Chapter IV. Available experimental data on isotopic activities

from this work and the literature were compared with the predictions based on this model.

The results of destructive analysis of the Dhajala meteorite are also discussed in chapter IV in context to the predictions from the meteorite model and also relative comparison between isotopes having similar modes of production (in respect of energy and target elements).

Chapter IV also contains a discussion of the results from track density and ^{53}Mn activity measurements carried out on the samples from cores of the four chondrites, mentioned earlier. The track density data were used for deriving the shapes and sizes of the meteorites and deducing the shielding depths of the samples in which ^{53}Mn activities have been measured. These data provide ^{53}Mn activity profiles in chondrites of four different sizes ranging from 6 to 20 cm.

The last chapter presents the conclusions of the studies undertaken in this work, which can be briefly summarised as below:

1. The ^{26}Al activity measurements in Lunar rocks show that the solar activity has remained constant within the limits of the experimental errors ($\pm$ 20%) for the last 2 million years.

2. The activities of the suite of radioisotopes measured in the Dhajala meteorite are consistent with the expected levels based on the present day GCR flux except for significant excess in two radioisotopes,

^{22}Na and ^{54}Mn, having half-lives of the order of years. A detailed analysis implies that this is due to a significant gradient of GCR fluxes perpendicular to the plane of the ecliptic during the solar minimum.

3. The activity profiles of ^{53}Mn, a low energy isotope, are now firmly established for chondrites of different sizes. The profiles show that for chondrites having effective radius less than 15 cm the increase in activity from near surface region to the centre is small (less than 10%). For St. Severin (20 cm) the increase is about 45 % thus indicating that the cascade of secondaries becomes important only for sizes greater than 15 cm.

A discussion on the future experiments in the field of cosmic ray effects in the Moon and meteorites is given at the end of the thesis.

Acknowledgements

I was initiated into the field of Moon and Meteorites by Prof. D. Lal, guided all along by Prof. N. Bhandari and got a thorough training in radiochemistry and neutron activation technique from Prof. M. Honda. My deep sense of gratitude to these mentors.

I had great pleasure in working with Dr. J.N. Goswami in the field of tracks. Mr. J.T. Padia and Mrs. N. Sinha supplemented the track studies by technical assistance.

Drs. M. Imamura and K. Nishiizumi taught me activation analysis of ^{53}Mn and helped me in experimental work. I am thankful to the Government of Japan for a Mombusho scholarship and grateful to the staff members of Prof. Honda's laboratory in the Institute for Solid State Physics, Tokyo, for making my stay enjoyable and fruitful.

I am grateful to NASA for providing the valuable Lunar samples and to Dr. R.C. Agarwala (Director, Jaipur Museum), Dr. B.P. Sinha (Director, Patna Museum) and Dr. P.L. Gupta (Curator, Patna Museum) for loan of the Indian meteorites. Thanks are also due to Drs. M.B. Duke, P. Butler Jr. and J. Warner & the NASA curatorial staff for careful preparation of the Lunar samples and for providing valuable information.

I am grateful to Dr. R. Reedy and Prof. J.R. Arnold for valuable discussions on production rate of radioisotopes and

providing me with their compilation of cross-section data. Dr. C.P. Kohl kindly measured the activities of two gamma-emitters in the Ge(Li) system at La Jolla.

Prof. S. Krishnaswami has been an invaluable friend and guide in academic life and otherwise. Thanks can never be enough to express my feelings to him and Mrs. Nanda Krishnaswami.

The constant push, encouragement and good humour from Profs. B.L.K. Somayajulu and K. Gopalan accelerated the writing of the thesis. Prof. Rao and Dr. T.R. Venkatesan kindly measured the rare gas ages.

M/s. N.R. Manchanda and A.R.S. Pandian maintained and improved the electronics. M/s. P. Sharma and M.M. Sarin assisted in atomic absorption measurements.

Mr. K.T. John has done an excellent job in typing the thesis. My thanks are also due to Mr. S.K. Bhavsar, Mr. D.R. Ranpura and Mr. N.D. Dave for their efficient and skillful drafting and photography.

LIST OF FIGURES

Figure		Page
1	Surface samples and core-samples from the Bansur chondrite. ...	33
2	Surface samples and core-samples from the Madhipura chondrite. ...	34
3	Surface samples and core-samples from the Udaipur chondrite. ...	35
4	Schematic of the beta-gamma coincidence spectrometer system	45
5	Beta-gamma ccincidence spectra for the top surface of the rock 61016 and the background. ...	54
6	Determination of half-thickness of positrons from ^{26}Al decay by external and self-absorption methods. ...	58
7	Gross positron signal from ^{52}Mn decay in the manganese fraction from the Dhajala chondrite versus the decay factor. ...	69
8	Expected track density profile in a radial direction (curve I), measured track densities (curve II) and ^{53}Mn activities (curve III) in the core-samples from Bansur (note that the scale for the ^{53}Mn activity is on the right). ...	88
9	Expected track density profile in a radial direction (curve I), measured track densities (curve II) and ^{53}Mn activities (curve III) in the core-samples from Udaipur (note that the scale for the ^{53}Mn activity is on the right). ...	91
10	Measured track densities (curve I) and ^{53}Mn activities in the core-samples from Madhipura (note that the scale for the ^{53}Mn activity is on the right). ...	94
11	Observed activity of ^{26}Al as a function of depth in various Lunar rocks. The solid lines indicate calculated profiles for the rock 61016 with erosion rate 1 mm/m.y. and without erosion. ...	101

Figure Page

12 Ratio of observed to expected ^{26}Al activity, Q(t) as a function of the saturation factor $(1-e^{-\lambda t})$ based on various rocks studied. The exposure age of 60335 is uncertain and, therefore, this rock has been excluded. ... 105

13 The depth profile of ^{53}Mn activity in the Marjalahti pallasite. The curves are calculated ^{53}Mn activity profiles for spherical pallasites of different radii. ... 112

14 Depth dependence of the shape parameter α deduced for the GCR flux, J (E > 1 GeV) = 1.7 protons/cm^2.sec (4π) for chondrites of different radii. ... 116

15 Depth dependence of the shape parameter α deduced for the GCR flux, J (E > 1 GeV) = 2.1 protons/cm^2.sec (4π) for chondrites of different radii. ... 117

16 Depth dependence of the integral flux of GCR particles (E > 1 GeV) inside chondrites of different radii corresponding to a free-space GCR flux, J (E > 1 GeV) = 1.7 protons/cm^2.sec (4π). ... 118

17 Calculated activity profiles of ^{22}Na, ^{26}Al, ^{53}Mn and ^{54}Mn in chondrites of radii 10, 20, 30, 40, 50 and 100 cm, for a free-space GCR flux, J (E > 1 GeV) = 1.7 protons/cm^2.sec (4π). ... 119

18 Calculated activity profiles of ^{22}Na, ^{26}Al, ^{53}Mn and ^{54}Mn in chondrites of radii 10, 20, 30, 40, 50 and 100 cm, for a free-space GCR flux, J (E > 1 GeV) = 2.1 protons/cm^2.sec (4π). ... 120

19 Saturated activity of ^{26}Al in chondrites against their pre-atmospheric sizes. The hatched band indicates the range of values expected for shielding greater than 2.5 cm for various sizes (based on Figure 17 and Table 20). ... 124

20 Saturated activity of ^{53}Mn in chondrites against their pre-atmospheric sizes. The hatched band indicates the range of values expected for shielding greater than 2.5 cm for various sizes (based on Figure 17 and Table 20). ... 127

Figure		Page
21	The variation of heliocentric and heliographic latitude, and heliocentric distance with time for the Dhajala chondrite calculated from the orbital parameters given by Ballabh et al. (1978). The mean lives of some of the isotopes are marked by arrows indicating the most important part of the orbital segments for evaluating their activities.	... 138
22	The measured activities of ^{53}Mn plotted against the effective pre-atmospheric shielding depths for Madhipura (R_o= 6.5 cm) and Udaipur (R_o = 9 cm) samples. The dotted lines indicate the best fit experimental profiles. The solid line for Udaipur is the theoretical profile expected from the model discussed in the text.	... 145
23	The measured activities of ^{53}Mn plotted against the effective pre-atmospheric shielding depths for Bansur (R_o = 15 cm) and St. Severin (R_o = 20 cm) samples. The dotted lines indicate the best fit experimental profiles. The solid lines are the theoretical profiles expected from the model discussed in the text.	... 146
24	Production profiles of ^{53}Mn in chondrites of radii 6.5, 9.0, 15.0, 20.0 cm. The curve for infinite radius refers to Moon (from Imamura et al., 1974) and is applicable to a very large size chondrite.	... 150

LIST OF TABLES

Table			Page
1	Description and mean chemical composition of Lunar rocks	...	27
2	Details of core-samples analysed for ^{53}Mn and tracks	...	36
3	Details of β-γ system: ARIES ON HORIBA	...	48
4	Description of Ge(Li) systems	...	52
5	^{26}Al counting data of Lunar rocks	...	60
6	^{26}Al activities and the shielding depths in chondrites	...	63
7	^{26}Al, ^{54}Mn and ^{22}Na activities in fragments of the Dhajala chondrite	...	65
8	Chemical and counting details of samples of the Dhajala chondrite	...	67
9	Cosmogenic radioactivities in fragments of the Dhajala chondrite (in dpm/kg)	...	73
10	Abundances of Fe, Ni and Mn in the analysed meteorites	...	74
11	^{53}Mn activities in meteorites	...	76
12	^{53}Mn activities in meteorites	...	78
13	Details of core-samples of four chondrites analysed for ^{53}Mn	...	81
14	Irradiation characteristics for n-irradiation of core-samples in JRR-3 reactor	...	83

Table		Page
15	^{53}Mn activities in core-samples from chondrites ...	84
16	Track density data for Bansur ...	87
17	Track density data for Udaipur ...	90
18	Track density data for Madhipura ...	93
19	Deviations in surface activity of ^{26}Al in Lunar rocks ...	103
20	Saturated activities of ^{53}Mn and ^{26}Al in chondrites and their pre-atmospheric sizes ...	122
21	Comparison of ^{54}Mn and ^{22}Na radioactivity with solar cycle and orbital inclination in different meteorites and a Lunar rock ...	136
22	Comparison of the observed and expected activities of ^{22}Na and ^{54}Mn in the Dhajala chondrite ...	140
23	The effective depths and ^{53}Mn activities in the core-samples from four chondrites ...	144

Chapter I

Introduction

The solar system is pervaded by high energy cosmic rays coming from all directions of the galaxy and moderately energetic solar flare particles derived from sporadic outbursts on the surface of the Sun. These two classes of energetic particles, galactic cosmic rays (GCR) and solar cosmic rays (SCR), have been extensively studied over the past few decades, by a variety of methods. These studies have led to a vast store of information regarding the contemporary cosmic rays.

It has been established that the contemporary galactic cosmic rays consist of about 93% protons, 6% alpha particles and small amount of heavier nuclei (Pomerantz, 1971). The differential energy spectrum of GCR in free space can be represented by a power law of the form:

$$dJ \propto (\alpha + E)^{-\gamma} dE \qquad \text{(for } E > 100 \text{ MeV)}$$

where J is flux, α is shape parameter (MeV) (about 1000 MeV for the free space flux at 1 A.U.), E is energy in MeV and γ is the spectral index. The value of γ ranges from 2.5 to 2.7. The integral flux of GCR at 1 A.U. ($E > 1$ GeV) is around (1.7-1.9) protons/cm^2.sec (4π) which fluctuates with the solar cycle. The average energy of primary cosmic rays is around a few GeV.

The energetic particles from the sun are emitted only during violent solar flares, the bulk of the particles being emitted in flares clustered near the sun-spot maximum. Studies of flares during solar cycle 19 (1954-1964) and solar cycle 20 (1965-1976) have shown that the intensity, spectral shape and composition vary from flare to flare (Reedy, 1977, and references therein). On the average, SCR consist of about 90 % protons, 10 % alpha particles and less than 1 % heavier nuclei. These particles have average energies of the order of a few tens of MeV and fluences (for E > 10 MeV) of the order of 10^8-10^9 particles/cm^2. (4π) over the short duration of a flare. The energy distribution of SCR particles can be described approximately by an exponential rigidity relation:

$$dJ \propto \exp(-R/R_o)\, dR$$

where J is flux, R is rigidity (= pc/ze) i.e. momentum per unit charge in MV, and R_o is shape parameter in MV. The value of R_o for contemporary flares varies between 40 and 200 MV. If the solar protons emitted during different flares over a solar cycle are distributed uniformly over the whole 11 yrs cycle, one can calculate an average equivalent steady-state flux. Such an average flux J (E > 10 MeV) for the last two cycles varied between 90 and 125 protons/cm^2.sec (4π) (Reedy, 1977).

The above summary of GCR and SCR characteristics refer to the past few decades of direct observations and periodic or aperiodic variations in these characteristics over the time

scale of tens of years have been well established. For example, the number of spots on the surface of the sun vary with about eleven year period. All solar activities, including the flares, tend to follow this eleven year periodicity and solar flares occurring near the maximum of the sunspot cycle are usually most intense. The intensity of GCR particles also varies with this eleven year cycle due to the variation in the modulation of GCR by solar magnetic field frozen into the plasma (solar wind) streaming radially away from the sun. For example, the intensity of the nucleonic component recorded by neutron monitor at a high latitude station increased by about 20 % from solar maximum to solar minimum during the 19th solar cycle (Pomerantz, 1971). This phenomenon is now well established and called as 'solar cycle modulation of galactic cosmic rays'.

Variations in SCR and GCR characteristics beyond the time-scale spanned by direct observations have been suspected from several independent studies. For example, over the time-scale of a few hundred years, historical reports on solar activity are available. Recently, Eddy (1976) has reviewed the observational reports on sunspots, auroral activities, and coronal activities during solar eclipses to show that the sun was comparatively inactive from 1645 to 1715 - the 'Maunder Minimum'. Measurements of ^{14}C activities in tree rings are consistent with the low solar activity for this period, and indicate that the sun was also inactive from about 1460 to 1550 (the 'Sporer Minimum'), was more active from about

1100 to 1250 (the grand maximum). Indications exist for similar variations in solar activity in the past.

Variations in solar luminosity over a much larger time-scale of a few million years have been invoked to explain (i) the frequent occurrence of terrestrial glaciation (Opik, 1950; Ezer and Cameron, 1972) and (ii) the low flux of solar neutrinos observed (Fowler, 1972; Rood, 1972; Ezer and Cameron, 1972; Ulrich, 1975). Davis (1972) and his colleagues (Davis and Evans, 1973) have observed a flux of solar neutrinos coming from the interior of the sun which is too low to be consistent with the standard solar model. To explain this discrepancy, Fowler (1972) proposed a variation in the standard solar model which involves a sudden mixing in the interior of the sun. Calculations carried out by Rood (1972) and Ezer and Cameron (1972) showed that such a mixing can explain a low neutrino flux and predicts luminosity variation over the time-scale of a few million years.

The above discussion refers to the evidences relating to possible variations in the solar activity in the distant past. It is possible, though not imperative, that changes in the solar activity are also reflected in the emission of SCR particles from the sun.

The most direct observational evidences regarding the extent of variations in the SCR and GCR intensity over the time-scale of a few million years come from the study of induced isotopes in the Lunar samples and meteorites. These objects have been continuously bombarded by SCR and GCR for

millions of years. The high energy of these particles is sufficient to induce nuclear reactions by spallation and neutron capture processes and produce a wide variety of stable and radioactive isotopes depending upon the available target elements. The heavier component of these particles also produce ionisation tracks in minerals of these samples. Arnold et al. (1961) have shown from a study of a wide variety of cosmogenic radioisotopes in iron meteorite Aroos that GCR intensity variation did not exceed a factor of 2 compared to the present day level during last b.y. Though this has ruled out any drastic variation in GCR intensity in the time-scale under consideration, a case for variation was made by Voshage and Hintenberger (1963) from the observed discrepancy between the cosmic ray exposure ages based on ^{36}Cl-^{36}Ar and ^{40}K-^{41}K methods. Schaeffer (1975) has recently reviewed the arguments and concluded that the GCR intensity was 50% higher in the last 0.4 m.y. than in the previous 600-900 m.y.

The variations in GCR and SCR characteristics in the long past are not yet unambiguously resolved. The present investigations were undertaken to augment the studies on the intensity and energy spectrum of SCR and GCR over the last few million years based on measurement of long-lived cosmogenic radioisotopes. In most of the cases, the radioisotope studies were supplemented by simultaneous analysis of nuclear tracks in the same samples. Track studies are crucial for a correct interpretation of radioisotope data since they provide valuable information regarding the exposure history and exposure geometry of the samples.

In addition to above, the activities of a variety of radioisotopes were studied in a fresh fall, Dhajala meteorite. The simultaneous measurement of short and long-lived radioisotopes provided a comparative analysis and the extent of solar cycle effect on GCR intensity along the Dhajala orbit could be evaluated.

A. Study of ^{26}Al activity in Lunar rocks

Lunar rocks are ideal detectors for monitoring any changes in the intensity and energy spectrum of SCR. They are well-documented hand-picked samples from a body maintaining a known distance from the sun. The nuclear reaction products of SCR protons and alphas are confined within the first few centimeters of Lunar rocks because of their relatively low energies compared to GCR. In this work, the radioisotope ^{26}Al was chosen on the basis of its half-life (0.72 m.y.) and abundant production in Lunar rocks. ^{26}Al is produced in Lunar rocks mainly by the following reactions:

SCR : $^{27}Al\ (p, pn)\ ^{26}Al$; $^{28}Si\ (p, 2pn)\ ^{26}Al$; $^{26}Mg(p, n)^{26}Al$

and

GCR : $^{27}Al\ (n, 2n)\ ^{26}Al$; $^{28}Si\ (n, p2n)\ ^{26}Al$

The cross-sections for these reactions have been discussed by Reedy and Arnold (1972) and tabulated by Dr. Reedy (priv. comm.). With these cross-sections and production models developed by Reedy and Arnold (1972) and Bhattacharya

et al. (1973) it is possible to calculate the production rate of ^{26}Al in Lunar rocks.

The GCR produced ^{26}Al activity is nearly independent of depth near the surface region whereas the SCR component falls off steeply and is many times greater than the GCR component near the surface. A comparison of ^{26}Al activities near and at the surface of several Lunar rocks having varying exposure times on the Lunar surface with the activities expected on the basis of model calculations can delineate the maximum extent of solar flare variation over this range of exposure times. A non-destructive β- γ coincidence technique having fine depth resolution was developed for measurement of ^{26}Al in a suite of suitable Lunar rocks. The results and their implications are discussed in chapter III and IV.

B. Study of production profile of ^{26}Al and ^{53}Mn activity in Meteorites

Meteorites suffer large and variable amount of ablation in atmosphere during their entry and thereby the region containing SCR effects is usually lost. The activities found in meteorites refer to interaction of GCR particles only. A typical meteorite orbit extends from little less than 1 A.U. to about 3 A.U. in space. Hence, the particle flux experienced by it refer to the integral over this orbit. Meteorites, thus, contain valuable records of GCR particles extended over a large domain of space and time. For example, a comparison of radioactivity in Lunar rocks and meteorites can elucidate the extent of modulation of GCR in space and time.

The production rate in a sample from a meteorite depends, among other things, upon the shape and size of the meteorite and also the shielding depth of the sample. For any valid interpretation of measured activities in terms of cosmic ray intensities and energy spectrum, detailed profiles are essential which should take into account (i) the target element abundances, (ii) the shape and size of the meteorite (i.e. choice of proper equivalent sphere), (iii) the class of the meteorite (the development of secondaries being different in different classes for the same size depending upon density and target element abundances), (iv) the cross-sections of the various reactions leading to the product isotope and (v) the modulation effect in space and time.

A simple parametric model which can take into account the above requirements independently from each other and thus deconvolute the problem into its separate components is desirable. An analytical method of calculating the primary and secondary particle fluxes inside a body was first proposed by Ebert and Wanke (1957) and later improved upon by Lavrukhina et al. (1969). In a different approach, Reedy and Arnold (1972) based on the work of Arnold et al. (1961) have proposed a simpler model for the Moon. In the present work, an extension of the Reedy-Arnold model coupled with the thick target approach (Kohman and Bender, 1967; Trivedi and Goel, 1973) applicable to the case of chondrites has been developed. The methods will be discussed in detail in chapter IV. The validity of the thick-target approach of Kohman and Bender (1967) was verified by measuring ^{53}Mn activities in a

pallasite. A comparison with the experimental data on ^{26}Al and ^{53}Mn is made to bring out the success and limitation of the model. Since the underlying assumptions in this model and that of the Reedy-Arnold model are the same, one can now compare the experimental results obtained in the case of Lunar rocks and meteorites (chondrites) directly in terms of cosmic ray intensities in a self-consistent way.

In addition to this theoretical attempt, experimental measurements were undertaken to get ^{53}Mn activity profiles in chondrites. Cores from four different size chondrites were studied simultaneously for cosmic ray tracks (to estimate the ablation and shielding depths) and ^{53}Mn activity at various locations. These studies bring out the essential features of development of secondaries inside a body as a function of size. The shape of the production profiles and the absolute magnitude of the predicted activities from the above-mentioned model are discussed in relation to the experimental profiles.

C. Radioisotope studies in Dhajala

On January 28, 1976 a meteorite fell in Gujarat having produced shower fragments distributed around the village Dhajala. The fragments of this meteorite were recovered with high efficiency and speed. An extensive multidisciplinary study was undertaken on this fresh fall which involved radioactivity measurement, rare gas investigation, nuclear track analysis and calculation of orbit. This work reports the studies on radioisotopes ranging in half-life from a few days to a few million years. The results are presented in

chapter III and discussed in chapter IV in terms of galactic cosmic ray intensities over the orbit of Dhajala during the different time-scales defined by the mean-lives of the radioisotopes.

The theoretical and experimental studies reported in this thesis lead to an overall picture of GCR and SCR characteristics over the past few million years and give interesting information on the GCR intensities in the recent past.

Chapter II

Experimental Techniques

The experimental procedures employed in this study involved sampling of Lunar rocks and meteorites, radiochemical separation and purification of elements, neutron activation analysis and counting of activities of various radioisotopes. Supplementary studies on nuclear tracks were carried out in the track laboratory of P.R.L. by our colleagues. The description of samples studied and the above-mentioned experimental methods are described below.

II.A. Sample description

Two types of extraterrestrial samples were studied in this work for determining the activities of cosmogenic radioisotopes. These are (1) Lunar rocks and (2) meteorites. The selection criteria and description of these samples are given below.

II.A.1. Description of Lunar rocks studied

Lunar rocks were studied for determining the content of cosmogenic radioisotope ^{26}Al. The selection criteria for the choice of rocks from among the variety of rocks brought by the astronauts were based on the following requirements:

(i) Concordance of rare gas and track exposure ages for a simple exposure history. This will be dis-

cussed in detail in chapter IV.

(ii) The isotope of interest in this work is ^{26}Al which is produced abundantly from ^{27}Al (p,pn) reaction. High abundance of target element Al was the second major consideration for rock selection.

(iii) For a nondestructive β-γ coincidence counting of the positrons from ^{26}Al decay the daughter products of U and Th cause interference. Low concentrations of U and Th in the selected rocks was an additional criterion.

(iv) The radioactivity at the Lunar top surface of a rock is expected to decrease with increasing zenith angle. Therefore at surfaces away from zenith, appropriate solid angle corrections have to be made. For estimation of this correction only rocks having unambiguous Lunar surface photo-documentation were suitable.

(v) Large size of the rocks to minimise the geometry corrections.

In addition, data on microcrater size distribution on the virgin surfaces and tracks were used to select rocks with a simple cosmic ray exposure history and preserved exterior surfaces. Four Apollo 16 rocks and one Apollo 17 rock chosen by us on the basis of the above considerations and allotted by NASA for these studies are described below (Interagency report: Astrogeology 51, 1972; Apollo 16 Preliminary Science report, NASA SP-315, 1972; Apollo 17 Preliminary Science

report, NASA SP-330, 1972).

Rock 61016

We received a vertical slice from the 11.7 kg Apollo 16 anorthosite clast rich breccia 61016, collected from the Cayley Plain (station 1) near the eastern rim of Plum Crater. The piece 61016,287 (Parent No.40) weighed 35.04 g. and had 3.3 cm^2 of preserved top surface. The thickness of the slice varied between 9 to 18 mm. The rock has a smooth glassy surface and the anorthosite crystals in the rock are severely shocked. Zap pits are present on all faces except the bottom. Our sample is from a face having a mean zenith angle for exposure to cosmic rays $\sim 30^{\circ}$.

The piece 61016,287 was sliced at a depth of 4 mm with the help of a slow speed Beuhler diamond saw with a 0.1 cm thick blade. This exposed two new internal faces at depths of 4 mm and 5 mm from the top. The saw dust was utilised for track measurements.

We also received a slice 61016,300 from a depth of about 2.8 cm from the surface for determination of ^{26}Al due to GCR only.

Rock 60335

This is a small (318 g) recrystallised breccia collected from the LM/ALSEP area near the bottom of a very subdued 150 m crater. The rock has vastly different crater densities from side to side indicating complicated surface history. We received a slice 60335,103 (Parent No.12) containing Lunar

top (face S) and weighing 2.34 g.

Rock 64435

This is a large breccia weighing 1.08 kg collected from station 4 on a high point on Stone Mountain. This region has an appearance which suggests derivation from South Ray Crater. Our sample was a small piece 64435,95 (Parent No.15) weighing 5.27 g. This had 3.2 cm^2 of Lunar top surface.

Rock 66095

This anorthosite rock weighing 1.19 kg was chipped from a big boulder at station 6 near the base of the Stone Mountain on the Cayley Plain. This region had probable ejecta from South Ray event. The face B had many zap pits and almost none on other faces thus establishing the Lunar orientation. Our sample 66095,145 (Parent No.6) weighed 5.74 g and had about 2.1 cm^2 of preserved Lunar top surface.

Rock 79215

79215 is a brecciated troctolite of 553.8 g collected from a distance of about 60 m (South East direction) away from Van Serg Crater, station 9 in Apollo 17 mission. The piece received by us 79215,78 (Parent No.3) was 3.32 g having a Lunar top surface of about 2.1 cm^2.

The details of the five rocks along with their major element composition are given in Table 1.

II.A.2 Sampling of rocks for nondestructive β-γ counting

The non-destructive β-γ coincidence counting method used for determining the ^{26}Al activity in the above-mentioned

Table 1

Description and mean chemical composition of Lunar rocks[1]

Rock	Location (crater)	Type	Size (cm)	Weight (kg)	Na	Al	Mg	Si	Fe	U	Th
					wt. %					ppm	
60335	L.M.	Breccia	10x6x5	0.318	0.23	13.23	4.64	21.65	3.3	1	2.81
61016	Plum	Anorth	28x18x16	11.7	0.25	13.0	6.11	20.3	0.05-4	0.1-0.5	0.5
64435	South ray	Breccia	12x10x11	1.079	0.126	16.98	1.81	20.82	0.4-3	0.03	0.1
66095	South ray	Anorth	18x16x7	1.185	0.178	12.17	5.82	20.98	4.5	1	2.7
79215[2]	Van Serg	Breccia	9x8x7.5	0.554	0.256	13.48	5.7	20.16	3.5-20	~1[3]	~3[3]

(1) The chemical composition is from J. Warner and P. Butler (priv. comm.)

(2) D.P. Blanchard (priv. comm.)

(3) Estimated from the analysis of the β-γ spectrum.

rocks minimizes the loss of the virgin surface of the rock that faced the sun and provides a high depth resolution in profile. It has been shown by studies of nuclear tracks, craters and destructive analysis of radioisotopes (Wahlen et al., 1972) that any major laboratory handling of rocks results in non-uniform abrasion of the surfaces. The extent of this loss is difficult to determine (especially for fine-grained breccias) and hence the surface activity may not always refer to zero depth. The present method enables one to determine the ^{26}Al activity precisely at the top face. The depth resolution is determined by the half-thickness of the positrons emitted by the decay of ^{26}Al.

The decay scheme of ^{26}Al is given in Samworth et al. (1972). ^{26}Al emits a positron 82 % time in coincidence with a gamma ray of 1809 keV. The positron has a maximum energy of 1.17 MeV. The β^+ annihilates into two 511 keV γ's on interaction with matter. The half-thickness of the ^{26}Al was determined by external absorption of betas from a ^{26}Al standard and also by self-absorption method. These results will be given in Chapter III. The best value is measured to be 60.5 $mg.cm^{-2}$ in Al metal. This value corrected for the composition of an anorthite rock like 61016 implies that about 90 % of the emerging positrons are emitted from a layer of 200 $mg.cm^{-2}$ thickness.

The signal strength in this method is limited by the available surface area of the rock facing the beta counter. All the samples provided by NASA were in the form of roughly

rectangular blocks having 1-3 cm^2 of virgin surface. The samples were packed inside plastic boxes with slots to match the exposed areas of the samples. The plastic box was carefully placed on top of the beta counter, so that the exposed area of the sample is in flush with the beta counter window through the slot. The area of the slot is the measure of the counting surface area. The plastic box without the sample inside was used for determination of background.

II.A.3. Sampling of meteorites for γ counting

Five meteorites Bansur, Parsa, Udaipur, Bruderheim and Dhajala were studied for gamma emitters using a simple NaI(Tl) γ -ray spectrometer.

Bansur is a 15 kg stone belonging to L5 or L6 group which fell in Rajasthan in 1892. This meteorite has a symmetrical conical shape which resulted from its oriented descent into the earth's atmosphere. This type of entry also resulted in its front face having pits like thumb prints and a thick fusion crust. The back face on the other hand has a crust of only a fraction of 1 mm. This meteorite has been extensively studied for rare gas (Gopalan and Rao, 1976) and tracks (Bhandari et al., 1978). ^{26}Al on 3 faces of this big stone was studied (face # 2, # 4, # 1) using a γ -ray spectrometer.

Udaipur is another Indian meteorite (1.2 kg) belonging to H4 or H5 group. It fell in Udaipur, Rajasthan. It also has a conical shape (Figure 3) indicating a possible oriented entry. This was also studied for rare gas and tracks. The

face of apex and base was put on γ-ray spectrometer for ^{26}Al. Both these meteorites were loaned to us by Dr. R.C. Agarwala, Director of Archaeology and Museums, Rajasthan.

Parsa and Dhajala are two other Indian meteorites. Parsa fell in Patna, Bihar and Dhajala in Gujarat. Several fragments from the fresh fall of Dhajala were studied within almost 2 days after the fall. The fall and sampling of Dhajala will be described below. A sample of Bruderheim was counted in the same system to serve as a standard and all the activities were normalised to the published ^{26}Al value of Bruderheim (Honda et al., 1961).

II.A.4. The fall and sampling of Dhajala

On January 28, 1976 a meteorite shower fell in Gujarat, India at 8.40 p.m. around the village of Dhajala ($22^{\circ}22'40"N$; $71^{\circ}25'38"E$). It was accompanied by brilliant light flashes and sound of detonations. A large number of fragments survived the ablation and dispersed over an elliptical area of about 50 km^2. About 500 fragments weighing a total of about 61 kg have been recovered so far. The phenomena associated with the fall of the meteorite, field observations and orbital characteristics have been described in detail by Bhandari et al. (1976 a), Lal and Trivedi (1977) and Ballabh et al. (1978). A few fragments of the meteorite arrived in PRL within a day of the fall.

A multi-faceted study involving particle tracks, rare gases and radionuclides was undertaken to characterise the meteorite. Six big fragments T-16, T-17, T-67, T-78, T-92

and G-1 each weighing between 1.5 kg to 6.5 kg were used for nondestructive gamma-ray analysis. In addition, three selected fragments, T-11, T-67 and T-68 were analysed using destructive methods for radionuclide concentrations. Aliquots of (1-1.5 gm) from T-11 and T-67 were analysed by Gopalan et al. (1977) for cosmogenic and radiogenic noble gases. All these fragments were investigated by Bagolia et al. (1977) for nuclear tracks.

II.A.5. Coring of meteorites for ^{53}Mn and track profile

Three Indian meteorites Bansur, Udaipur and Madhipura and one French meteorite St. Severin were studied extensively to ascertain the ^{53}Mn production profile in chondrites.

Five cores taken from St. Severin have been studied by Cantelaube et al. (1969) and Lal et al. (1969) for nuclear tracks. These studies have established that the core A-III is a near-radial core. The core CB4 is not quite as radial but the decrease in track density from the surface to the centre is about a factor of 250 which is nearly the same as for core A-III (Lal et al., 1969, Amin et al., 1969). Five samples from core CB4 and three samples from A-III were kindly provided by Prof. Lal for ^{53}Mn studies.

Cores were taken from Bansur, Udaipur and Madhipura by an electrometallic diamond drill-corer. Before coring spot samples from all the faces of these meteorites were studied for nuclear tracks to ascertain the faces which are least ablated. Coring locations and directions were decided on the

basis of these data so that they were along the direction of maximum gradient. Figures 1, 2 and 3 are the coring plans of the three meteorites and Table 2 gives the description of these cores and samples taken from various depth of the cores along with their weights.

Thirteen samples from these three meteorites were processed for ^{53}Mn determination. Aliquots from all these thirteen samples were also analysed for nuclear tracks.

II.B. Radiochemical methods

The γ-emitting radionuclides like ^{26}Al, ^{40}K in meteorites and lunar samples can be counted non-destructively for determining their activities. For example, in case of fresh fall Dhajala radioisotopes ^{22}Na, ^{54}Mn gave clear signals in singles γ counting. But for some isotopes the decay involves low β energy or X-ray emission. For determining such species a detailed radiochemical investigation was undertaken on three Dhajala fragments (section II.B.1).

Determination of ^{53}Mn in a number of meteorites by neutron activation analysis was also undertaken. This involves separation of Mn from metal or silicate phase (~ 1 g sample) of meteorites, irradiation to a highly thermalised dose of neutrons and post-irradiation radiochemical purification of Mn for determining ^{54}Mn activity produced by ^{53}Mn (n, γ) ^{54}Mn reaction. The technique has improved considerably by the work of Tokyo and La Jolla groups. Details of the methods are given in section II.B.2.

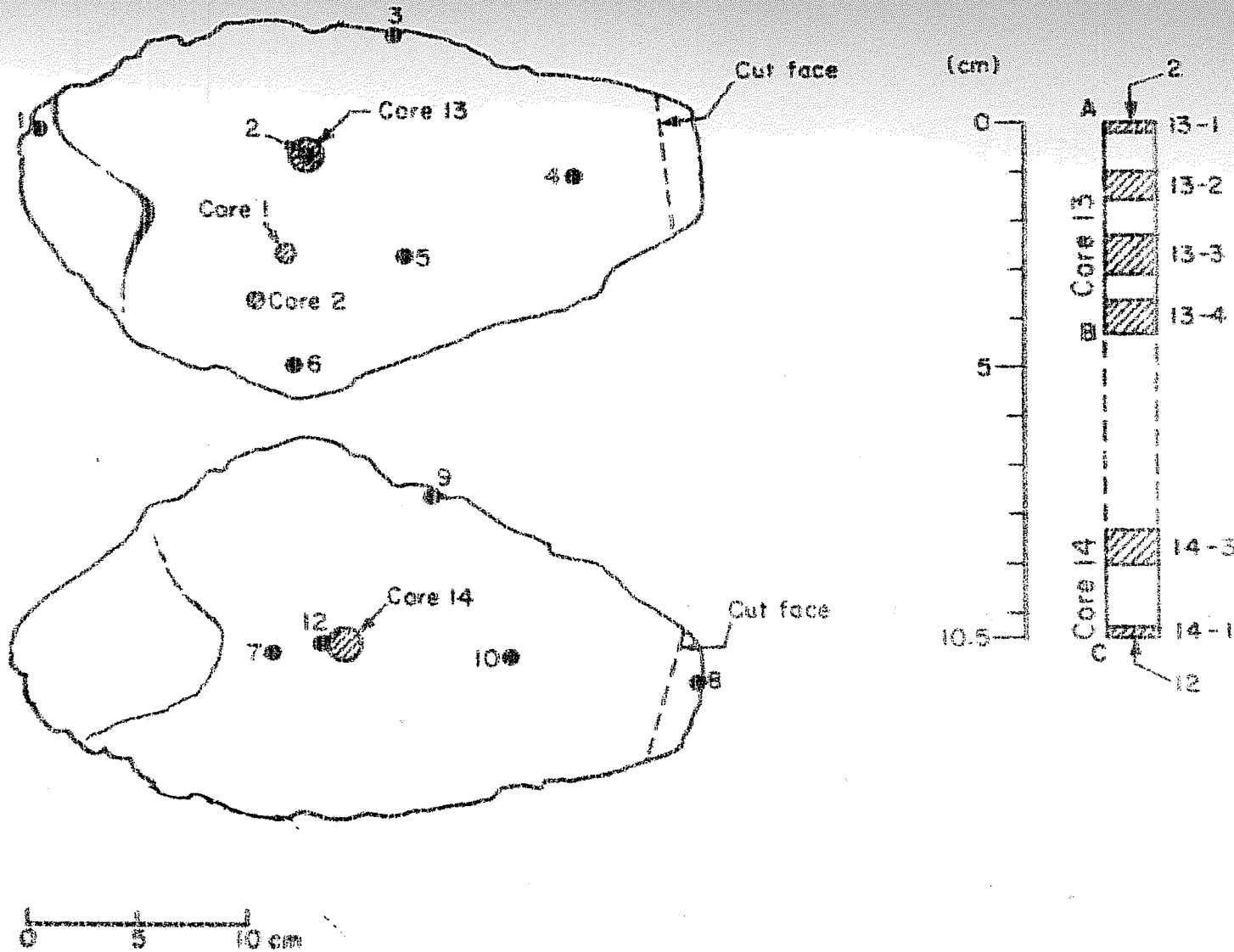

Figure 1. Surface samples and core-samples from the Bensaur chronicle.

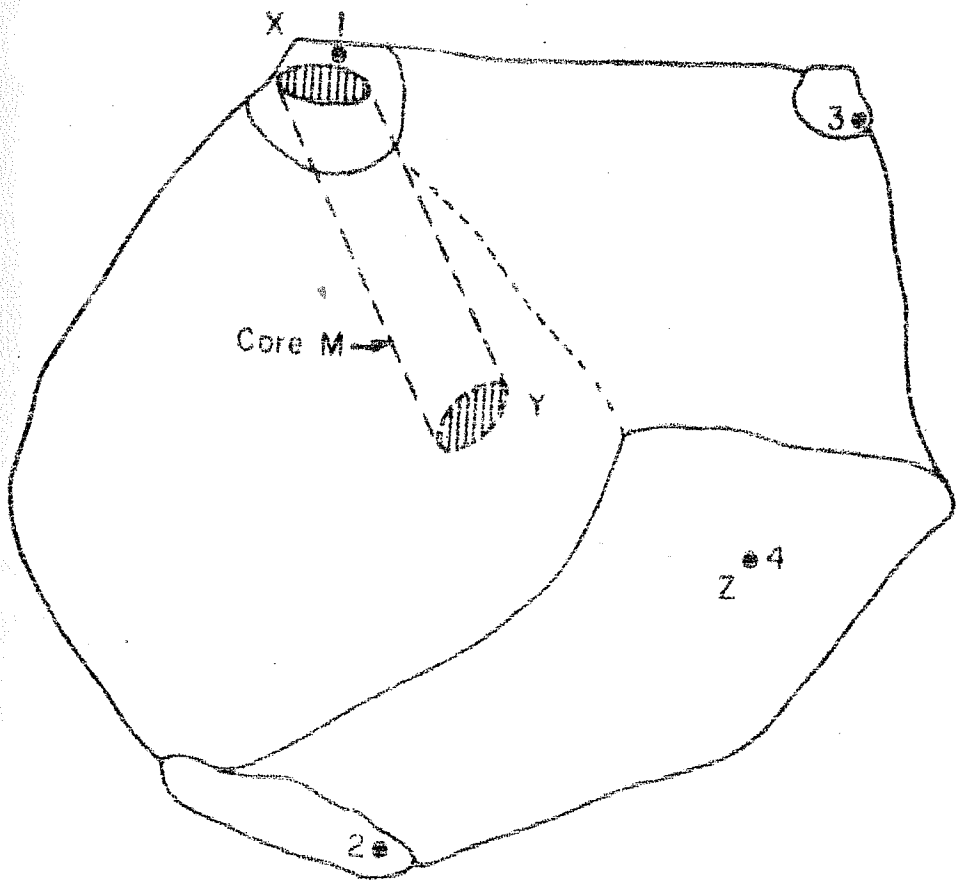

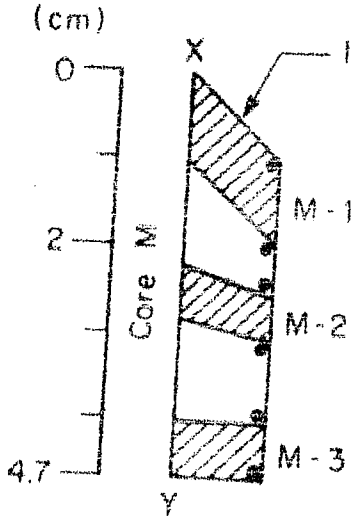

Figure 2. Surface samples and core-samples from the Madhipura chondrite.

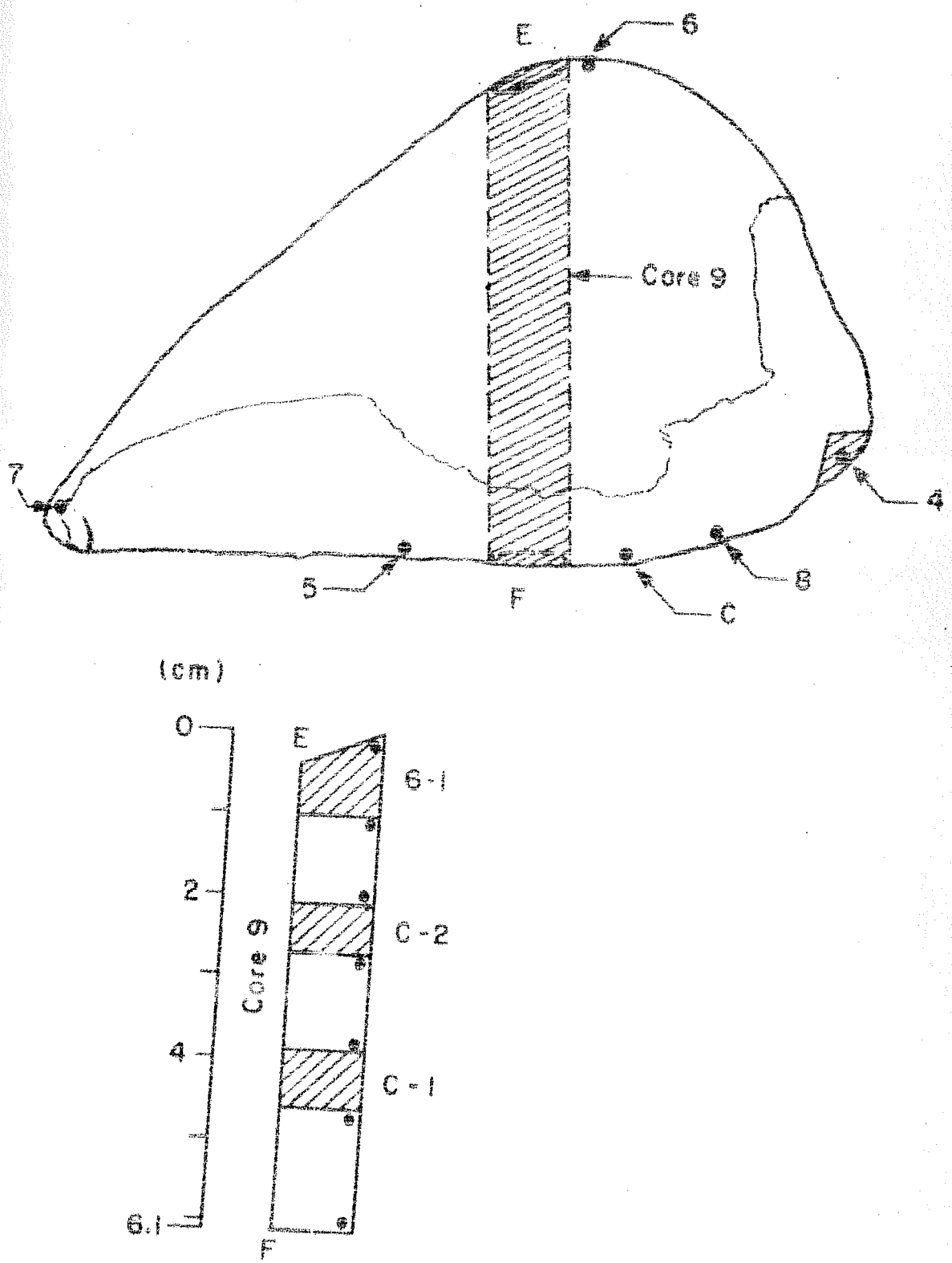

Figure 3. Surface samples and core-samples from the Udaipur chondrite.

Table 2

Details of core-samples analysed for ^{53}Mn and tracks

Meteorite	Exposure age (m.y.)	Core name	Sample	Code	Depth in core* (cm)	Weight (gm)
Bansur	10	# 13	13-1	A	0-0.2	0.9058
			13-2	B	1.0-1.6	0.7095
			13-3	C	2.3-3.1	1.0413
			13-4	D	3.6-4.3	1.0379
		# 14	14-3	E	8.3-9.0	0.9276
			14-1	F	10.3-10.5	0.6765
Madhipura	15	M	M-1	G	0-1.0	1.6025
			M-2	H	2.2-2.8	0.5501
			M-3	I	4.0-4.7	0.9175
Udaipur	22	9	C-1	J	3.9-4.6	0.7889
			C-2	K	2.1-2.7	0.6896
			6-1	L	0-1.0	1.0547
			# 4	M	~ 6.1	0.7024
St. Séverin	11.2	CB4	CB4-1	N	~0(-0.54)+	0.9114
			-2	O	0.13-0.26	0.9620
			-10	P	1.95-2.16	0.9319
			-25	Q	9.04-9.23	0.8644
			-32	R	15.98-16.23	0.9713
		A III	A III-10	S	2.65-2.97	0.8932
			-23a	T	7.35-7.61	0.7977
			-25b,c	U	23.45-23.63 28.45-28.62	0.3327

* See Figures 1, 2 and 3 for depth scale. For St. Séverin depth is from Lal (priv. comm.)

\+ The top with a hemispherical bulge ~ 0.54 cm.

II.B.1. Radiochemical investigation of Dhajala

Three fragments T-11, T-67 and T-68 of Dhajala were analysed destructively for radioisotopes ^{7}Be, ^{10}Be, ^{26}Al, ^{32}P, ^{33}P, ^{51}Cr, ^{52}Mn, ^{53}Mn, ^{54}Mn, ^{57}Co and ^{60}Co. These elements were separated and purified by following standard radiochemical procedures (Finkel, 1972 and references therein) outlined below briefly in case of sample T-11.

350 g of sample T-11 was crushed to less than 230 μ (60 mesh). 30 g of this was preserved as aliquot for mass spectrometric, fossil track and chemical composition measurements. 320 g was dissolved using HF, HNO_3 and HCl. About 45 g remained undissolved, which was fused with Na_2CO_3 and the melt was dissolved and mixed to the main solution. An aliquot was taken for the chemical estimation of elements. Carriers of Be, P and Co were added and equilibrated by vigorous boiling.

Fe was removed by ether extraction in 9N HCl. Al, Na and Mn were precipitated as chlorides by Gooch-Haven's method. Mn was separated as MnO_2 in a HNO_3-$NaBrO_3$ medium. Al, Be, Cr and P were separated from Fe, Ni and Co by hydroxide precipitation in a Na_2O_2-NaOH medium. Final separations were done by ion-exchange columns. The radiochemical purification was performed using characteristic precipitations or ion-exchange methods (Finkel, 1972).

14 g of sample T-68 and 13 g of sample T-67 were processed only for Al and Be to determine the activities of ^{26}Al and ^{10}Be.

II.B.2. Neutron activation analysis of ^{53}Mn in meteorites

^{53}Mn in meteorites was determined by intense neutron activation via ^{53}Mn (n, γ) ^{54}Mn (Millard, 1965). The technique involves pre and post-irradiation separation and purification of Mn following the detailed procedures of Imamura et al. (1969,1973), Nishiizumi (priv.comm.) on meteorites and Lunar samples.

Twelve chondrites, two pallasites, one mesosiderite and one iron meteorite were analysed. Chondrite samples (ca.500 mg) were crushed to 50 ~ 100 mesh size powder in an agate mortar. In 5 chondrites the samples available were large and for them the metal phase was separated by a hand magnet using isopropanol to wash away the fine dust fraction. The metallic fractions, so obtained were washed with dil HCl, water and iso-PrOH in an ultrasonic bath and inspected under microscope for silicate contamination. Metal blocks from non-chondritic meteorites (ca.300 mg) were also washed similarly before chemistry.

a. Pre-irradiation chemistry

After dissolution of the metal and other soluble minerals in stone (ca.500 mg) with a few ml of 1:1 HNO_3, the undissolved silicates were decomposed with 4-5 ml of 48% HF in a 50 ml teflon beaker. After dryness the residue was dissolved with 2-3 ml of 60% $HClO_4$ and fumed to dryness to remove fluorides. The fuming process was repeated three or four times by adding 40-50 mg of Boric acid to mask any residual fluorides. The

dry brownish cake was dissolved in 8N HCl. About one percent aliquot by weight was taken for chemical analysis.

Fe, Mn and Ni in these samples were determined by atomic absorption spectrophotometer (Perkin-Elmer model 305 A). Most of the Fe was extracted from the solution with isopropyl ether. The aqueous fraction was taken to dryness, and dissolved in mildly acidic solution. The solution was warmed and hydroxides were precipitated with NH_4OH at pH 8~9 and a few drops of H_2O_2 (30%). The solution was allowed to rest for about 2 hrs for completion of Mn precipitation. The thick brownish precipitate was separated by centrifuge and washed 2 times in ammoniacal water. This step removes most of the Mg, Ca, Na and part of Ni, Co. The precipitate was dissolved in a few drops of 9N HCl and loaded on a 7 ml anion exchange column (Dowex-1 x 8, 100-200 mesh, 0.5 cm^2 x 14 cm 9N HCl medium). The alkaline earths, Ni, Cr were separated in the first one column volume of 9N HCl. Mn was then eluted with the following 2.5 column volumes of 9N HCl. Co and remaining Fe were eluted with 3 column volumes of 0.5 N HCl.

In some cases, instead of a simple 9N HCl anion exchange column the medium used was a 'mixed solvent' (conc.HCl : iso-PrOH : H_2O = 45 : 40 : 15 by volume, Fritz and Pietrzyk, 1961). In this case the Mn fraction was taken in about 2 ml of 'mixed solvent' and loaded on a 7 ml anion exchange column in 'mixed solvent' medium. Ni, V, Ti were removed in the first 3 column volumes of the elute. Mn was then eluted with 2.5 column volumes of 7N HCl. The Mn fraction was

evaporated and converted to nitrate with about 10-15 drops of conc. HNO_3 by heating. The residue was dissolved in one or two drops of water and transferred to a 2.5 cm x 2.5 cm square foil of highly pure Aluminium (Nippaku Al 99.93 % Al, Mn = 0.2 ppm and Fe = 32 ppm) and evaporated under an IR-lamp. This process was repeated four or five times in order to transfer all the Mn on to the foil. The foil was heated on a hot-plate for complete dehydration and to a high temperature to form dark coloured oxide, Mn_3O_4. Finally the foil was folded and doubly wrapped, with another foil. Wherever required, Mn recoveries at the various steps were followed by atomic absorption spectrophotometer.

For iron meteorites or metallic phase of stony or stony-iron meteorites, the samples were dissolved with aqua regia, and about 200 µg of Mn carrier was added. Chemistry was followed as described above except for the step of hydroxide precipitation.

b. Neutron irradiation

The JRR-2 and JRR-3 reactors of the Japan Atomic Energy Research Institute, Tokai, Ibaragi prefecture, were used for the neutron activation analysis of ^{53}Mn in meteorites. The VT-4 position of JRR-2 ($\phi \sim 3.7 \times 10^{12}$ n/cm^2.sec) and VG-7-6 position of JRR-3 ($\phi \sim 2.7 \times 10^{12}$ n/cm^2.sec) were utilised. The irradiation times were 11 days in both the cases. Though JRR-2 has a higher flux, the VG holes of JRR-3 provide a higher thermal to fast neutron ratio which proved more satisfactory to reduce interferences from the $^{55}Mn(n,2n)$

^{54}Mn and $^{54}Fe(n,p)\ ^{54}Mn$ reactions. A set of samples wrapped in aluminium foil was irradiated with ^{53}Mn standards and Co as flux monitor, along with 5-10 mg of Mn metal and 2-10 mg of Fe metal for estimating interferences of (n,2n) and (n,p) reactions respectively. The standards of ^{53}Mn, Co, Mn-metal and Fe-metal were put on both sides of the samples arranged in the form of 'sandwich stack' and the whole stack was packed in a big aluminium foil to make a package of about 1.5 cm x 1.5 cm x 2.5 cm. The ^{59}Co standard measured the thermal neutron flux and the flux gradient across the stack. The flux variation from the top to the bottom of the stack was found to be within 5%.

c. Post-irradiation chemistry

The irradiated samples were usually cooled for 20-30 days before processing. The sample contained many radioactive impurities such as $^{46}Sc(t_{1/2}= 84\ d)$, $^{51}Cr(27.7\ d)$, ^{59}Fe (44.6 d), $^{60}Co(5.26\ yr)$ ^{65}Zn (244 d), ^{75}Se (120 d), $^{110m}Ag(250\ d)$ and ^{192}Ir (74 d). These were various (n, γ) products and particularly high activity of ^{46}Sc was formed from Sc impurity in the Al foil. The purpose of post-irradiation chemistry was to effect the radiochemical purification of ^{54}Mn from these radioactive impurities.

Extreme care and safety precautions were taken in handling the irradiated sample. The manganese oxide was dissolved from the inner aluminium foil using dilute HNO_3 and about 0.2% H_2O_2 in a beaker using IR lamp. About 1 mg each of hold back carriers of Fe, Co, Cr, Ir and Sc were

added to the solution. The foil was removed from the solution after complete dissolution of the manganese oxide. After evaporating off the solution, the residue was dissolved in a few drops of 6N HCl and made upto 0.5N HCl by adding water. The solution was loaded to a 5 ml cation exchange column (Dowex 50W x 8, 100-200 mesh, 0.5 cm^2 x 10 cm, 0.5N HCl medium) and then 5 ml of 2N HCl was passed through the column. Mn was collected in the next 13 ml of 2N HCl along with Co and Fe. In this step yellow coloured iron fraction eluted slightly faster than Mn.

The manganese fraction was evaporated and loaded on a 5 ml anion exchange column (Dowex-1x8, 100-200 mesh, 0.5 cm^2 x 10 cm, 9N HCl medium) with a few drops of 9N HCl. After 5 ml of 9N HCl was passed, Mn was collected in the next 13 ml of 9N HCl. Co was eluted with next 10 ml of 4N HCl and then Fe with 10 ml of 0.5N HCl. This iron fraction was evaporated in a plastic vial and the amount of iron was determined from the gamma activity of ^{59}Fe with a 3"x3'' NaI(Tl) scintillation detector. The iron content in the irradiated sample was necessary to know for correcting the contribution due to $^{54}Fe(n,p)\ ^{54}Mn$ reaction. The final purification of Mn was done by TTA (thenoyl trifluoroacetone) extraction. The TTA solution was made by dissolving 2.5 g TTA in 10 ml ethanol. The manganese fraction from anion exchange step was evaporated to dryness and dissolved with a few drops of 2N HCl. The solution was diluted with 5 ml of 10% ammonium tartrate as a masking agent and 5 ml of 20% ammonium acetate. About 100 mg of l-ascorbic acid was added and the pH was adjusted

to 8~9 with a few drops (1:1) NH_4OH. At this stage 1.5-3 ml of TTA solution was added which formed yellow precipitate of Mn-TTA complex. The complex was extracted into 10 ml of ethylacetate and the organic phase was washed with 10 ml of pH 8~9 buffer solution. Mn was back extracted into 10 ml of dil HNO_3. The back extraction was repeated. After drying the combined extracts the remaining ammonium salt was decomposed by boiling with aqua regia.

From the purified manganese solution a few percent aliquot was taken by weight for chemical yield determination. The remaining solution was transferred to a small plastic vial (counting sample holder) and evaporated to dryness under an IR lamp. The chemical yield was determined by atomic absorption spectrometry (Perkin-Elmer model 305).

II.C. Counting techniques and track measurement

The activity levels of the radioisotopes in samples of meteorites and the Moon are very low and hence require the use of special counting systems to yield high signal to background ratios. The background of counter from environmental radioactivity and muons and their interactions is reduced by the use of Pb shielding and anti-coincidence guard counters (Oeschger and Wahlen, 1975) while the efficiency is maximised by the choice of detectors. For isotopes decaying by emitting two coincident radiations e.g. ^{26}Al, ^{60}Co the specificity of detection is improved by using two detectors in coincidence with each other. Five high sensitivity counting systems were used in this study. The $\beta-\gamma$ coincidence system developed

in this study is described in detail here. In addition, the β, γ and X-ray counters used for this work will also be described. The ^{54}Mn counting for the irradiated ^{53}Mn samples was done in the Ge(Li) system in Prof. Honda's laboratory in Tokyo. A brief description of this is given. In addition, a short outline of the methods of nuclear track analysis is given for the sake of completeness.

II.C.1. The β-γ coincidence spectrometer

Radionuclides which emit β particles in coincidence with γ radiation can be measured by the β-γ coincidence spectrometer following the design by Bhandari (1969), Rajagopalan (1969) and Wogman and Brodzinski (1973). Three such radioisotopes were measured which included ^{60}Co (E_γ = 1.17, 1.33 MeV) and the positron emitters ^{26}Al and ^{52}Mn where the coincident γ rays were the annihilation photons (0.511 MeV) of the β^+ after its interaction with matter.

The schematic of the system is shown in Figure 4. The 12.5 cm x 12.5 cm NaI(Tl) scintillator supplied by Horiba Co., Japan was coupled to a EMI (9709 QKB) quartz face photomultiplier. The photomultiplier was run at 1200 V. The beta counters were flat rectangular Geiger-Muller counters. They were made of plexiglass (methyl-methacrylate) with 0.9 mg/cm^2 gold-coated mylar windows and S.S. central wire of dia.0.005 cm. For non-destructive analysis of Lunar rocks five such counters were made with different sizes and active areas to suit the available rock surfaces since larger surface area means a larger signal. The beta counters were placed flush against

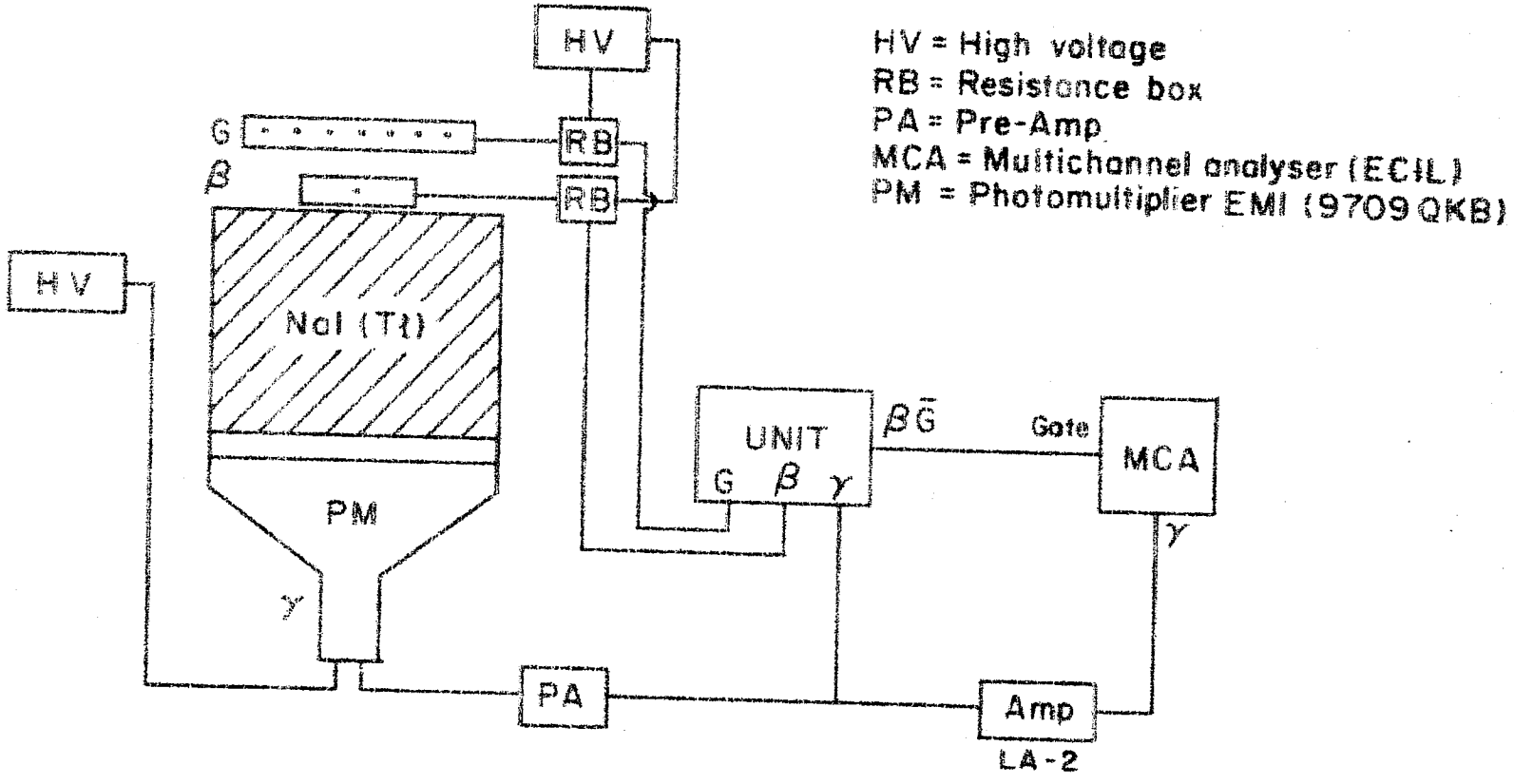

Figure 4. Schematic of the beta-gamma coincidence spectrometer system.

the top surface of the scintillator crystal. They were operated as flow gas counters with argon ethylene mixture (ethylene 1.25%) as counting gas. Commercial argon gas was found to be quite suitable for the purpose. The active area of the beta counters were between 4 to 12 cm^2. The beta counters had stable plateau of greater than 100 V and were usually operated at 70-80 V higher than the starting voltage. Periodic checks on starting voltage were done by using a ^{40}K beta standard.

A large (34 cm x 24 cm) Geiger-Muller counter was placed on top of this β- γ assembly to act as an anticoincidence mu-meson umbrella. It was also made of plexiglass and had 9 wires separated by 2.3 cm from each other. The window was made of aluminium coated mylar. This was also operated as a flow counter with (Ar + ethylene) gas mixture. The position of this guard was adjustable to accommodate various rock specimens on top of the beta counter. Use of this guard reduced the background of the system by a factor of about 3 in the present geometry. The whole system was placed inside a 15 cm thick lead shield and housed in the ground floor of a 8-storey laboratory.

Signals from the three counters, beta, guard and scintillator were monitored in a multi-purpose unit which also recorded the pure beta signal in anticoincidence with the guard and gamma signal. The gross count rates from the three detectors were checked to determine the stability of the system. Scintillator pulses in coincidence with beta

signal were stored in a 400 channel ECIL multi-channel analyser whose gate was opened by the output of beta pulses from the above mentioned multi-purpose unit. The schematic of the electronics is also shown in Figure 4.

The efficiency of the system was obtained by using ^{22}Na and ^{26}Al standards. The ^{22}Na standard (SMN ^{22}Na) was made from NBS standard (4921, parent solution had 1.09×10^4 β^+/sec/gm on 6 August, 1964). The ^{26}Al standard was made in the La Jolla laboratory of Prof. Arnold and intercalibrated with ^{22}Na standard. The backgrounds were counted by activity-free perspex pieces cut to fit the size of the counters. Typical efficiency and background of a system, Aries on Horiba, are given in Table 3. Activities for ^{26}Al were calculated using the 511 keV annihilation peak only. Integral rates at higher energies in the analyser spectrum were used as additional checks on the system stability. In the non-destructive counting of Lunar rocks the activity of the samples was low and it was necessary to count them for more than 5,000 minutes. Background and samples were usually counted alternately. The total background data for 30,000 minutes were pooled and used as mean background over the entire period. Individual background runs were found to be stable during the whole counting period.

II.C.2. The beta, X-ray and gamma counters

The radionuclides ^{10}Be, ^{32}P, ^{33}P were measured in the Dhajala meteorite after radiochemical separation of these elements. These isotopes are pure β emitters and the

Table 3

Details of $\beta-\gamma$ system: ARIES ON HORIBA

Crystal size (dia x thick)	12.5 x 12.5 cm
Active area of β counter	12 cm^2
GM(β) counter geometry	Flush on top surface of crystal
Ideal KCl β_2 efficiency (thin source over 3.5 cm^2)	48 %
Positron ($\beta^{\mp}-\gamma$) efficiency	13.2 %
Background (511 $\pm$ 50 keV) counts/day	10.9
Background (610 $\pm$ 25 keV) counts/day	4.0

activities were measured in a Geiger-Muller counter following the design of Lal and Schink (1960). Briefly, the beta counter was a rectangular counter with 2π - geometry and 4.1 cm^2 active are and operated with Q-gas (98.7% helium + 1.3% isobutane). The beta counter was used in anti-coincidence with a big rectangular guard counter and housed in a 10 cm thick lead shield. The background and counting efficiency are given in Table 8.

A duplicate sample of ^{10}Be was also measured in a lower background system designed following Bhandari (1969). This consisted of a rectangular G-M counter in anticoincidence with a NaI (Tl) scintillator. The scintillator has a well of 7.5 cm x 2.5 cm in which the G-M counter is placed. The counting gas was (Ar + Ethylene) mixture and the system was housed in a 15 cm thick lead shield. The background and efficiency of this system are also given in Table 8.

Radioisotopes ^{53}Mn and ^{57}Co were measured in the Dhajala chondrite after radiochemical separation of these elements. These are X-ray emitters and were counted in a big cylindrical X-ray counter. The proportional counter was made by Venkatavaradan (1970) and described in detail in his thesis. It was operated by P-10 gas as a flow gas counter. The signals were amplified by a Canberra spectroscopic amplifier and fed to a MCA for energy analysis. The efficiency was determined by a plated ^{55}Fe source. The background and efficiency are given in Table 8.

A simple γ-ray spectrometer was used for rapid non-destructive determination of ^{26}Al from various faces and

fragments of a meteorite. This method was first used by Van Dilla et al. (1960). The system consists of a 7.5 cm x 7.5 cm NaI(Tl) detector coupled with an ECIL multichannel analyser. The predominant γ-activities in chondrites are due to ^{26}Al in 511 keV and ^{40}K in 1460 keV channel. In the case of fresh fall Dhajala, the peaks due to ^{22}Na and ^{54}Mn were also very prominent. A simple iterative procedure was followed to calculate the net signal ratio of 511 keV to 1460 keV by counting standards of ^{26}Al and ^{40}K along with the sample. Final calculations of ^{26}Al activity were done on the basis of this ratio relative to the ratio found in the case of meteorite Bansur whose ^{26}Al was determined by $\gamma-\gamma$ spectrometry. The K-content of the sample was determined by atomic absorption spectrophotometry (Perkin-Elmer Model 305).

II.C.3. The Ge(Li) counting systems

The activation analysis of ^{53}Mn requires high resolution counting of 834.8 keV gamma of ^{54}Mn to discriminate from traces of several radioactive impurities carried through the post-irradiation chemistry. Solid state semiconductor detectors are ideally suited for this purpose. Three Ge(Li) detectors, located in Institute for Solid State Physics, Tokyo, were used in this work. One detector was supplied by Princeton Gamma-Tech (No.1292). It has a diameter of 49 mm and a length of 48 mm and a nominal active volume of 80 cm^3. It is encased in a stainless steel jacket and kept at liquid nitrogen temperature on a horizontal dip-stick cryostat. The other two detectors were supplied by Horiba Ltd., Kyoto, Japan.

All these detectors are housed in a room where temperature is controlled at $20^{\circ} \sim 22^{\circ}C$. The efficiency, background, resolution and other details of these 3 detectors are given in Table 4.

II.C.4. Measurement of nuclear tracks

All the samples of meteorites and lunar rocks studied in this work were analysed for nuclear tracks to estimate the pre-atmospheric depths and cosmic ray exposure ages. The detailed description of sampling, etching and counting in optical and electron microscopes have been described in several publications from this laboratory and summarised in Tamhane (1972), Bhandari et al. (1972) and Goswami (1977). In this work only the abundant minerals i.e. feldspar and pyroxene minerals were used for Lunar rocks and olivine and pyroxenes were used for meteorites. Standard procedures of mounting, etching and counting (Bhandari et al. 1975) were used and will not be described in more detail here.

Table 4

Description of Ge(Li) systems[a)]

Ge(Li) Detector	Energy range (keV)	Bias voltage (V)	Efficiency[b)]	Resolution[c)] (keV)	Background (cpm)	Shield
Princeton γ-Tech	834.8±2.5	3950	2.71	1.7	0.051	Pb 15 cm, OFHC 2 cm
Horiba-1	834.8±2.5	2400	2.16	2.7	0.061	Pb 10 cm
Horiba-2	834.8±2.5	2600	1.92	2.1	0.071	Pb 10 cm

a) These detectors are located at The Institute for Solid State Physics, Univ. of Tokyo, Tokyo, Japan.

b) The absolute efficiency was determined by a ^{54}Mn standard, made from standard supplied by Amersham; the diameter of the standard is 0.8 cm and kept at 0.1 cm from the surface of the Al can.

c) Resolution = FWHM (full width at half maximum).

Chapter III

Results

Radioactivities induced by solar and galactic cosmic rays in Lunar rocks and meteorites have been measured in the present work by a variety of techniques discussed in the previous chapter. Most of these activities are feeble and the signal strengths are only a few times higher than the backgrounds of the systems. The methods of analysis of signals and the calculation of activities for each isotope are described in this chapter. In addition, the results of measurements of track densities in samples from meteorites are also presented.

II.A. Analysis of $\beta-\gamma$ coincidence counting data in Lunar rocks

All samples of the Lunar rocks studied in this work for their ^{26}Al activities were counted at least 2-3 times in the $\beta-\gamma$ spectrometer interspersed with background runs. The counting data was pooled up and the analysis was done on the cumulative spectrum thus obtained. A typical coincidence spectrum obtained in the top face of rock 61016,287 is shown in Figure 5 alongwith the background. The ^{26}Al activity in the samples were ascertained from the 511 kev region in the measured spectrum, after making appropriate subtractions for other contributing nuclides like ^{22}Na and the daughter nuclides of U and Th. In the present case the contribution of ^{22}Na to the positron peak is estimated to be only 5 % of the total

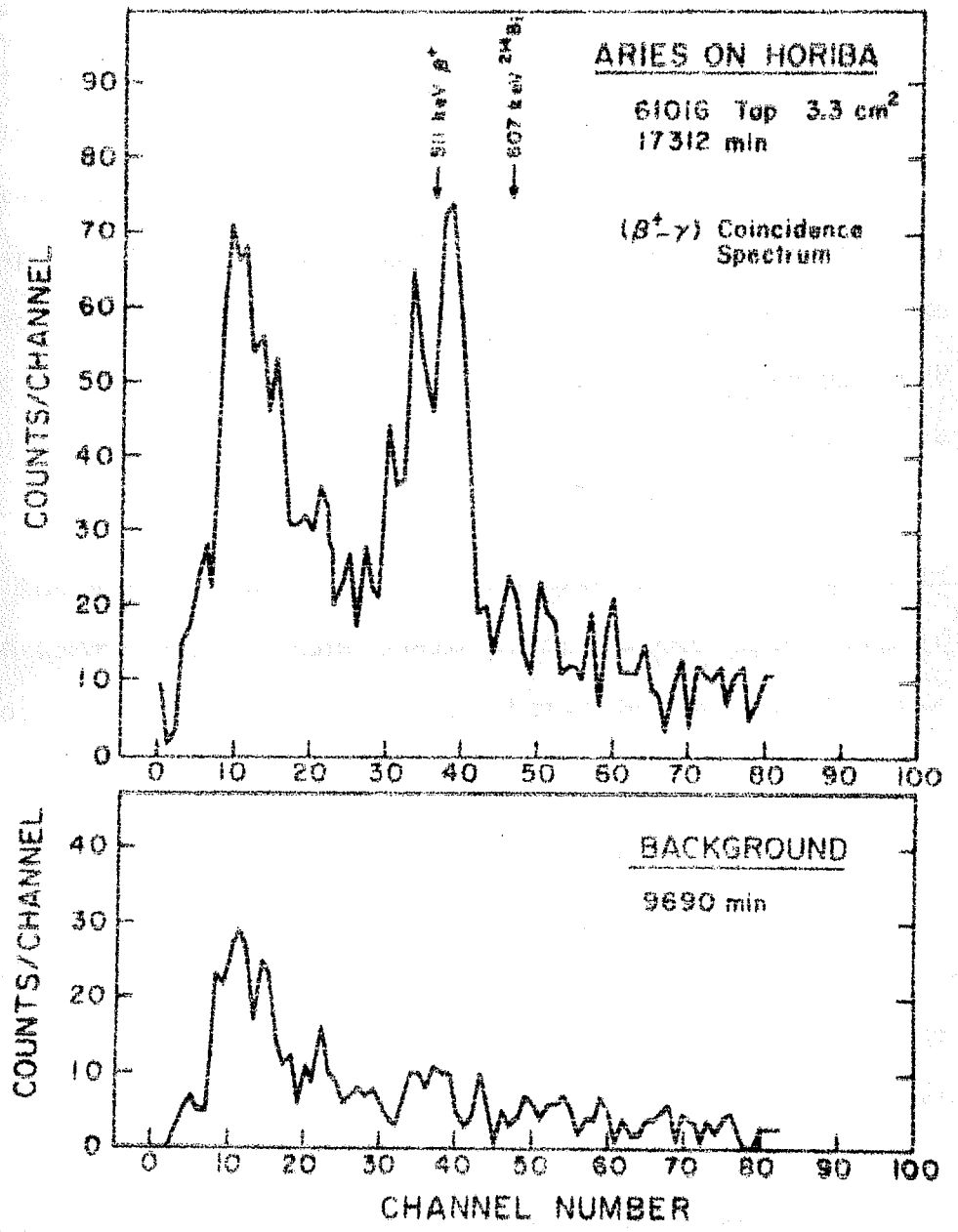

Figure 5. Beta-gamma coincidence spectra for the top surface of the rock 61016 and the background.

signal. The estimation is based on the following: (1) ^{22}Na production rate in all the chosen rocks is only about one-third that of ^{26}Al due to the low abundance of the target elements. (2) The samples were counted during the period April-September 1975 and the dates of collection of Apollo 16 and Apollo 17 rocks are April 22, 1972 and December 14, 1972 respectively. The decay of ^{22}Na in this interval range from 50 to 60 % (3) ^{22}Na has a low energy β^+ (E_{max} = 550 keV) which makes its contribution significant only from a layer of $\sim$ 30 mg.cm^{-2} thick compared to $\sim$ 100 mg.cm^{-2} layer for ^{26}Al.

The exact amount of contribution from ^{22}Na is difficult to estimate, but on the basis of the above three considerations we adopt a value of 5 % of the total signal for its contribution.

A more significant interference in deducing ^{26}Al activity is caused by the U, Th decay series nuclides. The estimation of this interference was done by a first order iteration process. The representative energy range for the positron was taken in 9 channels (511 $\pm$ 50) keV and for the Th, U series nuclides ^{208}Tl and ^{214}Bi in 5 channels (610 $\pm$ 25) keV. The (610 $\pm$ 25) region is separated by 24 keV from 511 keV tail and one can use the high energy side of the peaks of 583 keV (^{208}Tl) and 609 keV (^{214}Bi) which are the decay products of ^{232}Th and ^{238}U respectively. The iteration process was based on the ratios of count rates obtained for the standards of ^{26}Al,

terrestrial granite and basalt given below:

$$\frac{\text{Net counts in } (610 \pm 25) \text{ keV}}{\text{Net counts in } (511 \pm 50) \text{ keV}} = 0.07 \quad \text{for } {}^{26}\text{Al std.}$$

$$\frac{\text{Net counts in } (511 \pm 50) \text{ keV}}{\text{Net counts in } (610 \pm 25) \text{ keV}} = 1.37 \quad \text{for terrestrial granite}$$

$$\frac{\text{Net counts in } (511 \pm 50) \text{ keV}}{\text{Net counts in } (610 \pm 25) \text{ keV}} = 1.41 \quad \text{for terrestrial basalt}$$

The U/Th activity ratio in the granite and basalt is 1:3 and equal to that in the Lunar rocks studied here (Table 1). So the final net count rate in (511 ± 50) keV per 1000 min, denoted by FNCR, is given by 1st order iteration,

FNCR=(Net count rate in 511) - 1.37 (Net count rate in 610-0.07 (Net count rate in 511))

Since the signal is proportional to counted area of the rock face, a parameter CPTA, counts per 1000 mins per 1 cm^2 area is defined

$$\text{CPTA} = \frac{\text{FNCR}}{\text{area}}$$

The positron activity A_o of a thick sample, when the observed activity is A, is given by,

$$A = A_o \int_o^\infty e^{-\mu t}\, dt = \frac{A_o}{\mu}$$

So

$$A_o = A\,\mu$$

$$= \left(\frac{\text{CPTA} \times 10^3}{\eta}\right) \mu$$

where A_o = activity in dpm/kg

CPTA = net count rate in 511 keV after correcting for U, Th interferences

η = positron counting efficiency

$\mu = \frac{0.693}{t_{1/2}}$ and $t_{1/2}$ = half-thickness of positrons in rock in $mg.cm^{-2}$

Half-thickness, $t_{1/2}$

Since the half-thickness value of β^+ particles from ^{26}Al atoms in the rock determines the effective mass contributing to the signal, it was very important to know this value accurately in the present geometry. Half-thickness, $t_{1/2}$ of β in Al metal are related to the upper energy limit of the beta spectrum E_{max} (MeV) approximately by (Libby, 1956),

$$t_{1/2}\ (mg/cm^2) = 38(E_{max})^{3/2}$$

Libby also noted that for most highly forbidden spectra like ^{40}K and ^{36}Cl the formula underestimates the $t_{1/2}$ by about 10 -20%. ^{26}Al has a unique second forbidden spectra (I = 3, No) emitting β^+. To determine $t_{1/2}$ accurately we performed an external absorption experiment by placing Al-foils of varying thicknesses on the standard of ^{26}Al. We also performed self-absorption experiment by using varying thicknesses of powder standard. In Figure 6 the count rate obtained in the $\beta-\gamma$ mode is plotted against thicknesses of absorbers. The data points fall on a straight line indicating that the absorption is exponential in nature. It also gives a best fit value

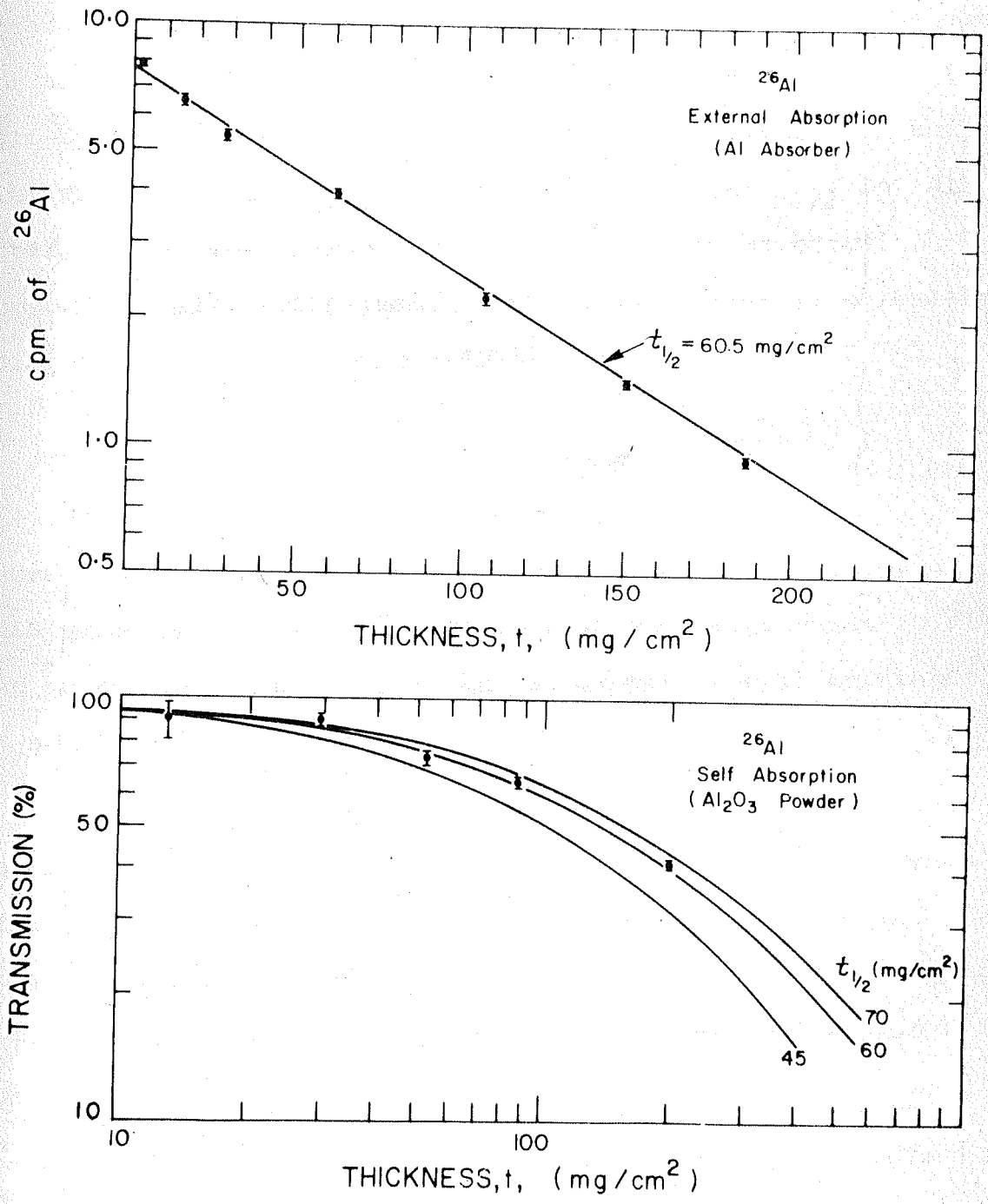

Figure 6. Determination of half-thickness of positrons from ^{26}Al decay by external and self-absorption methods.

for $t_{1/2}$ to be 60.5 mg.cm^{-2}. This contrasts with 48 mg.cm^{-2} obtained by using Libby formula and E_{max} = 1.17 MeV. The data for self-absorption in Al_2O_3 plotted in Figure 6 also fit a half-thickness value of 60 mg.cm^{-2}. For calculation of activity of ^{26}Al we take a value of 60.5 mg.cm^{2} for $t_{1/2}$ in Al metal. The half-thickness value in a rock of anorthositic composition like 61016 (mean atomic weight = 21) is calculated using the relation of Lerch (1953),

$$t_{1/2} \propto \frac{1}{1 + M/100}$$

where M is the mean atomic weight of the absorbing material. This value is 63.5 mg.cm^{-2} and is used for calculation in all the rocks since small variations in composition in anorthosites is not found to be important.

The Table 5 gives the details of the sample depths (available faces), counting data along with data for terrestrial granite and basalt and the ^{26}Al activity in dpm/kg. The activity of ^{26}Al in the bulk samples, reported by other investigators, are also shown. The counting efficiency was 10.4 % in the 1st set and 11.6 % for the 2nd set.

There are some differences between the data presented here and our earlier published data in Bhandari et al. (1976b). In most of the cases the difference is due to improved counting statistics and is well within the quoted uncertainties, except for two samples of 61016,287 from depth (1.1-1.2) and (1.5-1.6) g.cm^{-2}. In these two cases, we counted the faces in two other

Table 5

^{26}Al counting data of Lunar rocks

Rock	Depth[a] ($g.cm^{-2}$)	Surface area (cm^2)	Net counts/1000 min (511 keV)[b]	(610 keV)[b]	FNCR[c]	CPTA[c]	^{26}Al (dpm/kg)
60335,103	0-0.1	1.7	8.72	4.52	3.72	2.19	240 ± 115
	0.6-2.0	1.9	10.47	6.78	2.33	1.23	135 ± 110
	Bulk	-	-	-	-	-	140 ± 8[e]
61016,287[d]	0-0.1	3.3	22.04	3.04	20.0	6.10	740 ± 54
	1.1-1.2	5.0	8.80	0.68	8.72	1.74	210 ± 45
	1.5-1.6	7.0	9.73	1.00	9.30	1.33	160 ± 25
	2.7-5.4	6.7	10.75	1.02	10.38	1.55	190 ± 34
61016,300	7.5-9.0	3.1	11.24	5.65	4.58	1.48	160 ± 75
	Bulk	-	-	-	-	-	105 ± 5[f]
							65 ± 5[g]
64435,95	0-0.1	3.2	10.50	2.11	8.76	2.74	300 ± 50
66095,146	0-0.1	2.1	16.82	6.50	9.77	4.65	505 ± 100
	0-4	2.4	13.91	7.26	5.49	2.29	250 ± 200
	Bulk	-	-	-	-	-	107 ± 4[h]
79215,78	0-0.1	2.1	14.63	2.02	13.47	6.51	710 ± 100
	1.5-1.6	1.9	7.57	0.58	7.57	3.96	430 ± 100
Granite	-	5.0	104.8	76.5	-	-	-
Basalt	-	5.0	15.7	11.2	-	-	-
^{26}Al standard	-	5.0	6522	426	-	-	-
Background	-	12.0	7.6±.5	2.8±.3	-	-	-

a) Depth from the exposed surface of the moon.
b) Energy range: (511 ± 50) and (610 ± 25) keV. Counts in 610 keV region represent contribution from U,Th daughters and their interference to the positron region is based on data of granite, Basalt and ^{26}Al standard, as discussed in the text.
c) FNCR = Final net count rate per 1000 min in (511 ± 50) keV after U,Th correction. CPTA=FNCR/area.
d) 61016,287 data are from 1st set for which counting efficiency for β^+ was 12.7%. Rest are from 2nd set when counting efficiency for β^+ was 14.2%.
e) Apollo 16 preliminary Science Report NASA SP-315 (1972).
f) Wrigley (1973). (g) Eldridge et al., (1973). (h) Rancitelli et al., (1973).

systems. In the third system much larger CPTA values were observed. The published data in Bhandari et al. (1976b) were weighted average of these three sets of values. In the present table we have rejected the high CPTA values encountered in the third system because the background of the system was not stable and the previously adopted value may not be reliable.

Error analysis

The count rates in all the cases are small due to the smallness of the surface area counted. This fact is responsible for the large associated errors. The background was fairly steady for the duration of the counting period and the error in the background is taken to be 1 σ statistics from the total counts accumulated (in 511 $\pm$ 50 kev : 7.6 $\pm$ .5 CPT, in 610 $\pm$ 25 kev : 2.8 $\pm$ .3 CPT; CPT denotes counts per 1000 mins). The error is square root of the quadratic sum of errors in sample and background counts in (511 $\pm$ 50) kev.

III.B. Results of gamma counting in meteorites

Different faces of 4 Indian meteorites were counted in a gamma system to look for a possible depth variation of ^{26}Al activity. The results are given in Table 6 for Bansur, Parsa and Udaipur. The data for the fresh fall, Dhajala, will be presented in section III.B.1.

For old meteorites in which ^{22}Na has decayed, the positron signal is entirely due to cosmogenic ^{26}Al and the 1460 keV signal is due to ^{40}K inherently present. The ratio of these two signals can be used to calculate the ^{26}Al activity if the

bulk K content of the meteorite and $^{26}Al/^{40}K$ activity ratio in a suitable meteorite standard are known. The meteorite Bruderheim was used for this purpose. The ratio 1.67 found in Bruderheim was taken to represent ^{26}Al value of 60 dpm/kg found by Honda et al. (1961). Table 6 lists the faces counted and the net signal ratio of 511 keV to 1460 keV. The K content measured by AAS is also given in Table 6. With these data the ^{26}Al activities in the faces are calculated (Table 6).

The validity of the normalisation was checked by studying a piece of Bansur by $\gamma - \gamma$ spectrometry, (Bhandari et al., 1979) which gave values consistent with that found in this work.

The errors quoted are due to 1 σ counting statistics. The errors due to K content and original normalisation data (10 %) of Bruderheim have not been included. These data are representative of relative variation of ^{26}Al activity with respect to the Bruderheim value of 60 dpm/kg.

III.C. Radionuclides in Dhajala

In this section, initially the results of non-destructive gamma counting of six fragments of Dhajala are presented. The results of destructive analysis in three fragments will be presented subsequently.

III.C.1. Results of gamma counting

In the gamma spectrum clear signals were obtained at 511, 835, 1460 and 1810 keV due to positron emitters (^{22}Na and ^{26}Al), ^{54}Mn, ^{40}K and ^{26}Al respectively. The method of calculating gamma activities of ^{26}Al, ^{22}Na and ^{54}Mn from the gamma

Table 6

^{26}Al activities and the shielding depths in chondrites

Meteorite	Sample face	Track density[a] ($10^5/cm^2$)	Exposure[a] age (m.y.)	Pre-atmospheric[a] radius (cm)	Shielding[b] depth (cm)	K content (ppm)	Net signal ratio $^{26}Al/^{40}K$	^{26}Al (dpm/kg)
Bansur	2	27 (O)	10	15	1.9	870	1.24	48 ± 6
	4	50 (P)			3.5		1.39	54 ± 8
	1	27 (P)			4.5		1.23	48 ± 6
	10	1.1 (P)			7.5		1.30	51 ± 2
Parsa	whole	10-25 (P)	17	14	9.5	850	1.77	68 ± 7
Bruderheim	"	40 (P)	24	38	12	800	1.67	60[c]
Udaipur	Apex	47 (O)	22	9	2.5	730	1.57	52 ± 9
	Base	20 (O)			5.0		1.23	41 ± 8

a) Symbols O and P refer to track data in olivines and pyroxenes respectively. Track data, exposure ages and pre-atmospheric radius values taken from Bhandari et al. (1978), Gopalan and Rao (1976) and this work.

b) Shielding depth calculated from track densities by the method of Bhattacharya et al. (1973).

c) Normalisation value: 60±6 dpm/kg (Honda et al., 1961).

ray spectrum is outlined here. The 1460 keV signal due to ^{40}K was used as a relative internal standard for estimating the effective mass contributing to the signals. The Compton contribution of 1810 keV to 1460 keV was estimated by using a ^{26}Al standard. After this correction, the ratio of 1810 keV signal (^{26}S) to the 1460 keV signal (^{40}S) is calculated for each fragment of Dhajala. The ratio in Bansur was used as the meteorite standard. The average ^{26}Al activity of Bansur has been found to be 50 $\pm$ 5 dpm/kg from Table 6 and also by γ- γ measurements. The K contents of Bansur and Dhajala are measured to be 870 ppm and 840 ppm respectively. The ^{26}Al activity of the Dhajala samples is then calculated by,

$$^{26}Al \text{ activity} = \frac{(^{26}S/^{40}S)_S}{(^{26}S/^{40}S)_B} \cdot \frac{(840)}{(870)} \cdot 50 \text{ dpm/kg}$$

where the subscripts 'S' and 'B' denote ratios in sample and Bansur respectively. The activity of ^{22}Na was calculated from the total 511 keV signal using Compton corrected signals and subtracting the ^{26}Al contribution. The ^{54}Mn activity was determined from the 835 keV signal using the same procedure. The average of the ratios of the 835 keV signal to the 1460 keV signal was taken to correspond to 144 dpm/kg, the value measured in T-11 by destructive analysis.

The Table 7 gives the results of these calculations along-with the weight of the fragments, their distances along the fall-out track, the track density values in the fragments and

Table 7

^{26}Al, ^{54}Mn, ^{22}Na activities in fragments of the Dhajala chondrite

Sample	Weight (kg)	Distance along the fallout track* (km)	Track density** (cm^{-2})	Shielding depth (cm)	Activity (dpm/kg)*** ^{26}Al	^{54}Mn	^{22}Na
T-67	1.5	8	2.3×10^3	23	52 ± 5	123 ± 8	96 ± 10
G-1	2.39	17	6.7×10^3	18	62 ± 6	-	-
T-78	1.63	15	1.4×10^4	13	48 ± 5	-	-
T-16	2.02	14	3×10^4	12	55 ± 5	152 ± 10	120 ± 10
T-17	2.05	9	3×10^4	12	45 ± 5	-	-
T-92	6.5	17	3×10^4	12	53 ± 5	150 ± 10	126 ± 12
Average					53	144	111

* Bhandari et al. (1976a), Lal and Trivedi (1977).

** From Bagolia et al. (1977).

*** Errors are 1σ counting statistics.

the deduced shielding depths (by taking exposure age of Dhajala as 6.2 m.y. Gopalan et al., 1977).

III.C.2. Results of radiochemical analysis in Dhajala

In 3 fragments of Dhajala, T-11, T-68 and T-67 eleven radioisotopes (^{7}Be, ^{10}Be, ^{26}Al, ^{32}P, ^{33}P, ^{51}Cr, ^{52}Mn, ^{53}Mn, ^{54}Mn, ^{57}Co and ^{60}Co) were measured after their radio-chemical separation. Table 8 lists the details of the chemical and counting data of these samples. Carriers of Be, P and Co were added during dissolution and the amount expected is the sum of the added carrier plus the naturally occurring amount.

The elemental abundances in Dhajala were measured in PRL in two samples taken from T-11 (Sarin, priv. comm. 1976) and also by Noonan et al. (1976). These are given in column 2. (Note the changes in Co and Cr concentration from the values adopted in Bhandari et al. (1978). Co was taken as 0.04%. The bulk value obtained in PRL is 0.08 % and has been remeasured and checked to be correct. The Cr concentration found in P.R.L. was 0.215 % whereas Noonan et al. (1976) reported a value of 0.383 % which is in agreement with the average value 0.34 $\pm$ .05% (Mason 1971) found in H3 chondrites. The HF digestion method adopted in PRL measurement is now considered to be the reason for the discrepantly low value and Noonan et al's value is adopted now to be true. Column 3 lists the chemical form of the salt in which the elements were counted.

^{26}Al, ^{52}Mn and ^{60}Co were counted in the β-γ system described earlier. The ^{52}Mn has a short half-life of 5.6 days

Table 8

Chemical and counting details of samples of the Dhajala chondrite

Radio-nuclide	Elemental abundance (%)	Chemical form	Amount expected (g)	Amount counted (g)	Detection mode	Counting efficiency (ideal)	Back-ground (cpm)	Net signal (cpm)	Activity at the time of fall+ (dpm/kg)
Sample T-11 (320 g)									
^{7}Be*	-	BeO	0.111	0.026	γ	0.094	0.015	0.046	132 ± 12
^{10}Be	-	BeO	0.111	0.026	β^-	0.27	0.138	0.30	16.0 ± 1.5
^{10}Be**	-	BeO	0.111	0.050	β^-	0.24	0.033	0.07	17.3 ± 4.3
^{26}Al	1.15	Al_2O_3	6.954	0.148	$\beta^+-\gamma$	0.075	0.0086	0.017	45 ± 9
^{32}P***	0.126	$Mg_2P_2O_7$	1.449	0.414	β^-	0.36	0.1	0.51	22 ± 1.7
^{33}P***	0.126	$Mg_2P_2O_7$	1.449	0.414	β^-	0.15	-	0.04	7.2 ± 2.4
^{51}Cr*	0.383	Cr_2O_3	1.791	0.392	γ	0.122	0.026	0.062	91 ± 25
^{52}Mn	0.248	MnO_2	1.256	0.456	$\beta^+-\gamma$	0.085	0.010	0.012	28 ± 4
^{53}Mn	0.248	MnO_2	1.256	0.295	X-ray	0.027	0.24	0.24	76 ± 9
^{54}Mn	0.248	MnO_2	1.256	0.321	γ	0.148	2.27	2.61	144 ± 8
^{57}Co	0.08	Co_2O_3	0.501	0.187	X-ray	0.033	0.2	0.04	42 ± 10
^{60}Co	0.08	Co_2O_3	0.501	0.194	$\beta^-\gamma$	0.024	0.0027	0.013	15 ± 2
Sample T-68 (29.7 g)									
^{10}Be	-	BeO	0.111	0.025	β^-	0.24	0.036	0.040	18 ± 2
^{26}Al	1.15	Al_2O_3	0.646	0.266	$\beta^+-\gamma$	0.075	0.0086	0.038	61 ± 7
Sample T-67 (13 g)									
^{26}Al	1.15	Al_2O_3	0.246	0.088	$\beta^+-\gamma$	0.075	0.0086	0.016	56 ± 12

* These samples were measured by Dr. C.P. Kohl.
** Duplicate sample.
*** ^{32}P and ^{33}P were calculated by Biller's plot.
+ The time of fall: Jan 28, 1976.

and its decay was followed by counting over a long period till the gross signal became nearly equal to the background. Figure 7 shows the plot of gross counts (in β-γ mode) against the decay factor ($e^{-\lambda t}$). The net activity ^{52}Mn activity was derived from the best fit line to these data points.

^{10}Be, ^{32}P and ^{33}P were counted in two low-background G-M counters. ^{32}P and ^{33}P activities were calculated from the net count rates obtained over an extended period and from the analysis of the data by the method of Biller's plot.

^{54}Mn was counted in a well-type NaI(Tl) scintillator for its 835 keV gamma activity.

Combined X-ray activity of ^{53}Mn and ^{54}Mn was obtained by X-ray counting of Mn-fraction and ^{53}Mn activity was determined by subtracting from it the activity of ^{54}Mn measured by gamma counting. ^{57}Co was counted by the same X-ray counter. The ^{7}Be and ^{51}Cr samples were counted in a well type Ge(Li) detector by Dr. C.P. Kohl in Prof. J.R. Arnold's laboratory at La Jolla.

The activity A (dpm/kg) for each nuclide in each sample was calculated according to the formula,

$$A = N/\varepsilon . f_{sa} . f_{ch} . f_{d} . f_{br} . w$$

where N = Net counting rate (counts per min)

ε = detector efficiency

f_{sa} = self absorption factor

f_{ch} = chemical efficiency factor

f_{d} = decay factor

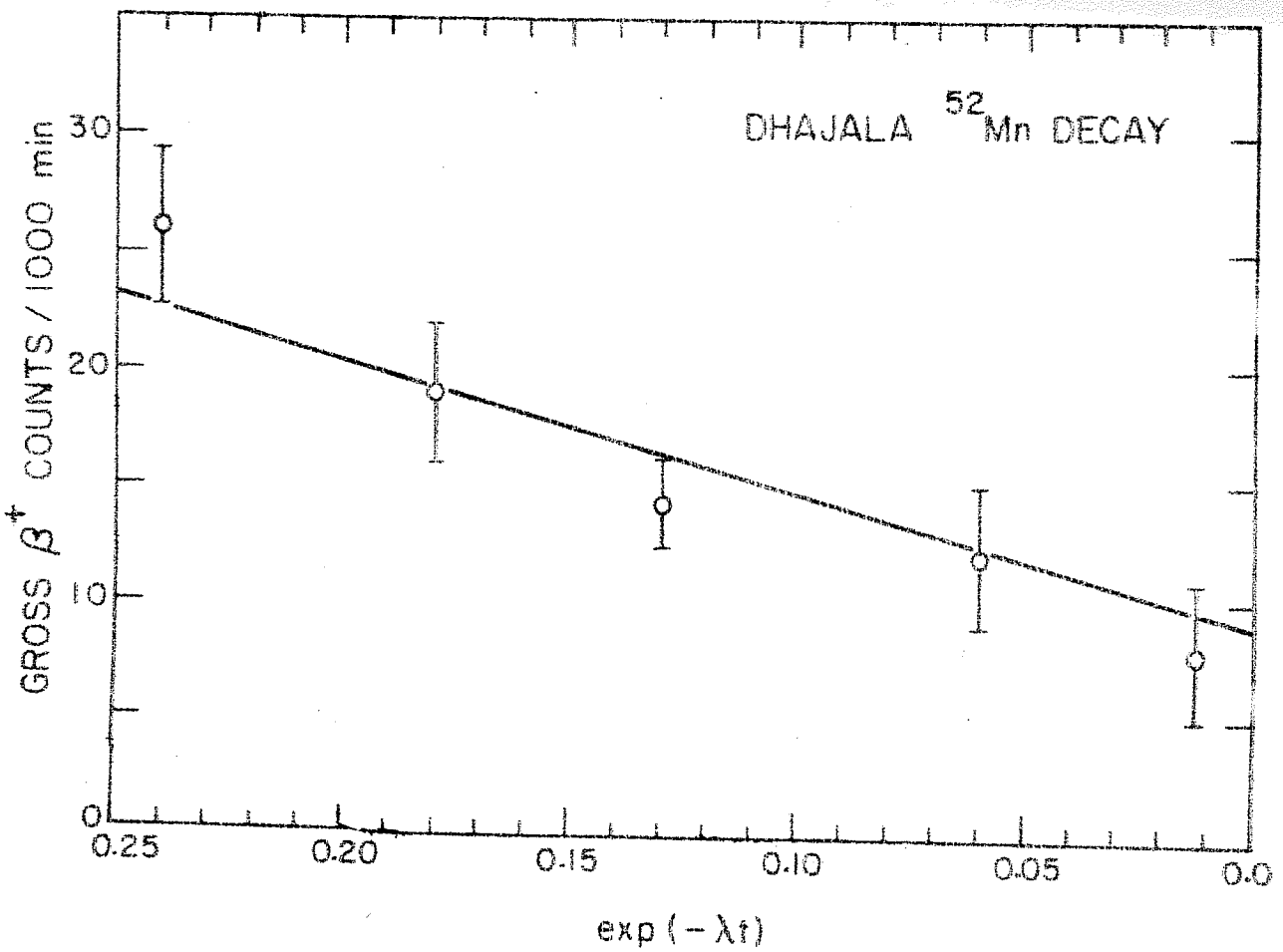

Figure 7. Gross positron signal from ^{52}Mn decay in the manganese fraction from the Dhajala chondrite versus the decay factor.

f_{br} = branching ratio

w = sample weight (kg)

The net counting rate (N) is obtained by subtracting the count rate of the blank or background from the count rate of the sample (gross count rate). The error in N is given by the square root of the sum of 1 σ errors of the gross signal and the background.

The efficiency of each detector system was determined by running appropriate standards. The counting efficiency (ε) is given by the ratio of the observed count rate to that expected. The self-absorption factor (f_{sa}) is required to correct for the attenuation of the radiation due to the finite thickness of the sample. For β emitters (^{10}Be, ^{26}Al, ^{32}P, ^{33}P, ^{52}Mn and ^{60}Co) f_{sa} is calculated by the formula for exponential absorption from a plain source,

$$f_{sa} = \frac{1 - e^{-\mu t}}{\mu t}$$

where $$\mu = \frac{0.693}{t_{1/2}}$$

$t_{1/2}$ = the half thickness in mg/cm^2

t = sample thickness in mg/cm^2

In most of the cases (^{10}Be, ^{26}Al, ^{32}P and ^{60}Co) the half-thickness values were determined experimentally by external absorbers. In other cases like ^{52}Mn, $t_{1/2}$ (in mg/cm^2) in Al-metal is found out by using the Libby formula (Libby, 1956).

$$t_{1/2}\ (Al) = 38\ (E_{max})^{1.5}$$

where E_{max} = the maximum energy of the β spectrum (in MeV) of the emitter.

The $t_{1/2}$ value in the compound actually counted is then determined by using the relation of Lerch (1953).

$$t_{1/2} \propto 1/(1 + 0.01\ M)$$

where M is the mean atomic weight of the compound. The values calculated were (by taking E_{max} values from Lederer et al., 1967)

^{10}Be in BeO	$t_{1/2} = 22.7$ mg/cm^2
^{26}Al in Al_2O_3	$t_{1/2} = 63.3$ mg/cm^2
^{32}P in $Mg_2P_2O_7$	$t_{1/2} = 88.9$ mg/cm^2
^{33}P in $Mg_2P_2O_7$	$t_{1/2} = 8.0$ mg/cm^2
^{52}Mn in MnO_2	$t_{1/2} = 16.3$ mg/cm^2
^{60}Co in Co_2O_3	$t_{1/2} = 6.2$ mg/cm^2

The X-ray self absorption of ^{53}Mn, ^{54}Mn and ^{57}Co in MnO_2 and Co_2O_3 respectively was calculated by using mass-absorption coefficients given by Compton and Allison (1968). The values are given below

^{57}Co (6.4 keV) in Co_2O_3	$t_{1/2} = 11.0$ mg/cm^2
^{54}Mn (5.4 keV) in MnO_2	$t_{1/2} = 9.2$ mg/cm^2

The branching ratios used were taken from Lederer et al. (1967) except for ^{26}Al which was taken from Samworth et al.

(1972) and were ^{7}Be (0.103), ^{10}Be (1.0), ^{26}Al (0.82), ^{32}P (1.0), ^{33}P (1.0), ^{51}Cr (0.09), ^{52}Mn (0.34), ^{53}Mn (1.0), ^{57}Co (1.0), ^{60}Co (1.0).

The efficiency of the X-ray counter was determined using a plated ^{55}Fe source. The fluorescence yields for ^{53}Mn and ^{54}Mn (decaying to ^{53}Cr and ^{54}Cr and giving Cr - X-rays)were taken 0.229 and for ^{57}Co (decaying to ^{57}Fe giving Fe - X-rays) was taken 0.293 for calculating the efficiencies for these isotopes (also from Lederer et al., 1967).

The calculated activities are presented in Table 8. In Table 9 a summary of the results obtained for various radio-isotopes is given alongwith the values obtained by other investigators on other fragments of Dhajala.

III.D. Neutron activation analysis of ^{53}Mn in meteorites

III.D.1. ^{53}Mn data from spot-samples

Of the 12 samples, 7 samples were taken from the separated metal phase and 5 samples from bulk of the meteorites. Fe, Ni and Mn contents of samples were determined by AAS and the data are presented in Table 10. The Table 10 also includes average Fe, Ni and Mn content of the core samples from 4 meteorites whose ^{53}Mn data will be presented in III.D.2.

The spot samples were processed in two batches of n-irradiation in two Japanese reactors JRR-2 and JRR-3. Tables 11 and 12 give details of these two irradiations and counting data. A brief explanation of the contents of the tables are given below.

Table 9

Cosmogenic radioactivities in fragments of the Dhajala chondrite (in dpm/kg)

Isotope	Half life	T-11	T-67	T-68	Other investigators*				
					A1	A2	B	C	D
^{53}Mn	3.7×10^6 yr	76±9	81±2+	–	–	–	69±7	–	
^{10}Be	1.6×10^6 yr	16±1.5	–	18±2	–	–	–	–	
^{26}Al	7.2×10^5 yr	45±9	52±5 56±12	61±7	44±1	48±1	52	46±4	48±6
^{60}Co	5.3 yr	15±2	–	–	13.5±.4	5.8±.3	–	14±2	82±8
^{22}Na	2.6 yr	–	96±10	–	109±2	100±2	–	94±8	126±9
^{54}Mn	312 day	144±8	123±8	–	156±6	140±5	–	140±15	201±15
^{57}Co	271 day	42±10	–	–	14.6±.6	16±1.1	–	–	38±6
^{7}Be	53.3 day	132±12	–	–	84±12	–	–		
^{51}Cr	27.7 day	91±25	–	–	95±14	–	–		
^{33}P	25.3 day	7.2±2.4	–	–	–	–	–		
^{32}P	14.2 day	22±1.7	–	–	–	–	–		
^{52}Mn	5.6 day	28±4	–	–	–	–	–		

* A1, A2: Dr. L. Rancitelli (Two samples, priv. comm.)
B: Dr. W. Herr (priv. comm.)
C: Dr. Gorin (priv. comm.)
D: Dr. G. Heusser (priv. comm.)
\+ by neutron activation.

Table 10

Abundances of Fe, Ni and Mn in the analysed meteorites

Meteorite	Class+	Phase*	Fe (%)	Ni (%)	Mn (ppm)
Bansur	L	B	22.3	1.30	2545
Barwise	H	M	79.9	7.9	105
Breitscheid	H	B	28.3	2.03	2335
Clovis(b)	L	B	21.5	1.10	2566
Dhajala	H3	M	87.6	9.8	24
Ladder Creek	L6	M	45.1	8.7	982
Madhipura	L	B	25.2	1.63	2416
Marjalahti	Pall	M	89.1	7.1	21
Odessa	Og	M	93.3	6.6	-
Plainview	H5	M	83.7	6.9	83
Ramsdorf	L	B	19.7	1.01	2682
Ranjitpura	SI	B	35.9	4.7	1989
St. Séverin	LL6	B	20.7	1.00	2718
Udaipur	H	B	28.2	1.69	2350
Wellman	H5	M	73.9	5.1	173

+ Pall = Pallasite, Og = Octahedrite, SI = Stony-iron.

* B = Bulk, M = Metal phase.

The neutron fluences were determined from Co-standards. The variation in n-fluence between the top and the bottom of the stack was less than 1 % for JRR-3 irradiation. For JRR-2 the extent of variation was not determined. ^{54}Mn activities induced in Mn-metal by (n, 2n) reaction and in Fe-metal by (n, p) reaction were estimated by irradiating two standards of each metal placed at the top and the bottom of the stack. The data for each metal are averaged and are given as ^{54}Mn cpm/mg Mn and ^{54}Mn cpm/mg Fe. These values are used to estimate the contribution to the ^{54}Mn signal in each sample from Fe contamination and stable Mn. Fe contamination in irradiated sample was determined by post-irradiation separation of Fe (by adding Fe-carrier) and counting the separated Fe in a NaI(Tl) scintillator for the 1099 and 1292 keV ^{59}Fe gamma-rays. Stable Mn in irradiated and counted samples were determined by AAS. The 9th column in the tables gives the ^{54}Mn count rate in each sample, after correcting for the (n, 2n) contribution from stable Mn, the (n, p) contribution from Fe contamination and applying small corrections due to decay and counting efficiency variations during the counting period. All samples were counted twice and the error in the 9th column is due to 1 σ counting statistics.

The conversion of ^{54}Mn cpm in each sample to ^{53}Mn dpm/kg Fe is done by the following method. Two standards of ^{53}Mn (made from Bogou iron meteorite and supplied by Dr. K. Nishiizumi) of known ^{53}Mn dpm/mg Mn were irradiated in each set. After irradiation, these were processed in the same way

Table 11

^{53}Mn activities in meteorites

Meteorite sample	Weight (mg)	Irradiation sample[b] Fe (mg)	Ni (mg)	Mn[c] (µg)	Counted sample Fe (µg)	Mn (µg)	^{54}Mn[e] signal (cpm)	^{54}Mn signal[f] 'corrected' (cpm)	^{53}Mn[g] (dpm/kg Fe)	^{53}Mn* [h] (dpm/kg Fe)
Dhajala	462.7	405.1	45.3	430.3	0.85	226.0	1.306±.031	1.178±.031	284±17	274±17
Plainview	264.6	219.4	18.1	240.9	1.23	166.1	1.218±.034	1.122±.034	380±23	370±23
Wellman	303.9	222.1	15.3	156.1	0.98	91.1	0.475±.021	0.421±.021	166±12	162±12
Barwise	309.0	244.4	24.1	250.6	5.53	168.5	0.934±.034	0.822±.034	256±17	248±17
Ladder Creek	676.8	302.2	58.0	868.2	1.33	503.5	0.582±.015	0.298±.016	87±7	82±7
Marjalahti-B	331.0	289.6	22.8	224.3	0.97	95.5	1.345±.036	1.289±.036	536±28	522±28
-C	325.8	285.1	22.0	224.3	1.56	95.3	1.307±.040	1.249±.040	528±28	515±28
^{53}Mn standard[a]	Solution (mg)								^{54}Mn cpm/^{53}Mn dpm	
^{53}Mn-1	328.3				0.44	275.9	4.114±.057	3.960±.057	19.50±.28	
^{53}Mn-2	312.4				1.44	260.0	4.110±.073	3.962±.073	19.51±.36	19.51±.22
Mn-metal	Mn (mg)								^{54}Mn cpm/mg Mn	
Mn-1	4.4				0.32	2970	1.719±.059	1.718±.059	0.578±.020	
Mn-2	8.4				0.23	4646	2.48 ±.052	2.480±.052	0.534±.011	0.556±.022
Fe-metal	Fe (mg)	Carrier Mn (µg)							^{54}Mn cpm/mg Fe	
Fe-1	5.7	200				182	16.00±.27	16.00±.27	3.08±.05	
Fe-2	3.7	200				184	11.92±.30	11.92±.30	3.50±.09	3.29±.29

Co-standard

	Co(μg)	^{60}Co(dpm)$^{d)}$	^{60}Co(dpm/μg)	Fluence (n/cm^2)
Co-A	0.0668	2.21×10^4	3.31×10^5	3.5×10^{18}

a) Tokyo Bogou-II standard: 0.781 dpm ^{53}Mn/mg Mn (±5 %) in solution of 1100 ppm Mn (courtesy of K. Nishiizumi)

b) Irradiation done in VT-4 position of JRR-2 reactor from 7 to 18 August, 1976 (1 cycle of 11 days).

c) Includes Mn carrier.

d) ^{60}Co activity refers to 18 August, 1976, the end of irradiation.

e) ^{54}Mn count-rates refer to 21 December, 1976, the beginning of counting in Horiba Ge(Li) system; Energy range = 834.8 ± 2.5 keV with counting efficiency = 2.16%.

f) 'Corrected' signal is obtained after (n, 2n) and (n,p) contributions are subtracted by using data of Mn and Fe-metals.

g) The uncertainty includes 1 σ counting statistics, 3 % for Fe concentration and 3% for Mn concentration (twice).

h) The contribution from Ni is based on ^{53}Mn dpm/kg Ni = $\frac{1}{3}$ x ^{53}Mn dpm/kg Fe (Nishiizumi, 1978). ^{53}Mn* denotes Ni-corrected value.

Table 12

^{53}Mn activities in meteorites

Meteorite sample	Weight (mg)	Irradiation sample[b] Fe (mg)	Ni (mg)	Mn[c] (µg)	Counted sample Fe (µg)	Mn (µg)	^{54}Mn[e] signal (cpm)	^{54}Mn signal 'corrected'[f] (cpm)	^{53}Mn[g] (dpm/kg Fe)	^{53}Mn*[h] (dpm/kg Fe)
Madhipura	429.1	106.7	7.5	1030.5	0.58	747	0.429±.018	0.383±.018	311±24	304±24
Odessa	360.7	207.8	17.3	185.6	0.82	95.6	0.378±.015	0.371±.015	218±16	212±16
Ranjitpura	268.3	83.7	12.9	182.9	1.44	77.7	0.234±.012	0.228±.012	402±31	382±31
Breitscheid	298.7	85.2	6.0	673.6	1.35	438.7	0.394±.019	0.366±.019	414±32	405±32
Ramsdorf	1010.7	196.6	10.1	2686	1.73	1702	0.763±.025	0.659±.025	332±23	326±23
Clovis (b)	617.8	130.9	6.7	1560	0.55	1055	0.660±.021	0.596±.021	423±29	416±29
Marjalahti-A	323.9	292.3	24.3	224.3	1.40	9.6	0.096±.006	0.094±.006	470±40	457±40
^{53}Mn standard[a]										
		Solution (mg)							^{54}Mn cpm/^{53}Mn dpm	
^{53}Mn-1		325.3			0.57	337.8	4.34±.07	4.32±.07	16.37±.27	15.93±.45
^{53}Mn-2		271.4			0.46	294.6	3.58±.05	3.56±.05	15.48±.23	
Mn-metal										
		Mn (mg)							^{54}Mn cpm/mg Mn	
Mn-1		7.330			0.04	6509	0.371±.019	0.371±.019	0.0570±.0029	0.0598±.0022
Mn-2		5.803			0.06	5222	0.327±.017	0.327±.017	0.0625±.0033	
Fe-metal										
	Fe (mg)	Carrier Mn (µg)							^{54}Mn cpm/mg Fe	
Fe-1	7.700	204.9			-	189.3	9.87±.17	9.87±.17	1.387±.024	1.38±.02
Fe-2	11.320	189.6			-	177.2	14.60±.24	14.60±.24	1.380±.023	

Co-standard	Co(μg)	^{60}Co (μc)[d]	^{60}Co (μc/μg)		Fluence (n/cm^2)
Co-1	0.1711	0.0201	0.1175	0.1171	2.75×10^{18}
Co-2	0.2314	0.0270	0.1167		

a) Tokyo Bogou-II standard: 0.781 dpm ^{53}Mn/mg Mn (± 5%) in solution of 1100 ppm Mn (courtesy K. Nishiizumi).

b) Irradiation done in VG-7-6 position of JRR-3 reactor from 6 to 17 June, 1977 (1 cycle of 11 days).

c) Includes also carrier of Mn, when added.

d) ^{60}Co activities refer to 17 June, 1977 at the end of irradiation.

e) All ^{54}Mn count-rates refer to 6 August, 1977, the beginning of counting in Princeton-gamma Tech Ge(Li) system; Energy range = 834.8 ± 1.7 keV and counting efficiency = 2.01%.

f) 'Corrected signal is obtained after (n,2n) and (n,p) contributions are subtracted by using data of Mn and Fe-metals.

g) The uncertainty includes 1 σ counting statistics, 3% for Fe concentration and 3% for Mn concentration (twice).

h) The contribution from Ni is subtracted based on ^{53}Mn dpm/kg Ni= $\frac{1}{3}$ x ^{53}Mn dpm/kg Fe (Nishiizumi, 1978). ^{53}Mn* denotes Ni-corrected value.

as the samples and ^{54}Mn activity in them determined. The average of these two standards determines the 'amplification factor' by (n, γ) reaction of ^{53}Mn. This is expressed as ^{54}Mn cpm/^{53}Mn dpm. From the 'corrected signal' of ^{54}Mn in a sample and the 'amplification factor' one gets the ^{53}Mn dpm in that sample. Since the Fe-content in the irradiation sample is known (by AAS) one can get the final value expressed as ^{53}Mn dpm/kg Fe. The uncertainty quoted in the 10th column is obtained by square root of the sum of squares of the percentage errors due to (i) 1 σ counting statistics, (ii) 3 % error in estimation of Fe, (iii) 3% error in determination of Mn in irradiation sample and another 3% in counted sample.

The final column in the tables gives the ^{53}Mn dpm/kg Fe in the sample if a small contribution from Ni in the sample is corrected for by using the relative value obtained by Nishiizumi, (1978) given below,

$$^{53}Mn \text{ dpm/kg Ni} = \frac{1}{2} \times {}^{53}Mn \text{ dpm/kg Fe}$$

III.D.2. ^{53}Mn data from core-samples

The locations, depth and other details of the samples from cores of Bansur, Madhipura, Udaipur and St. Severin meteorites are given in Table 13. The St. Severin samples were taken from core CB4 and AIII described in Lal et al. (1969), Amin et al. (1969) and Cantelaube et al. (1969). The 2nd column of Table 13 gives the sample code with reference to the Figures 1,2 and 3 and the 3rd column gives the

Table 13

Details of core-samples of four chondrites analysed for ^{53}Mn

Meteorite	Core-sample*	Code	Weight (gm)	Sample contents (total)** Fe (mg)	Ni (mg)	Mn (μg)	Fe/Mn
Bansur	13-1	A	0.9058	208.8	11.3	2258	92.47
	13-2	B	0.7095	158.4	9.16	1800	88.00
	13-3	C	1.0413	226.1	14.4	2554	88.53
	13-4	D	1.0379	222.0	11.6	2701	82.19
	14-3	E	0.9276	203.6	12.0	2448	83.17
	14-1	F	0.6765	157.6	10.1	1724	91.42
Madhipura	M-1	G	1.6025	371.1	22.1	3818	97.20
	M-2	H	0.5501	150.2	8.4	1322	113.62
	M-3	I	0.9175	234.5	14.3	2228	105.25
Udaipur	C-1	J	0.7889	216.8	13.0	1777	122.00
	C-2	K	0.6896	194.8	12.0	1636	119.07
	6-1	L	1.0547	298.3	17.1	2510	118.84
	# 4	M	0.7024	200.7	12.4	1684	119.18
St. Séverin	CB4 -1	N	0.9114	182.9	9.5	2506	72.98
	-2	O	0.9620	191.4	9.1	2617	73.14
	-10	P	0.9319	184.4	8.4	2505	73.61
	-25	Q	0.8644	179.7	6.1	2388	75.25
	-32	R	0.9713	190.5	8.6	2701	70.53
	A III-10	S	0.8932	179.1	8.1	2455	72.95
	-23a	T	0.7977	161.7	5.3	2173	74.41
	-25b,c	U	0.3327	84.2	6.4	854	98.59

* See Figures 1, 2 and 3 and Table 2 for sample locations and depth.

** The contents were determined from 2 independent aliquots and maximum deviations are: ± 1.8% for Fe, ± 2.1% for Ni and ± 1.9% for Mn. The assigned uncertainties are taken to be ± 2% for each.

irradiation code. The table also includes weight of each sample, depth along a specified direction (the direction along which track density decreases). Fe, Ni and Mn contents were determined from two independent aliquots. The mean values are given in Table 13. The maximum deviations from the mean were: ± 1.8% for Fe, ± 2.1% for Ni and ± 1.9% for Mn. We have assigned uncertainties of ± 2% for each of Fe, Ni and Mn contents.

The n-irradiation was done in VG-7-6 position of JRR-3 reactor. Two standards each of ^{53}Mn, Mn-metal and Fe-metal and 3 standards of Co were put in the stack in symmetrical fashion. The irradiation characteristics determined from these standards are given in Table 14. The thermal neutron fluence in position 1 was 6% higher than in position 2 as seen from Co-data and also ^{53}Mn standard data. The errors assigned in these numbers are 1σ counting statistics plus the propagated errors of Fe and Mn content. For ^{53}Mn standard the difference between the two determinations divided by 2 was taken as uncertainty on the average value of ^{54}Mn dpm/^{53}Mn dpm since that is larger than the statistical error.

Table 15 gives the ^{54}Mn activity found after post-irradiation chemistry in the samples. The Fe-contamination in the samples ranged from 0.6 to 7.4 µg (as determined by ^{59}Fe activity) and small corrections due to (n, p) reaction from Fe-contamination was applied using Fe-metal data from Table 14. The Mn-contents in the counted samples were determined by taking aliquots from the final counted samples. The con-

Table 14

Irradiation characteristics for irradiation of core samples in JRR-3 reactor

Description of standards			Counted Sample			Determined quantity++
			Fe (μg)	Mn (μg)	^{54}Mn activity+ (dpm)$_{t_o}$	
^{53}Mn standard**						^{54}Mn dpm/^{53}Mn dpm
S-1	-		0.4	503	327.8 ± 4.4	830 ± 10 } 813 ± 17
S-2	-		0.5	414	258.6 ± 3.8	796 ± 19 }
Mn-metal	Mn(mg)					^{54}Mn dpm/mg Mn
Mn-1	6.615		≤ 0.2	6520	19.60 ± 0.60	3.01 ± .11 } 3.07 ± .08
Mn-2	5.523		≤ 0.1	5480	17.11 ± 0.50	3.12 ± .11 }
Fe-metal	Fe(mg)	Carrier Mn(μg)				^{54}Mn dpm/mg/Fe
Fe-1	3.310	135.8		133.4	233.7 ± 4.3	71.87 ± 1.95 } 71.7 ± 1.4
Fe-2	2.865	134.3		131.1	199.9 ± 4.4	71.48 ± 2.12 }
Co-standard	Co(μg)	^{60}Co dpm*/μg Co				Fluence (n/cm^2)
Co-1	0.268	2.54 x 10^5				2.68 x 10^{18} } 2.61 x 10^{18}
Co-2	0.284	2.48 x 10^5				2.62 x 10^{18} }
Co-3	0.266	2-40 x 10^5				2.53 x 10^{18} }

** Tokyo Bogou-II standard: 0.781 dpm ^{53}Mn/mg Mn (± 5%)

* On 1st Jan. 1979; Irradiation period (4-15) Dec. 1978 - JRR-3, VG-7-6.

\+ t_o = Dec, 16; 1978

++ Error: 1σ counting statistics and 2% for Mn content in all calculations. In ^{53}Mn std. the difference between 2 values divided by 2 is used since that is larger error.

Table 15

^{53}Mn activities in core-samples from chondrites

Sample	Ratio Fe/Mn	Counted Sample: Fe (µg)	Counted Sample: Mn (µg)	Counted Sample: ^{54}Mn activity (dpm)$_{t_o}$	^{54}Mn activity+ corrected for (n,p) (dpm)$_{t_o}$	^{54}Mn activity per mg Mn corrected for (n,2n) & (n,p) (dpm)$_{t_o}$/mg Mn*	^{53}Mn activity** (dpm/kg Fe)
A	92.47	1.6	1723	52.21 ± 1.37	52.10 ± 1.37	27.17 ± 0.97	361 ± 19
B	88.00	1.6	1423	40.14 ± 0.87	40.03 ± .87	25.06 ± 0.80	351 ± 17
C	88.53	6.4	2042	56.61 ± 1.17	56.15 ± 1.17	24.43 ± 0.76	339 ± 17
D	82.19	7.4	2274	61.08 ± 1.43	60.55 ± 1.43	23.56 ± 0.79	352 ± 18
E	83.17	1.0	1966	53.63 ± 1.22	53.56 ± 1.22	24.18 ± 0.79	357 ± 18
F	91.42	1.6	1434	44.86 ± 1.06	44.75 ± 1.06	28.14 ± 0.93	378 ± 19
G	97.20	1.6	2509	61.59 ± 1.28	61.48 ± 1.28	21.43 ± 0.67	272 ± 13
H	113.62	0.6	1118	33.43 ± 1.09	33.39 ± 1.09	26.80 ± 1.12	290 ± 17
I	105.25	1.1	1933	51.51 ± 1.07	51.43 ± 1.07	23.54 ± 0.73	275 ± 14
J	122.00	0.9	1516	51.99 ± 1.08	51.93 ± 1.08	31.18 ± 0.95	314 ± 15
K	119.07	1.0	1306	41.47 ± 1.01	41.40 ± 1.01	28.63 ± 0.97	296 ± 15
L	118.84	2.7	2071	66.47 ± 1.46	66.28 ± 1.46	28.93 ± 0.92	300 ± 15
M	119.18	0.9	1227	41.51 ± .94	41.45 ± .94	30.71 ± 0.99	317 ± 16
N	72.98	2.3	2038	42.79 ± 1.04	42.63 ± 1.04	17.85 ± 0.63	300 ± 16
O	73.14	3.1	2180	47.52 ± 1.04	47.30 ± 1.04	18.63 ± 0.61	313 ± 16
P	73.61	2.9	2055	44.92 ± 1.22	44.71 ± 1.22	18.69 ± 0.71	312 ± 17
Q	75.25	3.8	2002	47.80 ± 1.16	47.53 ± 1.16	20.67 ± 0.72	338 ± 17
R	70.53	4.0	2222	51.72 ± 1.04	51.43 ± 1.04	20.08 ± 0.62	351 ± 17
S	72.95	7.0	1951	46.01 ± 1.04	45.51 ± 1.04	20.26 ± 0.68	342 ± 17
T	74.41	2.0	1489	40.83 ± 1.05	40.69 ± 1.05	24.26 ± 0.86	401 ± 21
U	98.59	1.1	700	26.30 ± 0.67	26.22 ± 0.67	34.39 ± 1.18	429 ± 22

+ t_o = Dec.16, 1978. Error: 1σ counting statistics.

* Error: 1σ counting statistics, 2% in Mn content and errors of standards.

** Error: 1σ counting statistics, 2% in Fe content, 2% in Mn content of sample 2% in Mn content of counted sample and propagated errors of standards.

tribution from the stable Mn by (n, 2n) reaction was subtracted by using Mn-metal data. After these two corrections one obtains the net ^{54}Mn activity per mg Mn in the 7th column. The 'amplification factor' expressed as ^{54}Mn dpm/^{53}Mn dpm obtained from Table 14 and the Fe/Mn ratio in each sample then give the ^{53}Mn dpm/kg Fe in the samples. The errors in the final numbers are calculated by taking square root of the sum of percentage errors due to (1) 1 σ counting statistics (2) 2 % uncertainty in Fe content (3) 2 % uncertainty in Mn-content (4) 2 % uncertainty in the Mn-content of counted samples and (5) the propagated errors of all the standards.

III.D.3. Track data in core samples

Samples from several locations of the cores and also from various faces of each meteorite were analysed for nuclear tracks to find out the pre-atmospheric size and shape of the meteorite. In addition, these data are used to find out the shielding depths of the samples in which ^{53}Mn activities were determined.

a. St. Severin

The cores of St. Severin used in this work are CB4 and AIII and a detailed description of these are given in Cantelaube et al. (1969).

Track data in these cores were taken from Lal et al. (1969) and Amin et al. (1969). The exposure age, as discussed in Marti et al. (1969) is 11.2 m.y. The recovered mass of the St. Severin is 271 kg. These three data viz. track densities,

exposure age and recovered mass are used to find out the pre-atmospheric size and shielding depths of the samples by the method of Bhattacharya et al. (1973). The pre-atmospheric shape of St. Severin has been shown to be similar to an ellipsoid of axial dimensions 40 cm x 45 cm x 75 cm(Cantelaube et al., (1969)). But the directions of cores CB4 and AIII are along the shorter axes and the best choice of equivalent spherical size for the present work is a sphere of radius 20 cm. The core AIII has been shown to be a near-radial core (Lal et al., 1969). The ablation for the high density face of this core is estimated to be 1.8 cm. The 'equivalent radial depths' (henceforth called 'effective depth') for three samples from this core were obtained by using 1.8 cm ablation of a sphere of 20 cm radius. The effective depths of 5 samples from non-radial core CB4 are discussed and given in Amin et al. (1969).

b. Bansur

Track density was measured in olivines taken from several locations of the core 13 and core 14. These data are given in Table 16. The depth is measured along ABC (Figure 1) with the highest density face taken as zero. These data are plotted in Figure 8 and the best fit line is shown by dotted curve II.

Samples from several faces of Bansur have been investigated by Bhandari et al. (1978). Taking the exposure age of Bansur to be 10 m.y. (Gopalan and Rao, 1976) Bhandari et al. (1978) estimate the pre-atmospheric size of Bansur equivalent to a sphere of effective radius 15 cm.

Table 16

Track density data for Bansur

Serial No.	Sample+	Depth (cm)	Track density in olivine (in $10^6/cm^2$)
1	B-2	~0.0	2.58 ± .10
2	13-1	0-0.2	3.17 ± .22
3	13-2	1-1.6	1.75 ± .11
4	13-3-2	2.7	1.68 ± .15
5	13-4	3.6-4.3	0.84 ± .13
6	B-15-3	4.3-4.5	0.97 ± .11
7	B-15-B	5.8	1.0 ± .10
8	14-3	8.4	0.54 ± .06
9	14-2-2	9.4	0.57 ± .06
10	14-2	9.9	0.46 ± .07
11	14-1	10.3-10.5	0.64 ± .06
12	B-12	10.5	0.73 ± .05

+ Sr. Nos.1 to 5 from core 13; Sr. Nos.8 to 12 from core 14
Depth from face #2 of core 13, along ABC (see Figure 1).

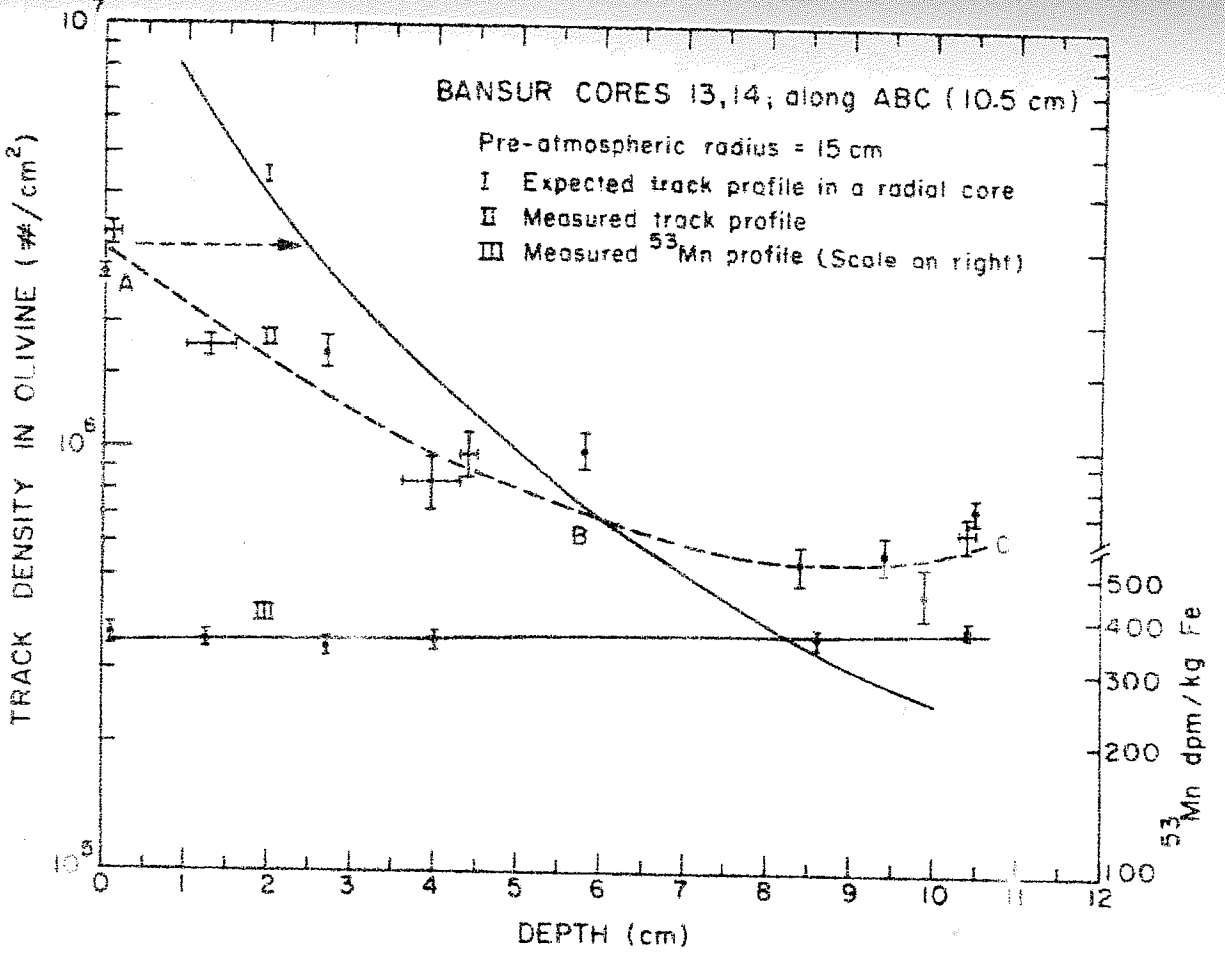

Figure 8. Expected track density profile in a radial direction (curve I), measured track densities (curve II) and ^{53}Mn activities (curve III) in the core-samples from Bansur (note that the scale for the ^{53}Mn activity is on the right).

The expected radial profile of track density in olivines for a spherical chondrite of 15 cm radius is also shown in Figure 8 by curve I. The track density in olivines is lower by a factor of 2 than in pyroxenes in case of Bansur. This factor has been obtained by measurement of tracks in olivines and pyroxenes from the same location. Using this scaling factor 2 and an exposure age of 10 m.y. the theoretical profile was obtained from Bhattacharya et al. (1973).

A comparison of the measured profile with that expected for a spherical chondrite of 15 cm radius shows that the pre-atmospheric shape of Bansur was not spherical. The effective depth for each sample of ^{53}Mn was obtained by taking the measured track density from curve II and reading off the depth corresponding to that density value from curve I, which corresponds to an effective radius of 15 cm.

c. Udaipur

Track densities were measured in pyroxenes taken from several locations of core 9 and also from various faces of Udaipur. The data are given in Table 17, where the depth is measured along EF direction shown in Figure 3. These data are also plotted in Figure 9 as a function of depth, and the best fit line is shown as curve II.

A detailed analysis of track data from various faces along with the adopted exposure age of 22.0 m.y. (Gopalan and Rao, 1976) show that Udaipur can be approximated by an equivalent sphere of radius 9 cm. The expected track profile

Table 17

Track density data for Udaipur

Serial No.	Sample+	Depth (cm)	Track density in pyroxene (in $10^6/cm^2$)	TPM* ($10^5/cm^2$ .m.y.)
1	Udp-4	0.1	11.0 ± .4	5.0 ± .2
2	Udp-3	0.7	10.2 ± .4	4.6 ± .2
3	Udp-2	2.2	8.0 ± .3	3.6 ± .2
4	Udp-1-3	2.9	7.3 ± .3	3.3 ± .2
5	Udp-1-2	3.6	6.7 ± 1.0	3.0 ± .5
6	Udp-1	4.8	5.7 ± .6	2.6 ± .3
7	Udp-0	5.6	4.5 ± .2	2.0 ± .1
8	U-8	6.1	4.6 ± .4	2.1 ± .2
9	U-4	-	3.7 ± .3	1.7 ± .2
10	U-5	-	5.0 ± .5	2.3 ± .2
11	U-7	-	3.0 ± .3	1.4 ± .1

+ Sr. Nos. 1 to 8 from core 9, (6-c); Sr. Nos. 9, 10, 11 from orthogonal direction on face containing U-8. Depth from face # 6 (see Figure 3) along EF.

* TPM = track density in pyroxene per m.y. taking exposure age = 22.0 m.y. (Gopalan and Rao, 1976).

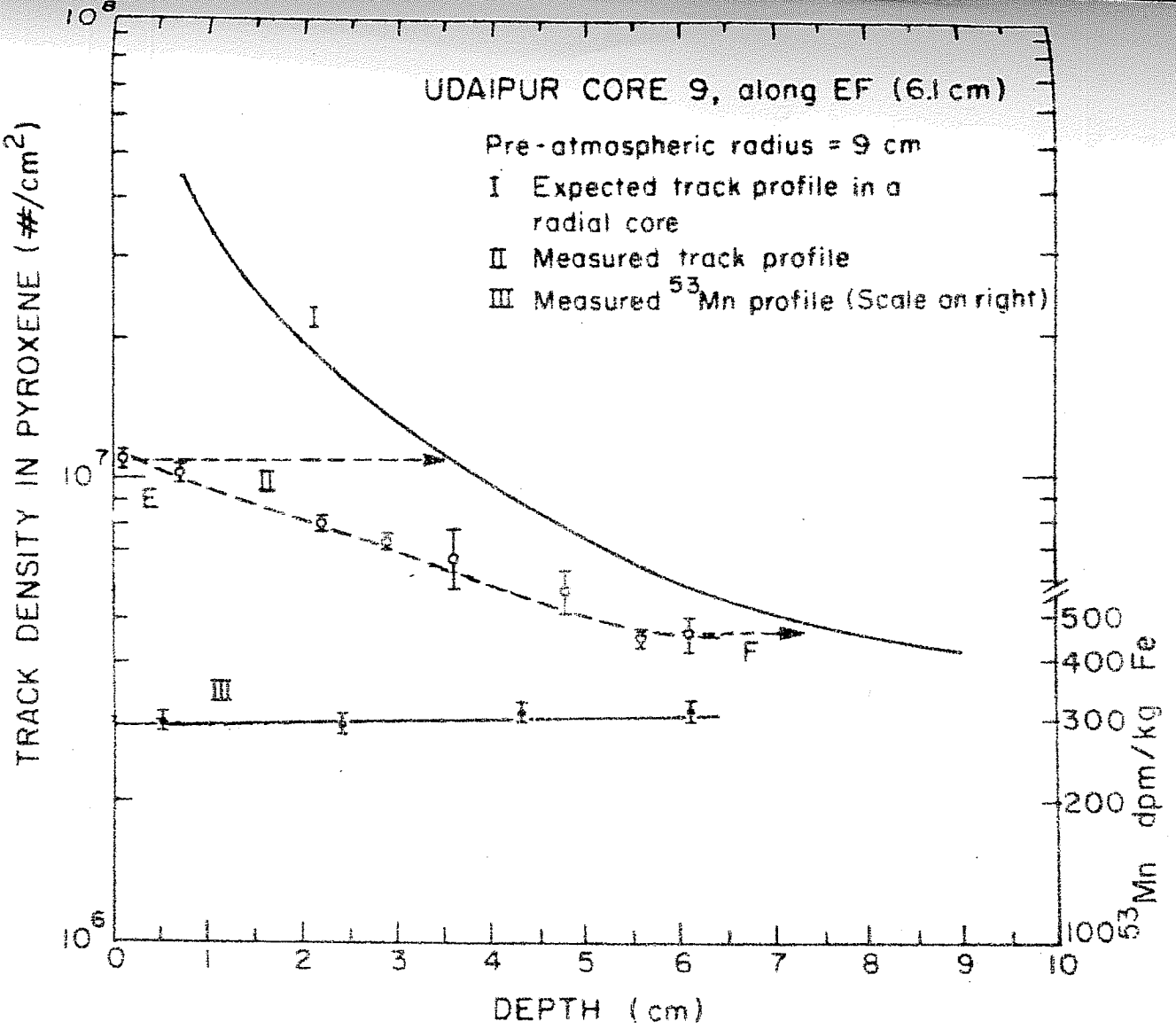

Figure 9. Expected track density profile in a radial direction (curve I), measured track densities (curve II) and ^{53}Mn activities (curve III) in the core-samples from Udaipur (note that the scale for the ^{53}Mn activity is on the right).

in pyroxenes for a body of 9 cm radius and 22.0 m.y. exposure age is shown as curve I. (from Bhattacharya et al., 1973).

A comparison of curve I with curve II shows that the core 9 is a near radial one. The effective depth for each sample of ^{53}Mn is obtained by the same method as outlined in case of Bansur.

d. Madhipura

Track densities were measured in olivines from samples taken from the core-M and in pyroxenes from surface samples. These data are presented in Table 18. The depth is measured along XYZ direction shown in Figure 2. The core data are also plotted in Figure 10 as a function of depth and the best fit line is shown as curve II.

The exposure age of Madhipura has been recently determined in P.R.L. and the value is 15 m.y. (Rao and Venkatesan, priv. comm.). An analysis of surface track densities with 15 m.y. age shows that the core-M is a near radial one. The similar values of densities found on all faces also support this fact. The analysis also shows that Madhipura can be approximated by an equivalent sphere of 6.5 cm radius, and the ablation near zero depth of core-M is about 3.0 cm. The effective depths of the samples for ^{53}Mn were obtained by adding 3.0 cm to the physical depths in the core.

Table 18

Track density data for Madhipura

Serial No.+	Sample+	Depth (cm)	Track density ($10^6/cm^2$) in Olivine*	Pyroxene
1	M-1-1	0.0	4.93 ± .24	-
2	M-1-2	1.0	4.00 ± .20	-
3	M-2-1	2.2	3.04 ± .25	-
4	M-2-2	2.8	2.24 ± .12	-
5	M-3-1	4.0	1.81 ± .11	-
6	M-3-2	4.7	2.44 ± .28	-
7	1	0.0	5.0 ± .3	9.0 ± .5
8	2	-	-	6.5 ± .4
9	3	-	-	14.8 ± .9
10	4	7.6	-	7.0 ± .4

+ Sr. Nos. 1 to 6 from core M; depth measured along XYZ. Sr. Nos. 7, 8, 9, 10 are spot samples as shown in Figure 2, taken from Bhandari et al. (1978).

* Track density ratio: $\rho(Pyx)/\rho(Ol) = 1.8$ from sample 1.

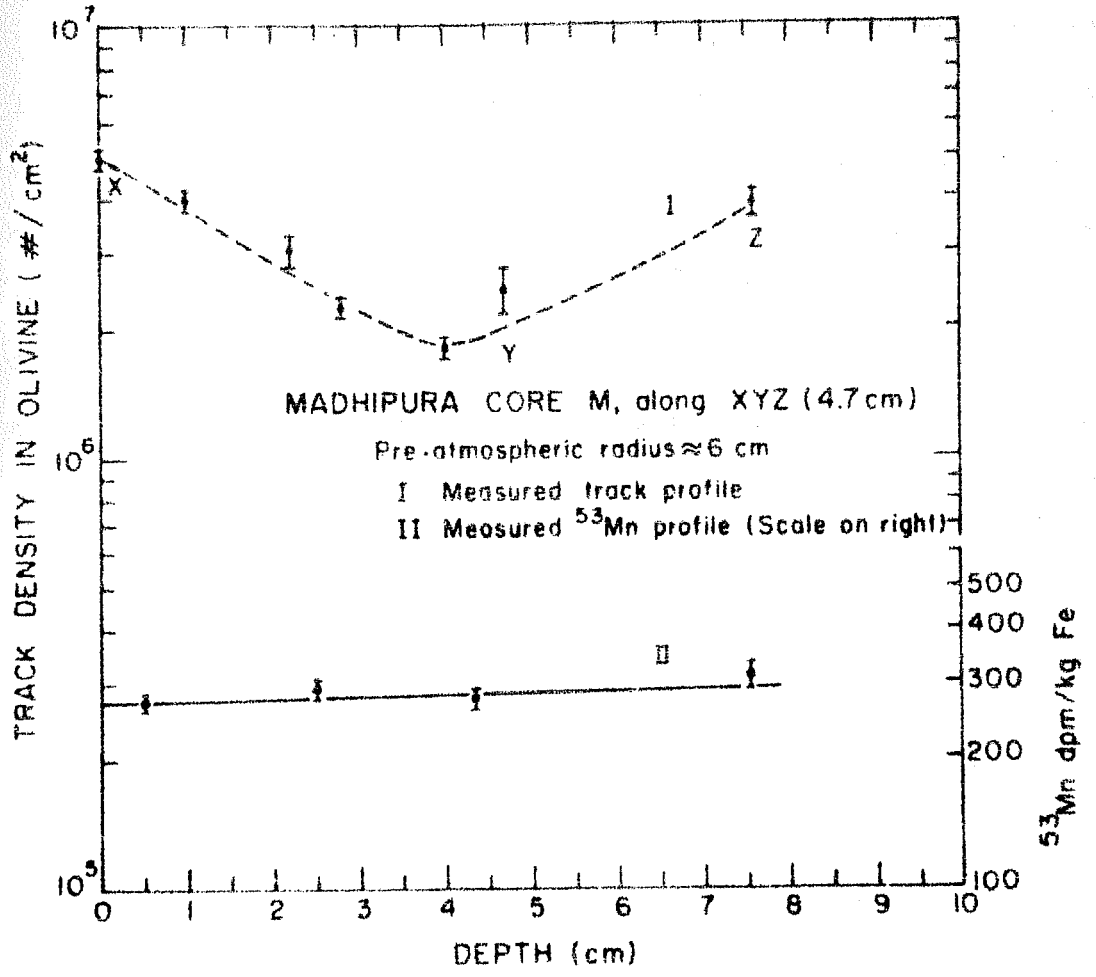

Figure 10. Measured track densities (curve I) and ^{53}Mn activities (curve II) in the core-samples from Madhipura (note that the scale for the ^{53}Mn activity is on the right).

Chapter IV

Discussions

The results of measurement of ^{26}Al and various other radio-isotopes in Lunar rocks and meteorites are useful in deriving information on the flux and energy spectrum of solar and galactic cosmic rays over different periods of time in the past. The discussions of the data presented in chapter III are motivated by these considerations. We will first discuss the results of ^{26}Al studies in Lunar rocks and derive the SCR parameters from these data. In the next section the nature of interaction of GCR in meteorite bodies and possible time and space variation of GCR fluxes will be discussed.

IV.A. ^{26}Al studies in Lunar rocks

The purpose of the measurement of ^{26}Al in Lunar rocks was to derive information on the solar cosmic ray (SCR) characteristics in the past few million years. For the interpretation of ^{26}Al activity of a rock it is essential to know the exposure period of the rock on the Lunar surface and the erosion rate under micrometeorite bombardment. The surface exposure age or 'sun-tan' age is to be distinguished from the integral galactic cosmic ray exposure age, which is derived from rare gas analysis. In the present study nuclear tracks induced by solar and galactic cosmic rays were used for the deter-

mination of surface exposure ages. The method has been described in detail in Bhattacharya and Bhandari (1975) and will be discussed here only in brief.

IV.A.1. The surface exposure age and erosion rate

Tracks induced by SCR and GCR VH nuclei in feldspar group of minerals were measured and track density profiles were constructed in all the 5 rocks. Track production rate in 2π geometry applicable to the case of a spherical rock on Moon was calculated using the energy spectrum discussed in Bhattacharya and Bhandari (1975). From these data we construct residence time, $\tau(x)$, as a function depth using the relation:

$$\tau(x) = \rho_{obs}(x) / \rho(x)$$

where $\tau(x)$ = residence time at present depth x

$\rho_{obs}(x)$ = track density at x

$\rho(x)$ = track production rate at x.

Since the rocks are subject to a variety of effects, like continuous erosion, occasional fragmentation and turn over, the residence time curves have positive slope in near surface regions. It has been shown in Bhattacharya and Bhandari (1975) that a plateau in residence time curve represents one stage exposure with negligible shielding whereas absence of a plateau can be taken as an indication that the rock has undergone complex irradiation history on the Lunar surface, with small surface exposure in the final geometry. Since the track production rate is a steep function of depth, the slope of the residence

time curve also gives erosion rate for short exposure ages. For ages greater than a few million years the slope attains erosion equilibrium value and cannot be used for estimating erosion rate. The major error in the age estimate from tracks is due to the uncertainty in the energy spectrum which is ~ 30% in this energy region.

In the present study, three rocks 61016, 66095 and 79215 showed well developed plateau in residence time curves (Bhandari et al., 1976b)indicating simple surface exposure ages of 1.5, 1.0 and 3.7 m.y. respectively. In rock 64435, rarity of transparent crystals in the small sample available made it difficult to obtain a continuous track profile. Two data points indicate that the exposure age is quite low, close to 0.5 m.y. In the case of 60335, the data show a burial (sub decimeter) age of ~ 50 m.y. with a surface exposure age of ~ 0.5 m.y. but these estimates are only approximate because of its complex exposure. The estimated erosion rate for these rocks is about (0.5 - 1.0) mm/m.y.

An attempt was made to measure the microcrater density in the surfaces of the rocks to get independent estimates of surface exposure ages and erosion rates. The model production rates given by Hartung et al. (1973) were used for this purpose. In 61016, the method was successful and the data have been presented in Bhandari et al. (1975). For other rocks only approximate estimates were obtained. The erosion rate for 61016 from microcrater data is consistent with (0.5 - 1.0) mm/m.y. as deduced from nuclear tracks.

IV.A.2. ^{26}Al activities and SCR parameters

The activities of ^{26}Al reported in the chapter III have large associated errors ranging from 10% to 80%, due to the small surface area of the rock samples available (1.3 to 7.0 cm^2). Depth profiles constructed from these data can only be used to put a large range on the solar flare parameters. Calculations were carried out towards this end and are outlined below.

The adopted model was from Reedy and Arnold (1972) and Bhattacharya et al. (1973). The energy distribution of SCR particles is represented by

$$\frac{dJ}{dR} = k\, e^{-R/R_o}$$

where J = flux in units of particles/cm^2 sec (4π)

R = rigidity of particles (pc/ze, momentum per unit charge) in units of MV.

k = normalisation constant

R_o = shape parameter in units of MV

This free space flux attenuates in Lunar rocks mainly due to ionisation energy loss, and the modified energy distribution at any depth inside a spherical rock on Moon can be obtained by summing up the contributions from various directions in this 2π geometry.

^{26}Al is produced from nuclear reactions induced by these particles on the targets of Al, Mg and Si. These cross-sections have been summarised by Reedy and Arnold (1972). The production

rate P (x) at a point x, is calculated by the formula:

$$P(x) = \sum_i \frac{N_o W_i}{A_i} \iiint \frac{dJ}{dE}(x,E) \quad \sigma_i(E) \quad \sin\theta \, d\theta \, d\phi \quad dE$$

where N_o = Avogadro's number

W_i = Weight percentage of the target element i.

A_i = atomic weight of the target element i.

$\frac{dJ}{dE}(x,E)$ = differential energy spectrum at a point x inside the rock

E = kinetic energy of the particles

$\sigma_i(E)$ = cross section of production from target element i

ϕ = zenith angle

θ = azimuthal angle

For ^{26}Al production, i refers to Al, Mg and Si. A finite contribution of ^{26}Al activity also comes from GCR particles. The model adopted for this computation again follows closely that of Reedy and Arnold (1972). It will be described in detail in section IV.B. dealing with production rate in meteorites. The main difference between the case of Lunar rocks and meteorites is due to 2π and 4π geometry respectively. The calculations of ^{26}Al activity due to SCR and GCR particles were carried out for composition of 61016 and the production function P(x) was constructed. The effect of erosion on P(x) is given by

$$Q(X) = \int_o^T P\,(x(t))\, e^{-\lambda t} \, dt$$

where $x(t) = X + \varepsilon t$ = depth (mm)

X = the present depth (mm)

ε = erosion rate (mm/m.y.)

$P(x(t))$ = production function at $x(t)$

λ = decay constant for ^{26}Al ($m.y.^{-1}$)

T = exposure age of the rock (m.y.)

$Q(X)$ = activity at the present depth X

This integration was carried out by fitting the production function $P(x)$ with a 5 degree polynomial in x.

Figure 11 shows the activities of ^{26}Al found in the samples plotted against their depths from the Lunar top surface for all the five rocks. The production profiles for rock 61016 (taking the composition from table 1 and the exposure age 1.5 m.y.) with erosion rates ε = 0 and 1 mm/m.y. are also shown for the SCR parameters, R_o = 150 MV and J = 140 protons/ cm^2 sec (4π, E > 10 MeV).

For a comparison with the theoretical production profile drawn, the differences in chemical composition of the five rocks have to be taken into account. The other main correction is due to the difference in exposure ages. If we correct all rocks in the exposure age 1.5 m.y. of 61016 we have to multiply the activities by the factors given in bracket for each rock: 60335(2.0), 64435 (2.0), 66095 (1.23) and 79215 (0.80). Following this analysis we see that the solar flare proton fluxes can best be represented by

$$(R_o, J) = (150, 140)$$

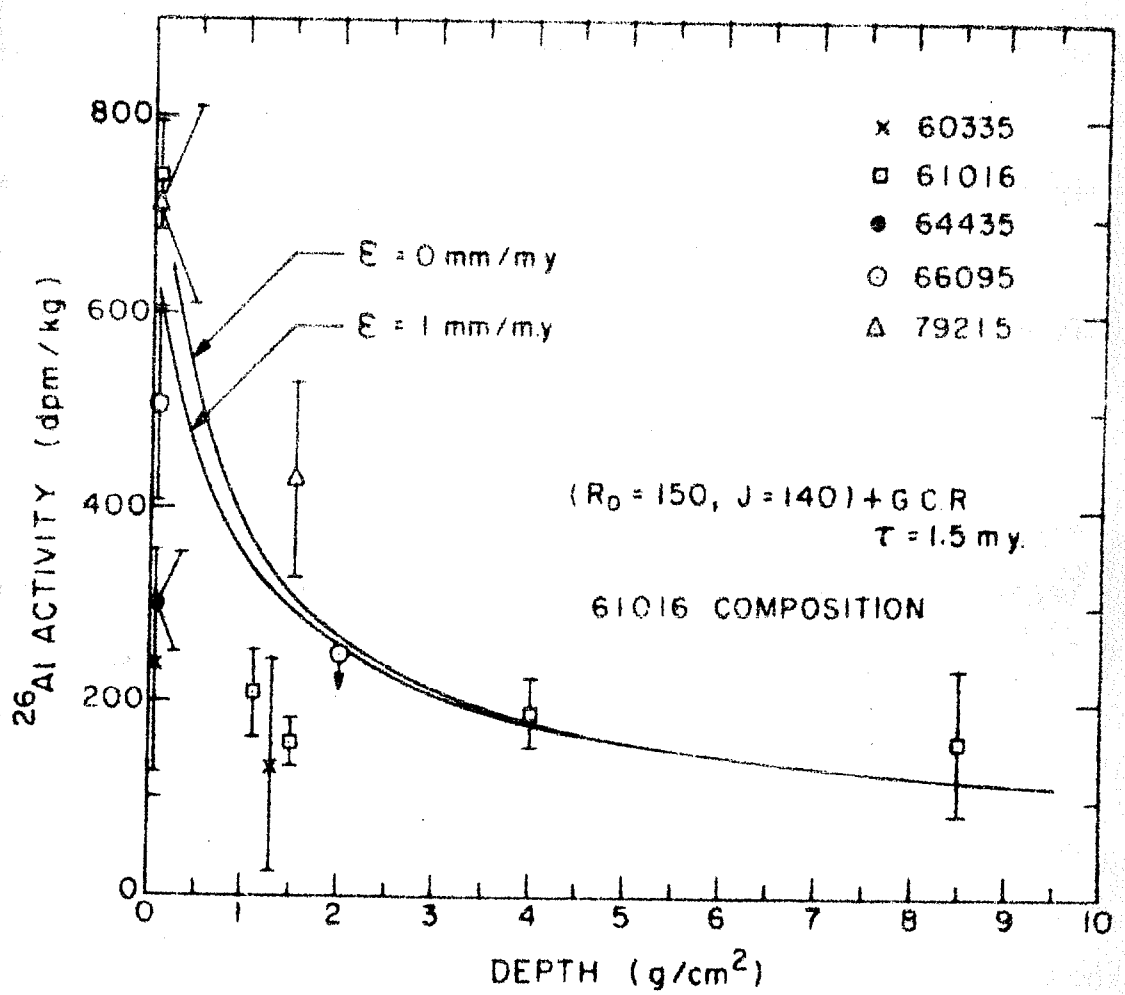

Figure 11. Observed activity of ^{26}Al as a function of depth in various Lunar rocks. The solid lines indicate calculated profiles for the rock 61016 with erosion rate 1mm/m.y. and without erosion.

The surface activities of all the five rocks studied here is consistent with SCR parameters deduced from the depth profiles. Table 19 shows the calculations only for surface activities for which signals were larger. The deviation 'δ' given in the final column indicates that the values of J can at most vary between 100 and 150, the average being about 130. This value is consistent with J=140 deduced from the depth profiles, as discussed in the previous paragraph.

These values of R_o and J are higher than those (100,70) deduced by Kohl et al. (1978) based on the radioactivity measurements of rocks 68815, 12002, 14310 and 14321. For 68815, the method adopted by La Jolla group is destructive analysis of samples prepared by grinding layer after layer from the upper region of the Lunar top surface. The resolution of the grinding method is about 150 mg/cm^2. In the present study the resolution is essentially given by the value of mean-thickness of positrons from ^{26}Al decay and corresponds to about 100 mg/cm^2 ($1/\mu$ = 92 mg/cm^2). In addition, in the present method there is no risk of possible loss (attrition) of surface material during grinding. This is especially troublesome for friable rock like 14321 for which estimated attrition is about 120 mg/cm^2 (Wahlen et al., 1972).

The SCR parameters based on radioactivity data are most sensitive to the surface exposure age of the rock. It has been established from studies of nuclear tracks and rare gases, that GCR ages do not refer to the surface exposure, (Bhattacharya and Bhandari, 1975; Rao et al., 1979). The plateau method,

Table 19

Deviations in surface activity of ^{26}Al in Lunar rocks

Rock	Rare gas exposure age (m.y.)	Track exposure age[4] (m.y.)	Microcrater exposure age[6] (m.y.)	Observed ^{26}Al at surface (dpm/kg)	Calculated[7] production rate at surface (atom/min.kg)	Expected[8] ^{26}Al at surface (dpm/kg)	$\frac{^{26}Al_{obs}}{^{26}Al_{exp}}$	Deviation δ[9] (%)
60335	-	~0.5[5]	-	240 ± 115	1130	375	0.64	-36
61016	1.71±.20(Ar)[1] 1.23±.20(Ne)[1]	1.5	1.2	740 ± 54	1100	652	1.13	+13
64435	0.6±.3(Ne)[2] 0.7±.35(Ar)[2]	0.5	0.2-2	300 ± 50	1305	364	0.82	-18
66095	1.1±.5(Ne)[3]	1.0	~0.2	505 ± 100	1070	560	0.90	-10
79215	-	3.7	~0.8	710 ± 100	1120	745	0.95	-5

(1) Solar flare rare gas age (Rao et al., 1979).
(2) Bogard and Gibson (1975).
(3) Heyman and Hubnar (1974).
(4) Track exposure age is based on the plateau method (Bhattacharya and Bhandari, 1975).
(5) Shows multiple exposure history.
(6) Based on production rates given by Hartung et al. (1973).
(7) Based on SCR parameters $J(E > 10\ MeV) = 140\ p/cm^2.sec\ (4\pi)$ and $R_o = 150$ MV and GCR (after Reedy and Arnold, 1972). Surface is defined as 0-100 mg/cm^2 depth.
(8) Taking exposure ages from column 3, assuming erosion rate of 0.5 mm/m.y. and applying corrections for exposure geometry (zenith angle η) after Bhattacharya et al. (1973). 60335,103 and 66095,146 had $\eta = 0$ and, therefore, no correction was applied. For 61016,287; 64435,95 and 79215,75 this correction was determined to be 5, 20 and 10% respectively.
(9) Deviation $\delta = (^{26}Al_{obs} - ^{26}Al_{exp})/^{26}Al_{exp}$ expressed in percentage.

described in detail in Bhattacharya and Bhandari (1975), show that rocks 12002, 14310 and 14321 do not have simple exposure history and hence their surface exposure ages cannot be identified with GCR ages. Dust and Crozaz (1977) measured track densities in 68815 and obtained three profiles. They conclude that though large scale chipping did not occur for this rock the three profiles and the variations among them indicate that small scale chipping cannot be ruled out. The data of Dust and Crozaz (1977) treated by the plateau method do not yield a simple surface exposure age of 2.0 m.y. as assumed in the calculations of Kohl et al. (1978).

Only in the present work the surface exposure ages of the rocks have been properly evaluated and appropriate corrections for the growth of radioactivity have been applied. Furthermore, in view of our better depth resolution with no loss of virgin surface and the consistency in five samples analysed, these parameters should represent the average solar proton spectrum reasonably well.

The five rocks, studied in this work, span different windows of time, namely 0.5 m.y., 1.0 m.y., 1.5 m.y. and 3.7 m.y. in the past. The ratio Q of the observed surface activity of ^{26}Al to that expected (on the basis of exposure time, exposure geometry, erosion and chemical composition of the rocks) is directly proportional to the variation in the average solar flare activity over the period of exposure. These computations are given in Table 19. As shown in Figure 12 the surface activities are mutually consistent within $\pm 20\%$

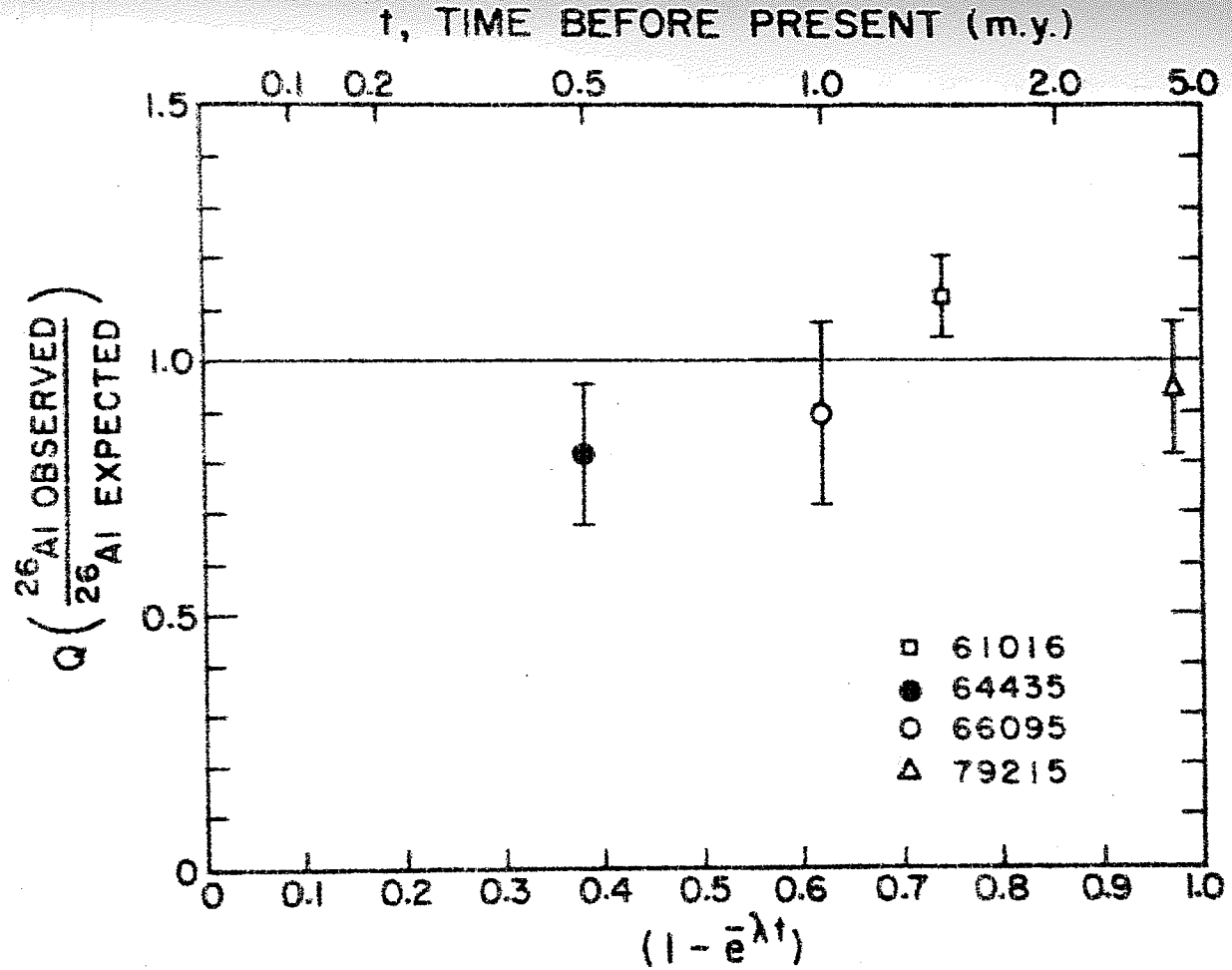

Figure 12. Ratio of observed to expected ^{26}Al activity, Q(t) as a function of the saturation factor $(1-e^{-\lambda t})$ based on various rocks studied. The exposure age of 60335 is uncertain and, therefore, this rock has been excluded.

and agree with the expected activities based on (J,R_o) = (140, 150) within experimental errors. These observations exclude major changes in solar flare particle fluxes over the last few (2-3) m.y.

Recently, Fowler (1972) and Ezer and Cameron (1972) have invoked the possibility of a variation in solar luminosity based on solar neutrino experiment. To explain low neutrino fluxes from the sun observed by Davis (1972), these authors have postulated 'sudden mixing' in the solar core whose consequence is a decrease in solar luminosity over the time scale of a few million years. The manner in which the average solar flare activity and the solar luminosity may be related is not known at the present time. The solar constant appears to have only slight dependence on the sun-spot activity. It, however, appears reasonable to assume that the solar luminosity, solar flare activity and solar wind efflux would be significantly affected by any major structural changes in the Sun. If this reasoning is valid, our observations rule out any appreciable change in solar luminosity over the time-scale of a few million years.

IV.B. Production rates of radioisotopes in meteorites

The activity of radioisotopes induced by galactic cosmic rays in meteorites (and also in Lunar rocks) depends, among other things, on the primary cosmic ray flux and the energy spectrum of the secondaries inside the body. The latter in turn depends upon the size and shape of the meteorite and the shielding depth of the sample.

A comprehensive review of the methods adopted till 1967 has been given in Kohman and Bender (1967). Basically there are three approaches to this problem: (1) calculations based on particle fluxes and nuclear cross-sections (2) Monte Carlo calculations of cascade generation (3) translation of thick-target bombardment data to spherical bodies in an isotropic flux.

The first method has the advantage that once the fluxes of primary and secondary particle are correctly evaluated production rate of any stable or radioactive isotope can be calculated by plugging in the appropriate thin-target cross-section data and the target element abundance. This allows for more and more refinement as and when improved and new cross-section data become available.

A simple analytical method of calculating the particle fluxes inside a body was first proposed by Ebert and Wanke (1957) and later improved upon by Lavrukhina et al. (1969). Lavrukhina et al. (1969) calculated the integral fluxes of primary and secondary particles in a spherical stone meteorite. Using Rudstam type of formula (Rudstam, 1966) for cross-section these authors calculated production profiles of several isotopes in stones of various radii (Lavrukhina and Ustinova, 1972).

Reedy and Arnold (1972) (hereafter called RA), based on the work of Arnold et al. (1961), proposed a semi-empirical model for calculating the energy spectrum of all nuclear active particles inside a large size body like Moon. Their

model describes the secondary spectra in terms of a single shape parameter α, which is depth dependent. The relevant equations are:

$$\frac{dJ}{dE}(E, d) = K(\alpha + E)^{-2.5} \quad \text{for } E > 100 \text{ MeV} \quad \ldots \quad (1)$$

where E = energy in MeV

d = depth in the body

K = normalisation constant

α = spectral shape parameter

The spectra of secondary neutrons with $2.5 < E < 100$ MeV at depth d is given by

$$\frac{dJ}{dE}(E, d) = (\alpha + 100)^{-2.5} \{M(E) - (\alpha - 50)\delta(E)\} \ldots \quad (2)$$

where K, α are the depth dependent parameters of eqn. (1) and

$$M(E) = 94E^{-1} + 603E^{-2} - 300E^{-3} \quad \ldots \quad (3)$$

$$\delta(E) = 0.3E^{-1.26} - 0.00091 \quad \ldots \quad (4)$$

The genesis of these particular expressions have been outlined in detail in RA.

This model has been applied in the interpretation of data on radioisotopes, like ^{26}Al and ^{53}Mn, and also rare gas isotopes in Lunar cores and rocks. It was shown that the model predicts the shape of the depth dependence of the production accurately but as far as absolute magnitude is concerned ^{53}Mn production is under-predicted by about 40 % (Kohl et al., 1977) and ^{26}Al

and ^{22}Na productions are over predicted by about 15% (Rancitelli et al., 1975). The implication of these results will be discussed later.

In this work an attempt has been made to extend the flux model of RA to the case of chondrites. There are two basic differences in the calculations made for Moon and for meteorites. Firstly, for a meteorite, the attenuated primary flux inside the body originates from a 4π isotropic irradiation whereas for moon it is 2π. Secondly, the depth dependence and magnitude of the shape parameter α is different from that for Moon while the geometry effect is straightforward (Bhattacharya et al., 1973). The derivation of α for stony meteorites (chondrites) is done by a logical extrapolation of thick target calculations. The rationale for estimation of α is based on the results obtained for the pallasite Marjalahti. It is shown below that the depth profile of ^{53}Mn in the pallasite Marjalahti agrees reasonably well with that predicted from thick-target calculations of Kohman and Bender (1967) (hereafter KB), giving credence to the thick-target approach. The thick-target calculations for ^{22}Na profile by Trivedi and Goel (1973) are, then, used for estimation of α. The discussion on the results of ^{53}Mn measurement in Marjalahti is presented in the following section.

IV.B.1. ^{53}Mn activity profile in Marjalahti

Marjalahti has been studied in detail for track (Kolesnikov et al., 1977), and for rare gas isotopes (Megrue, 1968). Based on ^{3}He, ^{21}Ne and ^{38}Ar cosmic ray exposure ages of 205, 204 and 178 m.y. respectively were calculated (Megrue,

1968). However, these ages may need revision in view of better estimates of production rates and shielding corrections determined for chondrites (Cressy and Bogard, 1976). Begemann et al. (1976) determined the exposure age to be 180±18 m.y. by ^{36}Cl - ^{36}Ar method which is in good agreement with the value of 174±11 m.y. determined by Kolesnikov et al. (1977) using the ^{39}Ar-^{38}Ar method. An exposure age of 180 ± 18 m.y. is adopted here for the purpose of calculating the pre-atmospheric radius and the shielding depths. An uncertainty of ±10 % in age introduces only about ±3 % uncertainty in the value of shielding depths of the samples of Marjalahti A,B,C studied here.

Using the exposure age of 180 ± 18 m.y. and the published track data a pre-atmospheric radius of 20 cm for this meteorite can be calculated following the method of Gupta and Lal (1978). This is consistent with the estimate of 135 kg (±30%) given by Kolesnikov et al. (1977), which is equivalent to an effective radius of 19 cm (density = 4.9 gm/cc).

The three samples A,B,C were selected from the exterior surface of the Marjalahti. The large olivine inclusions present in the samples were analysed for nuclear tracks and the metal phase was processed for ^{53}Mn. The ^{53}Mn data have been presented in Tables 11 and 12. The track data have been presented in Bhattacharya et al. (1979) and used for calculating the shielding depths of these three samples. The samples A, B and C have shielding depths (cm),

6.3 (A) , 11.8 (B) and 14.9 (C)

and the ^{53}Mn activities (dpm/kg Fe)

$$457 \pm 40 \quad (A), \quad 522 \pm 28 \quad (B) \quad \text{and} \quad 515 \pm 28 \quad (C)$$

respectively. Based on these shielding depths the depth profile of ^{53}Mn is plotted in Figure 13.

The calculated profiles of ^{53}Mn for pallasites of different radii are not available. Kohman and Bender (1967) from an analysis of thick iron target data calculated the ^{54}Mn production rate in iron meteorites of various radii. ^{53}Mn production profile in pallasites can be obtained from these curves in the following manner. We assume that

$$X_{pall} = X_{iron} \times \frac{\rho_{iron}}{\rho_{pall}} \times \frac{\lambda_{pall}}{\lambda_{iron}}$$

where X is the depth (cm), ρ is the density (g/cc) and λ is the absorption mean free path (g/cm^2) of high energy protons ($\sim$ 1 GeV). The subscripts iron and pall refer to iron meteorites and pallasites respectively. The adopted values are:

$$\rho_{iron} = 7.9 \text{ g/cc} \quad , \quad \rho_{pall} = 4.9 \text{ g/cc}$$

Using the expression (Venkatavaradan, 1970),

$$\frac{1}{\lambda} = N_o \Sigma \frac{\sigma w}{A}$$

λ in iron and pallasite are calculated to be 141 and 127 g/cm^2 respectively, where N_o is Avogadro's Number, σ is the proton absorption cross-section (Booth, 1957), A is the atomic

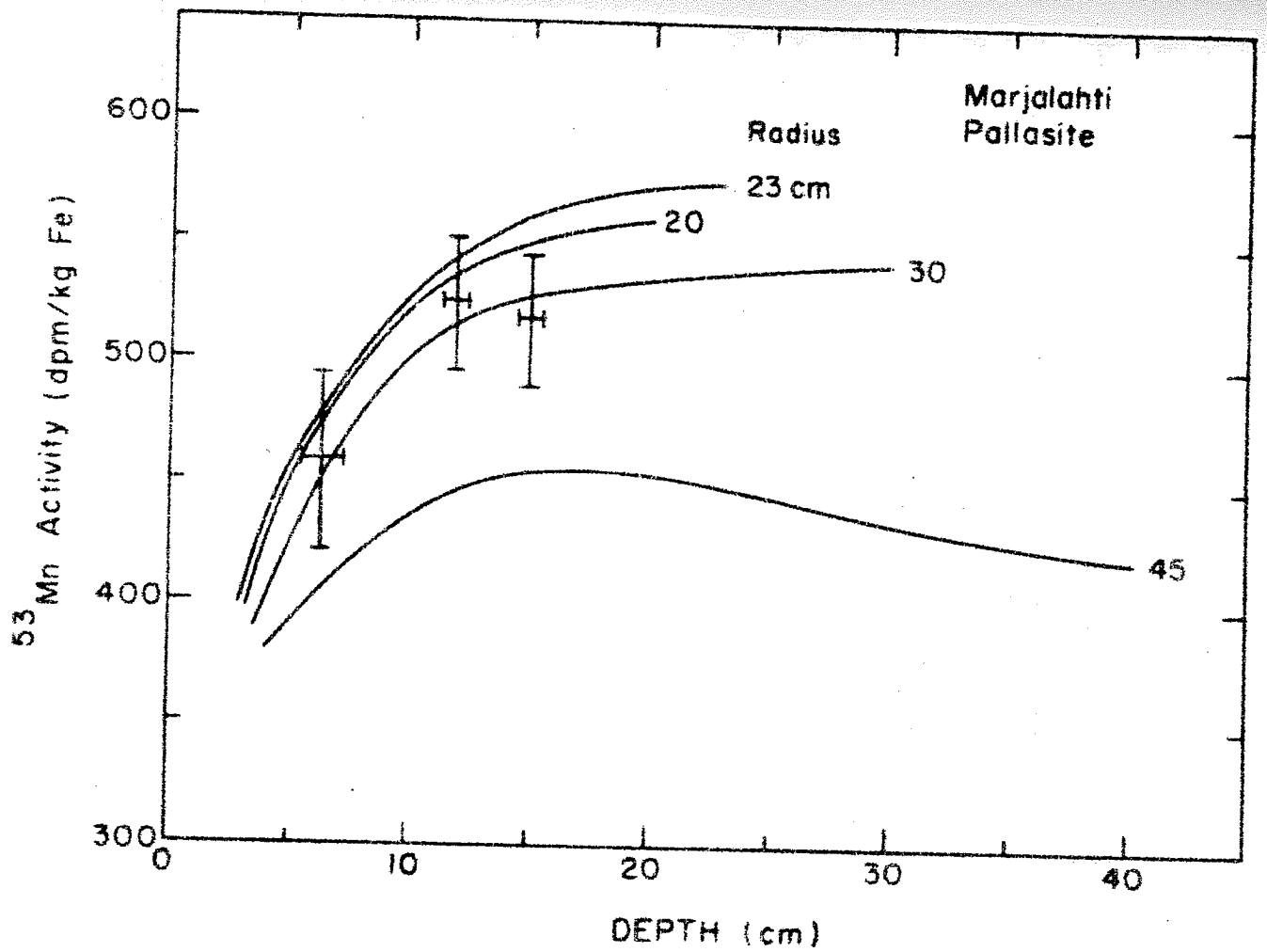

Figure 13. The depth profile of ^{53}Mn activity in the Marjalahti pallasite. The curves are calculated ^{53}Mn activity profiles for spherical pallasites of different radii.

number, and w is the weight percentage of various elemental constituents. The bulk composition of the Marjalahti type pallasite is taken to be 55 % iron-nickel and 45 % Mg-rich olivine (Mason, 1962).

The ^{54}Mn profiles, thus translated to the case of pallasites, show that for bodies less than about 23 cm radius, production at any depth increases with the size of the meteorite, reaching a peak production at the centre of a pallasite of radius about 23 cm. For bigger bodies the production rate is smaller and the depth profile shows a broad maximum around a depth of 15 cm. ^{53}Mn depth profile is expected to be similar within $\pm$ 10 % to that of ^{54}Mn from a consideration of their cross-sections (Reedy, priv. comm., 1976; Gensho et al., 1977). In Figure 13 the depth profiles of ^{54}Mn for pallasites are thus assumed to apply to the case of ^{53}Mn.

A comparison of the observed data and the depth profile for a 20 cm pallasite indicates that the KB calculations are about 5 % higher than the observed values, which is well within the uncertainties discussed above.

Thus the present study leads to the conclusions that (a) the KB calculations predict reasonably well the magnitude of ^{53}Mn production in 15-30 cm size irons or pallasites and (b) the data are also consistent with the shape of the depth profile predicted by KB for 15-20 cm size body.

IV.B.2. Cosmic ray flux in meteorite orbits and the shape parameter α

In the earlier section the validity of thick-target

calculations was established within certain limits. Using similar thick-target approach, Trivedi and Goel (1973) (hereafter TG), have determined the production profiles of ^{22}Na in chondrites. Their calculations for ^{22}Na have been found to agree well with the observations in some meteorites. In this work, these ^{22}Na profiles of TG were used to deduce the RA shape parameter α for chondrites of various sizes as a function depth. The method is briefly described below.

The production integral P(x), at a depth X, inside a spherical meteorite is,

$$P(X) = \frac{N_o W}{A} \int \int \int \frac{dJ}{dE}(E,X) \quad \sigma(E) \sin\theta \, d\theta \, d\phi$$

The calculations were done by a computer program. The cross-sections for ^{22}Na production for the reactions ^{23}Na (n,2n) ^{22}Na, Si(n,x) ^{22}Na, ^{27}Al (n,x) ^{22}Na and Mg (n,x) ^{22}Na were taken from a literature survey and Dr. Reedy (priv. comm.). The composition for H-chondrite was assumed as that of Dhajala, Si = 17.2%, Mg = 14.2%, Al = 1.13%, Na = 0.6%, Fe = 27.16% and Mn = 0.25%. The expressions for fluxes at two energy ranges, $2.5 < E < 100$ MeV and $E > 100$ MeV, have been given in section IV.B. The normalisation for flux is discussed below.

The long term average flux, J, of GCR protons (> 1 GeV) taken by RA is 1.7 protons/cm^2.sec (4π) and this also probably represents the observations made during solar cycle 19 near the earth (at 1 A.U.). However, observations of GCR spectra during solar cycle 20 (1965-1976), analysed by Potdar and

Bhandari (1979), yield an average value of 1.9 protons/cm^2.sec (4π). Allowing a maximum of +7% per A.U. increase with aphelion distance (Bhattacharya and Bhandari, 1976) over the value 1.9 one can at most expect a value of 2.1 protons (unit omitted) for the flux applicable to meteorite orbits. The values of 1.7 and 2.1 protons are adopted to represent the range of average long term flux. The values of the shape parameter α depend on the choice of this normalisation flux and were derived by fitting TG profiles of ^{22}Na for both these fluxes and are given in Figures 14 and 15 as a function of depth for six different sizes.

The flux of particles above 1 GeV was calculated as a function of depth (J(d)) using the same approach as in RA, and is shown in Figure 16 for the case of free-space flux of 1.7 protons.

Based on these values of α and normalisation flux J (> 1 GeV) and the reaction cross-section (Reedy, priv. comm.) the production rates of three radioisotopes ^{26}Al, ^{53}Mn and ^{54}Mn were calculated for the composition of H-chondrite. The activity profiles for these three isotopes (along with the fitted ^{22}Na) are shown in Figures 17 and 18 for the free-space fluxes of J = 1.7 and J = 2.1 respectively.

IV.B.3. Comparison between calculated and experimental values

For a proper comparison between the predicted values from the above model and the measured activities in the meteorite the pre-atmospheric size of the meteorite must be known.

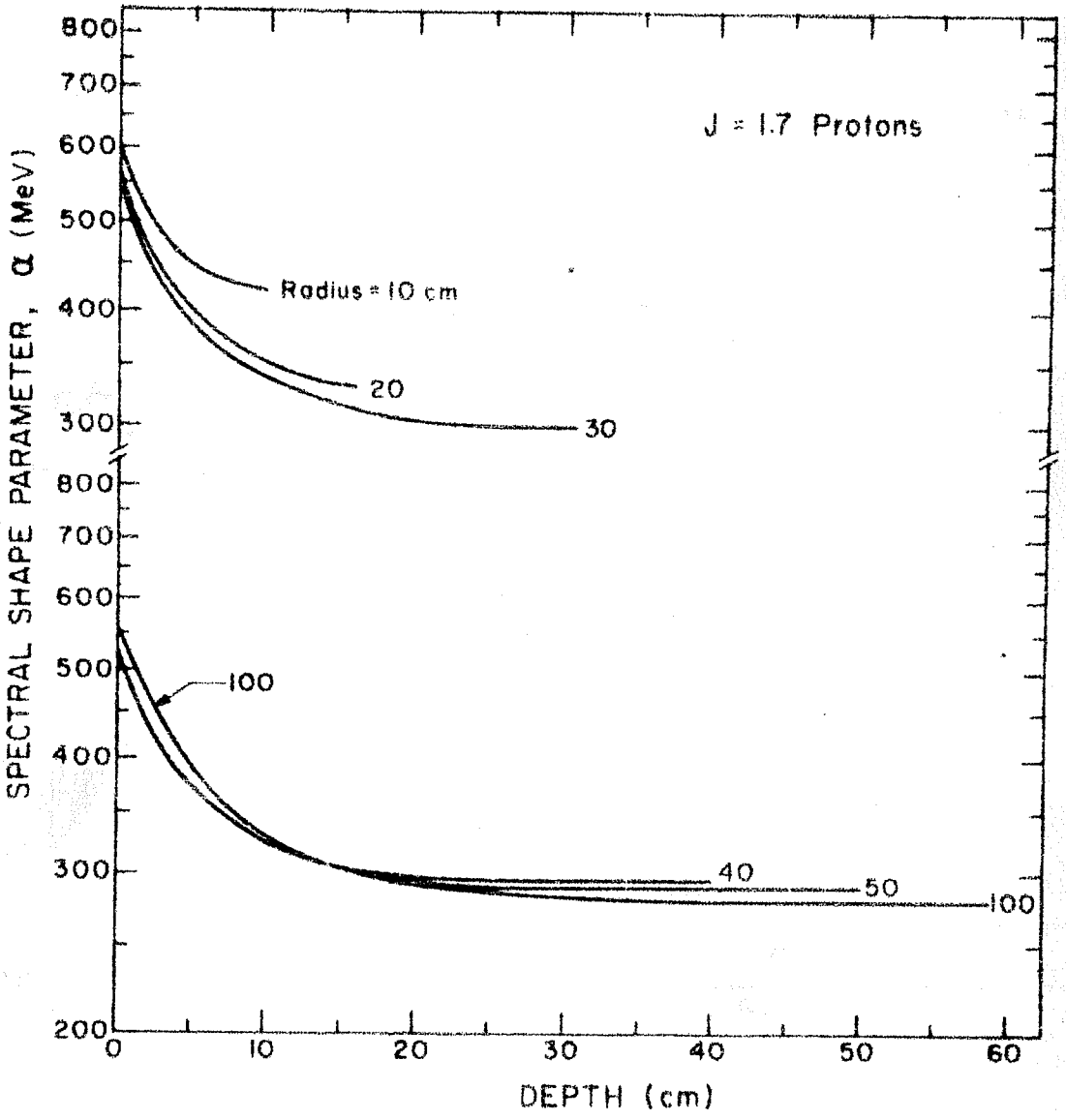

Figure 14. Depth dependence of the shape parameter α deduced for the GCR flux, J (E > 1 GeV) = 1.7 protons/cm^2. sec (4π) for chondrites of different radii.

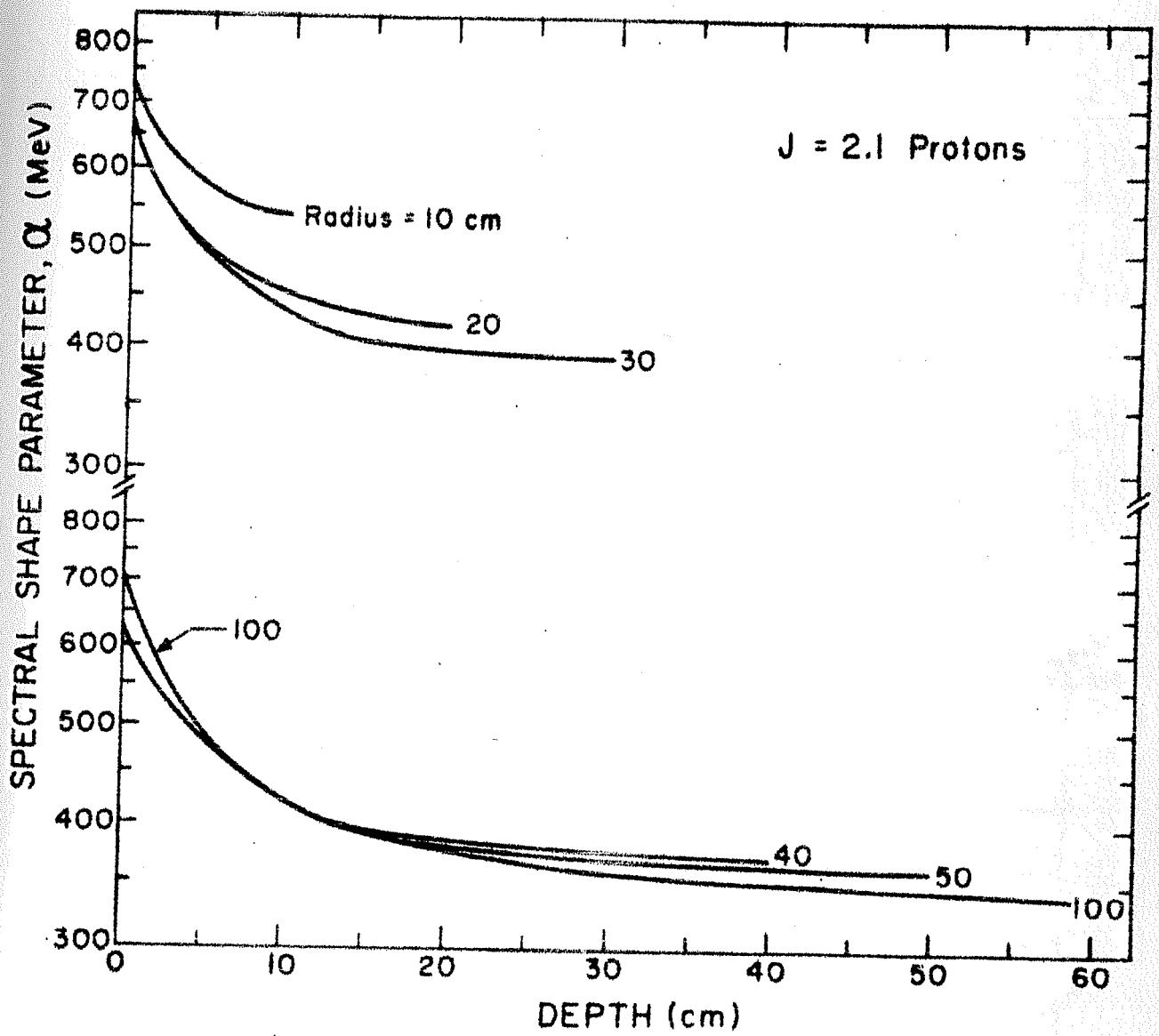

Figure 15. Depth dependence of the shape parameter α deduced for the GCR flux, J (E > 1 GeV) = 2.1 protons/cm^2.sec (4π) for chondrites of different radii.

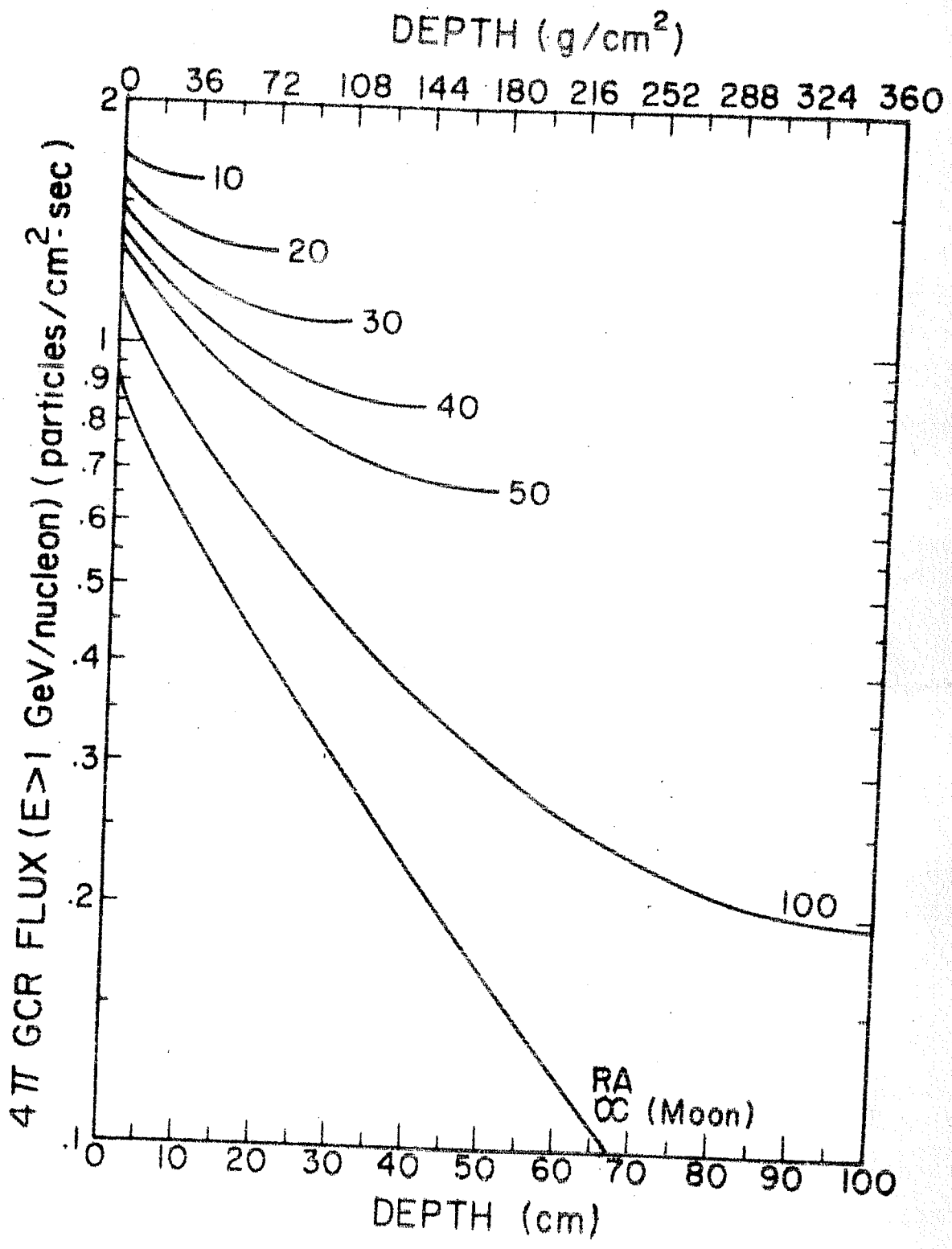

Figure 16. Depth dependence of the integral flux of GCR particles (E > 1 GeV) inside chondrites of different radii corresponding to a free-space GCR flux, J (E > 1 GeV) = 1.7 protons/cm^2.sec (4π).

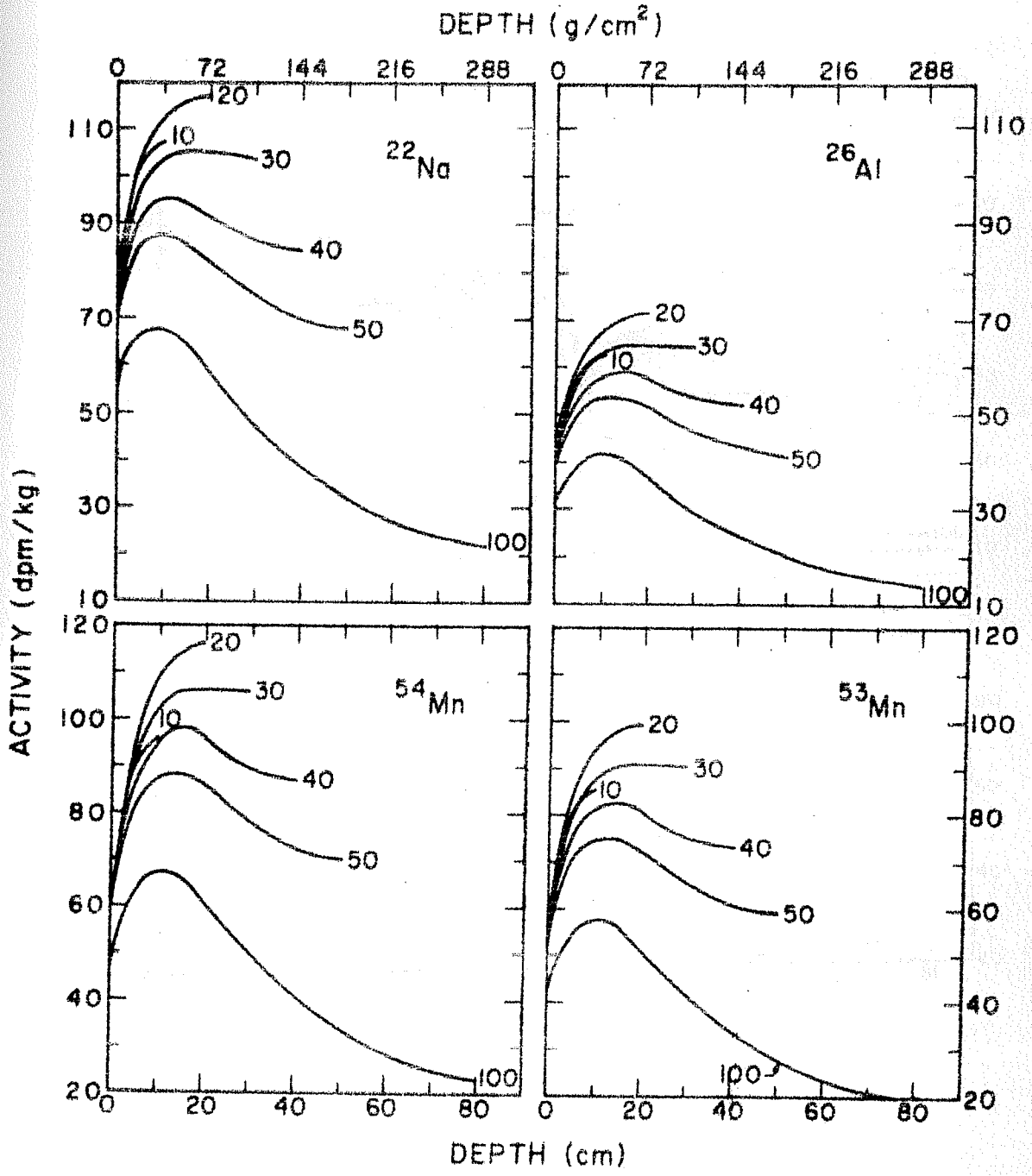

Figure 17. Calculated activity profiles of ^{22}Na, ^{26}Al, ^{53}Mn and ^{54}Mn in chondrites of radii 10, 20, 30, 40, 50 and 100 cm, for a free-space GCR flux, J (E > 1 GeV) = 1.7 protons/cm^2.sec (4π).

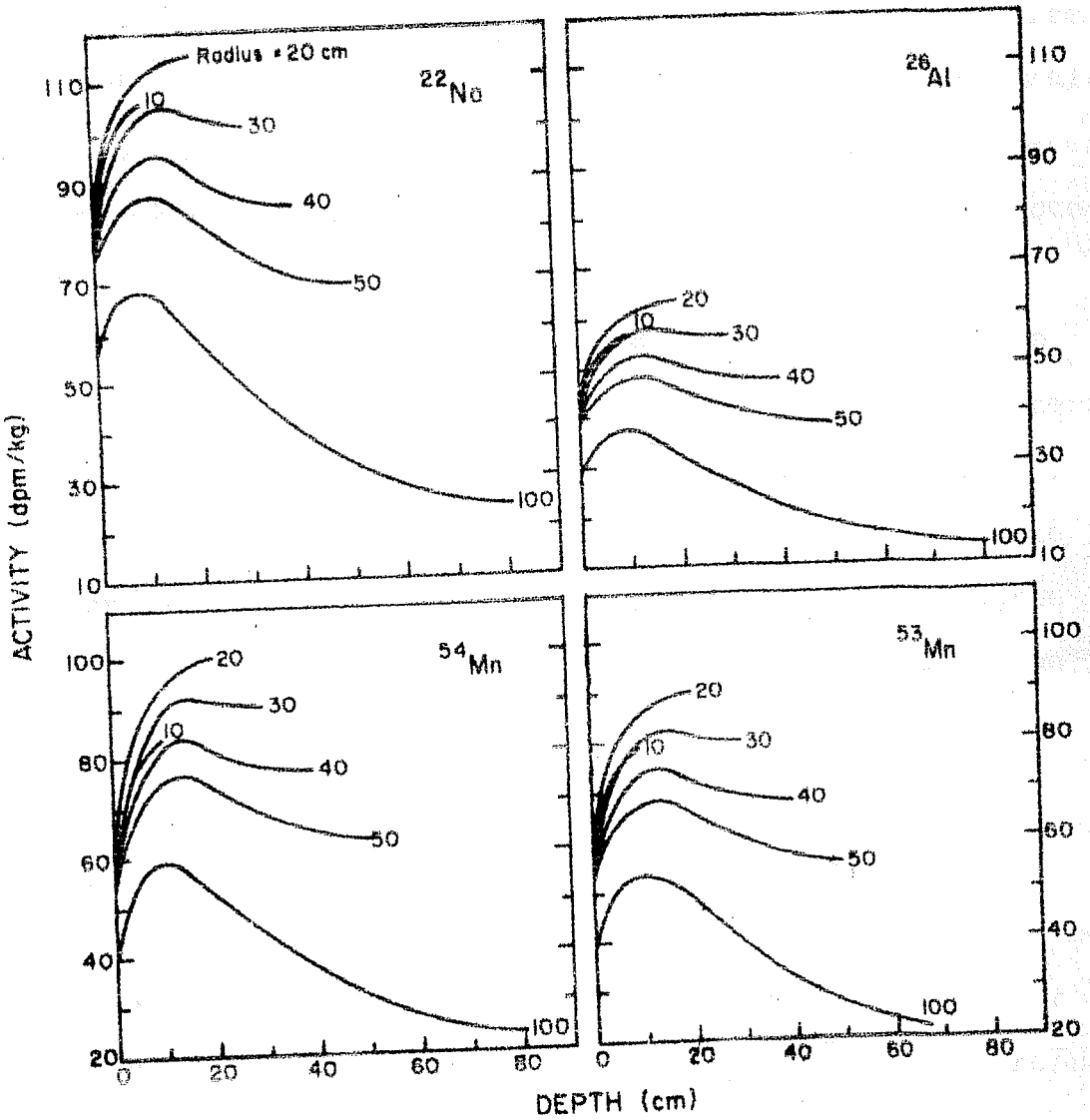

Figure 18. Calculated activity profiles of ^{22}Na, ^{26}Al, ^{53}Mn and ^{54}Mn in chondrites of radii 10, 20, 30, 40, 50 and 100 cm, for a free-space GCR flux, J (E > 1 GeV) = 2.1 protons/cm^2.sec (4π).

Recently, Bhandari et al. (1978) have estimated the equivalent pre-atmospheric radii (R_o) of a large number of meteorites. From a survey of literature data in addition to the present work on ^{26}Al and ^{53}Mn activities in chondrites, 30 chondrites were found for which R_o have been estimated. This compilation is presented in Table 20. Confident estimates of R_o are available for eleven meteorites from this group of 30. The quoted list of activities is not a complete list of measurements available. Selection of activity data, when more than one measurement is available, was done by the following criteria: (a) the measurement with the lowest quoted error was taken, (b) usually more recent measurements for the same meteorite were found more reliable, (c) if several measurements agree within errors one representative value was taken. Small variations in chemical compositions among the chondrites do not affect the conclusions in any major way.

The activities of ^{26}Al and ^{53}Mn are plotted in Figures 19 and 20 as a function of R_o of the meteorites. The hatched band shows the range of ^{26}Al values predicted for depths greater than 2.5 cm for various radii. 2.5 cm is taken to be a representative lower limit for shielding depth in chondrites. Several interesting trends follow from these figures.

Comparison for ^{26}Al

The ^{26}Al activities are best predicted for the long-term average flux of $J = 1.7$ p/cm^2 sec (4π). This is also supported by the ^{26}Al data in cores of the Keyes chondrite (Cressy, 1975). Lorin (1975) and also Bhandari (priv. comm.) have shown

Table 28

Saturated activities of ^{53}Mn and ^{26}Al in chondrites and their pre-atmospheric sizes

Meteorite	Equivalent pre-atmospheric radius R_o[a] (cm)	Saturated ^{53}Mn (dpm/kg Fe)	Reference	Saturated ^{26}Al (dpm/kg)	Reference
Akron	22	560	c	-	-
Archie	18[b]	-	-	57	g
Bansur	15[e]	420	e	50	h
Batsura	16	-	-	40	h
Bruderheim	38	424	c	58	i
Crab Orchard	23	520	d	-	-
Dhajala	50[e]	411	e	53	e
Finney	28	418	c	50	j
Hamlet	16[b]	-	-	64	k
Harleton	18[b]	251	f	50	l
Holbrook	35	436	d	58	i
Keyes	23[e]	369	c	56-69	m
Kunashak	33	458	f	59	n
Lecoville	10	587	d	47	o
Lost City	24[b]	-	-	57	p
Madhipura	6.5[e]	338	e	-	-
Mocs	35	501	c	-	-
Modoc	17	543	f	59	i
Murchison	30	586	c	-	-
Peace River	21	403	d	55	l
Pribram	26[b]	-	-	56	q
Ramsdorf	14	415	c	60	j
Richardton	23	333	d	45,59	f,i
Roy	27	501	c	-	-
San J. Capistrano	8[r]	305	d	44	r
Shaw	15	487	c	-	-
St. Severin	20[e]	440,397	d,e	56	s
Temple	19	527	c	-	-
Ucera	24	-	-	66	t
Udaipur	9[e]	312	e	42	h
Wellman	24	287,475	e,c	72	u

a = Bhandari et al. (1978) except when noted;
b = Confident estimate of R_o.
c = Englert and Herr (1978a).
d = Nishiizumi (1978)
e = This work
f = Cressy (1964)
g = Rowe and Clark (1971)
h = Bhandari et al. (1979, and priv. comm.)
i = Cameron and Top (1974)
j = Herpers et al. (1969)
k = Heymann and Anders (1967)
l = Shedlovsky et al. (1967)
m = Cressy (1975)
n = Spannagel and Heusser (1969)
o = Heimann et al. (1974)
p = Bogard et al. (1971)
q = Fireman E.L. (priv. comm., 1979)
r = Kohl (1975)
s = Cressy (1970)
t = Bhattacharya and Bhandari (1976)
u = Herzog and Cressy (1974)

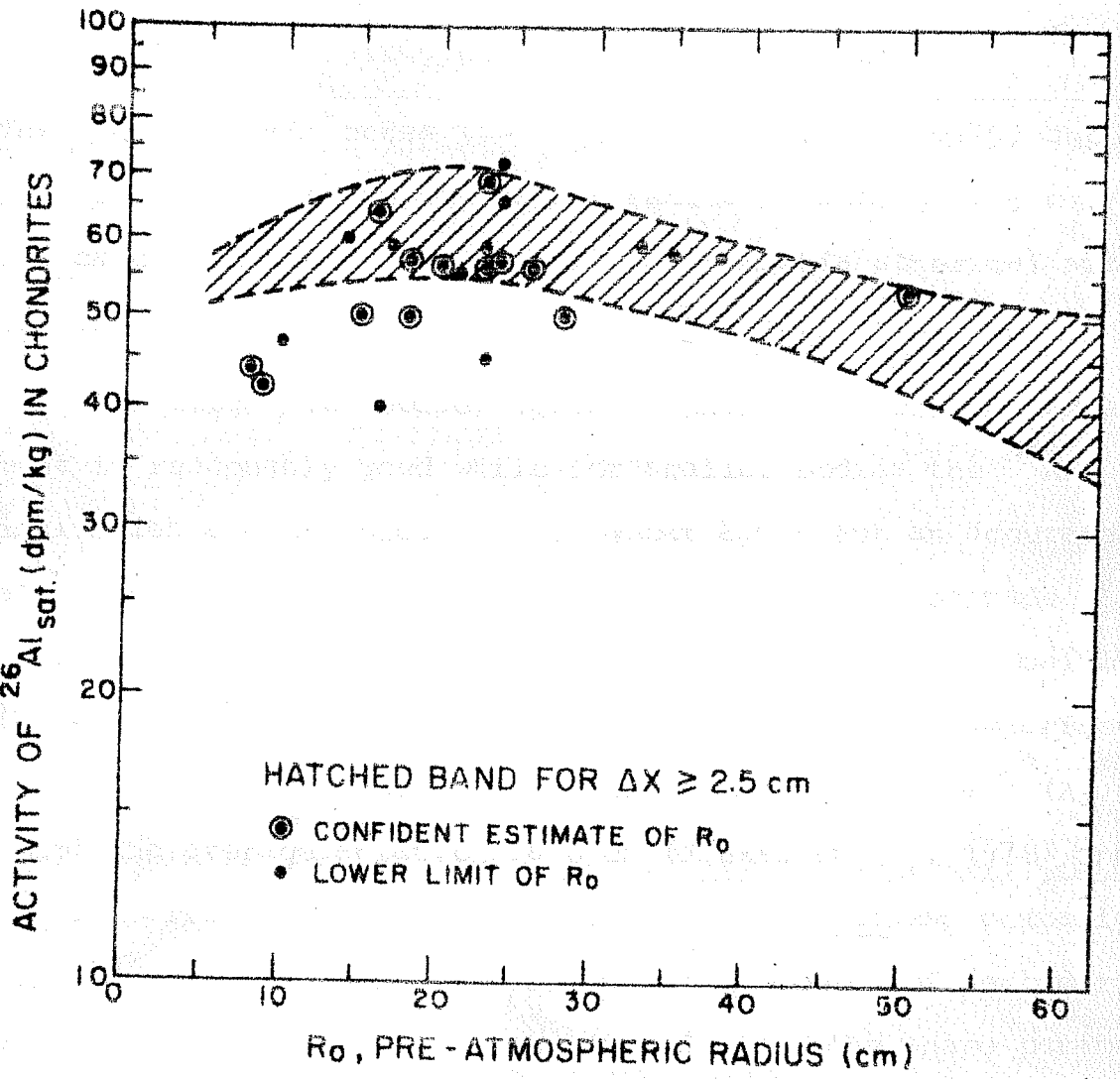

Figure 19. Saturated activity of ^{26}Al in chondrites against their pre-atmospheric sizes. The hatched band indicates the range of values expected for shielding greater than 2.5 cm for various sizes (based on Figure 17 and Table 20).

that Keyes had an oblong pre-atmospheric shape given by lengths (a,b,c)

along core (3-5) a = 61 cm

along core (2-4) b = 65.4 cm

along core 1 c = 37.4 cm

The ^{26}Al data for cores (3-5) and (2-4) (Cressy, 1975) should thus correspond to an equivalent radius of about 20-25 cm. The calculated depth profile of ^{26}Al for this spherical size (Figure 17) agrees very well with the observations.

For large size bodies (greater than ~ 15 cm) the agreement is reasonably good while for smaller bodies the ^{26}Al activities are overpredicted by about 25%. But an accurate estimate of the extent of over-prediction cannot be made unless shielding depths are taken into account. For Udaipur (R_o = 9 cm) the ablation values are known and the comparison shows an excess of about 27%. For San Juan Capistrano (R_o = 8 cm) the average ablation is 6 cm (Finkel et al., 1978) and the comparison shows an excess of about 23%. These comparisons suggest that for smaller bodies the development of secondary particles is not as much as predicted, i.e. the shape parameter α should be increased by about (25-30)% for agreement with the observation.

For very large bodies like Allende, Kirin etc. the model predicts ^{26}Al values less by about 18%. The reason for these departures i.e. over-prediction for lower sizes and under-prediction for very large sizes are suspected to be due to the

limitation in size of the original thick silicate target experiment of Trivedi and Goel (1973). Their targets were of medium size (equivalent to about 20-30 cm meteorite) so the diffusion parameters deduced from this size range is not applicable to the small size (less developed secondaries) and the very large size (extremely developed secondaries). In conclusion, we can say that the model (i.e. shape parameter α) is applicable for ^{26}Al activity in the size range 20-40 cm chondrites. For the size range around 10 cm the α's have to be increased by about 25% and for sizes greater than 50 cm α's have to be decreased by about 20%.

Comparison for ^{53}Mn

The ^{53}Mn activity expressed in dpm/kg Fe between meteorites is directly comparable since iron is the major target element for production of ^{53}Mn (with a few per cent contribution from ^{55}Mn and Ni). In Figure 20 the saturated activities of ^{53}Mn (dpm/kg Fe) are plotted against the equivalent pre-atmospheric radius R_o of the meteorites. The hatched band represents the range of ^{53}Mn activities (calculated from the present model with J = 1.7 protons) for various radii expected with an ablation or shielding of 2.5 cm. In addition to the present work, the experimental data have been taken from various publications (listed below Table 20) of Tokyo group, W. German group and Dr. Cressy. The earlier work of Cressy (1964) was done by X-ray counting while the other three by neutron activation and there may be problem of intercalibration of standards as discussed later in section IV.B.5. The experimental points

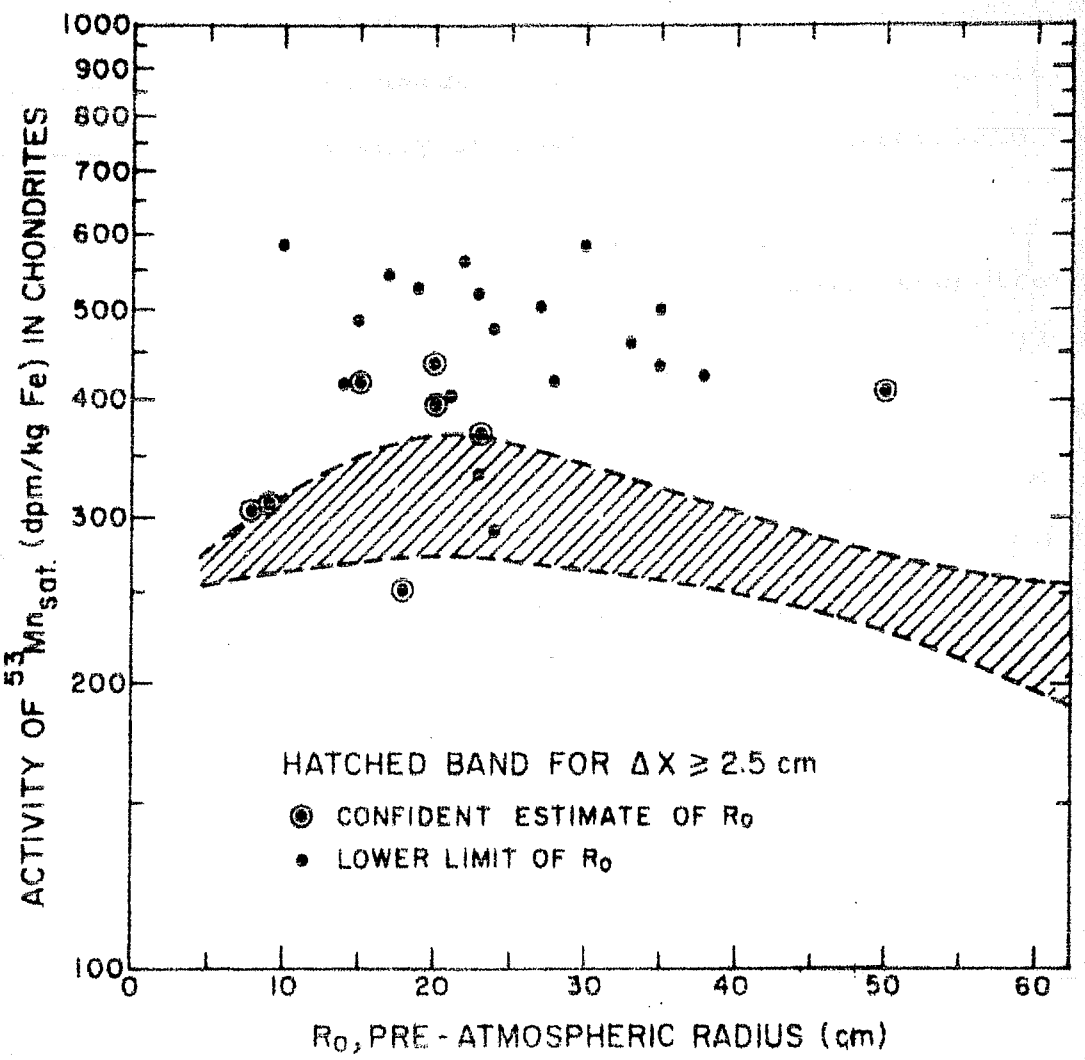

ure 20. Saturated activity of ^{53}Mn in chondrites against their pre-atmospheric sizes. The hatched band indicates the range of values expected for shielding greater than 2.5 cm for various sizes (based on Figure 17 and Table 20).

lie mostly above the hatched band indicating under-prediction by about 45% for moderate size range. It is to be noted that the same magnitude of discrepancy has been seen in the case of Lunar core data on ^{53}Mn (Kohl et al., 1977). Since ^{26}Al data in this size range is in reasonable agreement with the calculations we assume that the model is applicable. To explain the discrepancy in case of ^{53}Mn we investigate two possibilities:

(1) The flux value of J = 1.7 protons is lower than that applicable over ^{53}Mn time scale (Rancitelli et al., 1975). This point could be checked by comparing the expected activities for short exposure age meteorites (< 2 m.y.). From this work and that of Englert and Herr (1978 a) we have 4 such cases: Ladder Creek (0.95 m.y.), Murchison (1.3 m.y.), Scurry (1.3 m.y.) and Shaw (0.5 m.y.). The observed ^{53}Mn activities are (from Englert and Herr, 1978a) (in ^{53}Mn dpm/kg Fe):

Ladder Creek	85±9
Murchison	121±8
Scurry	92±9
Shaw	43±7

The value for Ladder Creek obtained in this work is 87±7 dpm/kg Fe (Table 11), in excellent agreement with that of Englert and Herr (1978 a).

When corrected for exposure ages given in Englert and Herr (1978) the saturated activities for these meteorites lie about 40-50% higher than the hatched band shown in Figure 20.

This comparison shows that time variation in the flux cannot explain the observed discrepancy with theoretical prediction. Deep samples (> 20 $g.cm^{-2}$) from under-saturated (exposure age < 4 m.y.) Lunar rocks will be useful in establishing this point still firmly. From the available exposure ages, the rocks 61016, 64435, 66095, 68815 and 79215 having exposure ages of 1.5, 0.6, 1.1, 2.0 and 3.7 m.y. could be used for this purpose.

(2) The second possibility is that the cross-section have been underestimated by about 45 %. For high energy the proton induced cross section is applicable to GCR interactions but the same may not be true in the low energy region. In the high energy range there is a small discrepancy in the literature values. Perron (1976) have reported $\sigma = 45 \pm 4$ mb for reaction Fe (p, x) ^{53}Mn at E = 600 MeV which is slightly higher than the value of Honda and Imamura (1971): $\sigma = 37 \pm 15$ mb at E = 730 MeV. Gensho et al. (1977) have given the best fit curve for proton induced reaction Fe(p, x) ^{53}Mn over the large range 10-1000 MeV. As a check, this curve was run in the present model, but still the predicted activities were lower by at least 25%.

From the above discussions it is clear that from the limited amount of data we cannot still make a case for either of the two possibilities. More experiments for the determination of cross-section and ^{53}Mn activity in short exposure age meteorites and Lunar samples are needed to settle this point. In the subsequent discussion we will apply a normalisation factor of 1.45 for ^{53}Mn production rates for moderate

size bodies like Dhajala. This factor is identical to the one used by Kohl et al. (1977) for the case of Lunar samples.

IV.B.4. Radionuclides in Dhajala

Twelve radionuclides of half-lives ranging from 5.6 days (^{52}Mn) to 3.7 m.y. (^{53}Mn) were measured in Dhajala. These can be conveniently divided into 3 groups according to their half-lives: (A) half-lives less than about 60 days (^{52}Mn, ^{32}P, ^{33}P, ^{51}Cr, ^{7}Be), (B) half-lives in the scale of years (^{57}Co, ^{54}Mn, ^{22}Na and ^{60}Co), (C) larger half-lives (^{26}Al, ^{10}Be and ^{53}Mn).

a. Short-lived activities and solar cycle effect

Radioisotopes in groups A and B can be used for estimating the magnitude of the solar cycle effect. For example, ^{7}Be, mainly produced from oxygen by high energy GCR can be ideally used for estimating high energy cosmic ray fluxes during different phases of the solar cycle. Its value of 132 $\pm$ 12 dpm/kg in T-11 is 14% higher than 116 $\pm$ 12 dpm/kg for Canon City meteorite (Kohl, 1975), which fell in 1973 during solar maximum. This suggests that the solar cycle effect is atmost $\pm$ 20 % over the mean. Fireman (1967) considered ^{22}Na/^{26}Al ratio in six falls and came to a similar conclusion that the production of low energy isotopes does not vary by more than $\pm$ 15 % from the mean value (see Figure 2 in Fireman, 1967). The data of ^{7}Be activity will be further discussed in the next section in relation to ^{10}Be activity.

The value of ^{51}Cr in our sample (91 $\pm$ 25 dpm/kg) is in excellent agreement with that found by Dr. Rancitelli (priv.

comm.) in another sample. This value is lower than 132 ± 28 dpm/kg (quoted in Kohl, 1975 from Rancitelli priv. comm.) found in Canon city. This isotope is a medium energy product from Fe and production rates in a medium size body like Dhajala (~50 cm) and a small body like Canon City are not well known for a fine comparison. Similarly, considering the uncertainty of shielding effects and production rates the activities of ^{33}P (7.2 ± 2.4) and ^{32}P (22 ± 1.7) dpm/kg compare favourably with 18 ± 9 (^{33}P) and 14 ± 5 (^{32}P) dpm/kg found in St. Severin meteorite which also fell at the time of solar minimum in 1966 (Marti et al., 1969). The 5.6 day ^{52}Mn activity 103 ± 15 dpm/kg Fe is much lower than 177 ± 30 dpm/kg Fe in St. Severin (Tobailem 1967 and Cressy 1970) but closer to 123 ± 40 in Lost City which fell in 1970 (Cressy 1971). These differences may partially be due to the size effects but again the production rates are not known. Once the production rate is established this isotope is ideal for indicating the GCR flux near the earth.

b. Long-lived isotopes and comparison with calculations

The experimental values of five isotopes ^{10}Be, ^{53}Mn, ^{54}Mn, ^{26}Al and ^{22}Na can be compared with the calculations presented in section IV.B.2. The observed average values are

^{10}Be = 17 dpm/kg

^{53}Mn = 284 dpm/kg Fe (from n-activation)

^{54}Mn = 144 dpm/kg

^{26}Al = 53 dpm kg

^{22}Na = 111 dpm/kg

The ^{53}Mn activity of 280 dpm/kg Fe by X-ray counting of Mn-fraction in T-11 is in excellent agreement with 284 dpm/kg Fe found by n-activation.

To compare the above mentioned activities with the calculations it is essential to know the pre-atmospheric radius of Dhajala. Bagolia et al. (1977) gave an estimate of 38 cm for equivalent pre-atmospheric radius based on cosmic ray studies. They studied samples from about 25 % of the total number of recovered fragments. The lowest track density value observed was $(6.5 \pm 1.6) \times 10^2$ cm^{-2} which they assigned to the centre of the meteorite. If this assumption is not made their data give a lower limit of 40 cm for Dhajala. A more reliable way for estimating R_o is from the measured ^{26}Al activities in various fragments studied in this work and by others. Table 9 gives data of 8 measurements and 4 more measurements have been reported by Bhandari et al. (1979). The measured values vary from 37 to 62 dpm/kg with seven values being less than 50 dpm/kg. The weighted average of all the measurements is 46 dpm/kg. The shielding depths (ΔX) of all these samples are not known (for the known cases ΔX varies between 10 to 20 cm, except for a single case, T-9 where ΔX is 31 cm with a low ^{26}Al activity of 37 ± 8 dpm/kg (Bhandari et al., 1979). If we adopt an average ΔX of about 15 cm the calculated profiles discussed in section IV.B.2 show that for Dhajala, an equivalent radius of 50 cm is the best choice. The range of values predicted for a 50 cm radius is from (55-42) whereas the range of values corresponding to 40 cm radius does not go below 53 dpm/kg. In

the subsequent discussion we will use an equivalent radius of 50 cm as the pre-atmospheric radius of Dhajala.

To obtain the expected activities we use the profiles corresponding to 50 cm radius, obtained in section IV.B.2, the shielding depths from Table 7 and an exposure age of 6.2 m.y. (Gopalan et al., 1977). The mean calculated values for the following 4 isotopes are,

$$^{53}Mn = 276 \text{ dpm/kg Fe}$$
$$^{54}Mn = 87 \text{ dpm/kg}$$
$$^{26}Al = 54 \text{ dpm/kg}$$
$$^{22}Na = 82 \text{ dpm/kg}$$

The observed values of ^{53}Mn, ^{54}Mn, ^{26}Al and ^{22}Na differ from the mean calculated ones by + 3 %, + 66 %, -2 %, and + 35 % respectively. For the high energy product ^{10}Be (also for ^{7}Be) produced from O, Mg, Al, Si and Fe the present model underestimates the production by a large factor. As discussed in Kohl (1975), the same discrepancy is observed in case of Lunar samples. The reason for this discrepancy is still not clear, though it was discussed by Kohl (1975) that the proton induced cross-sections used for calculation of the production rates of ^{7}Be and ^{10}Be (particularly from the light element O) are, perhaps, gross underestimates for the case of cascade neutrons from GCR. The $^{10}Be/^{7}Be$ (observed production ratio) in Dhajala is 0.14 $\pm$ .04 in good agreement with the values 0.13 $\pm$ .03 reported by Kohl (1975) for Lunar rock 78481 and Canon City meteorite. This shows that the activity of the short lived

isotope (53 days) ^{7}Be in Dhajala is consistent with the expected flux sampled by a Lunar rock in Nov-Dec 1972 (at 1 A.U.) and a meteorite in 1973.

The levels of activities in case of ^{22}Na and ^{54}Mn are affected by the solar cycle variations in the GCR fluxes (Bhandari et al., 1979) which have not been taken into account in the calculations given above. For these isotopes, detailed variations in measured GCR fluxes over the year 1965-1975 have to be taken into consideration. Observations of GCR spectra over these years were used by Bhandari et al. (1979) to calculate the modulation effect and the predicted activities for Dhajala are

$$^{54}Mn = 110 \text{ dpm/kg}$$
$$^{22}Na = 98 \text{ dpm/kg}$$

i.e. the net effect of GCR flux variation on ^{54}Mn activity is 26 % and on ^{22}Na activity + 20%. This analysis shows that the magnitude of the solar cycle effect is too small to account for the observed excess activities of ^{22}Na and ^{54}Mn.

c. Excess activity of ^{22}Na and ^{54}Mn in Dhajala

Many uncertainties in the calculations can be removed if we consider the ratio of activity of the isotopes, produced in similar reactions rather than the individual radionuclides. The $^{22}Na/^{26}Al$ (observed production ratio) in Dhajala is 2.1 and $^{54}Mn/^{53}Mn = 1.3$. These are higher than those reported in any other meteorites where $^{22}Na/^{26}Al$ is usually between 1.2 and 1.6 and $^{54}Mn/^{53}Mn$ is around 1.0. The excess of ^{22}Na and

^{54}Mn by about 15% and 40% over and above the solar minimum effect, therefore, appears to be genuine.

A comparison of the observed activities of ^{54}Mn and ^{22}Na with other meteorites is made in Table 21. Since ^{54}Mn is almost totally produced from Fe, a direct comparison of activity per kg of Fe is possible if we ignore small corrections due to the differences in the shielding effects for various meteorites. Table 21 shows that Dhajala has the highest ^{54}Mn dpm/kg Fe value observed. The Allende meteorite has a comparable value of 503 ^{54}Mn dpm/kg Fe and similar to Dhajala it has a high orbital inclination ($> 20^{o}$). From the available data presented in Table 21, it appears that the ^{54}Mn activity does not correlate inversely with the solar cycle effect but depends on the orbital inclination of the meteorites.

From the above discussion, it can be concluded that the long-term (m.y.) average GCR flux in the interplanetary space encompassed by the Dhajala orbit has been the same as around the Moon. The activities of shorter lived isotope (5-53 days) also seem to be consistent with the same flux, although for some of them the calculations are not reliable, nor do adequate observations exist in other meteorites or the Moon to allow an accurate comparison. The solar cycle effect from minima to maxima is generally within $\pm$ 20% of the mean flux adopted here. For the isotopes ^{54}Mn and ^{22}Na with half-lives of around a year, however, there seems to be a clear excess above the values expected from the GCR fluxes at the time of solar minimum near the ecliptic.

Table 21

Comparison of ^{54}Mn and ^{22}Na radioactivity with solar cycle and orbital inclination in different meteorites and a Lunar rock

	St. Severin	Allende	Murchison	Lost City	Ucera	Dhajala	Rock 14321
Type	LL6	C3	C2	H5	H5	H3	-
Date of fall	27/6/1966	21/2/1969	28/9/1969	3/1/1970	16/1/1970	28/1/1976	5/2/1971[p]
V_∞(km/s)	14[a]	-	-	14.2[c]	-	21[d]	-
Inclination(^{o})	~ 1[a]	20[b]	-	12[c]	-	28[d]	0
Shielding depth (cm)	2-5[e]	≳ 20[e]	≳ 10[e]	5-12[e]	~20[e]	11-23[f]	13.3
^{54}Mn (dpm/kg)	81±2[g]	99-128[h] (± 4)	83 ± 8[i] 101 ± 2[j]	65 ± 6[i] 85 ± 4[j]	61 ± 4[j]	144 ± 8[k]	27 ± 5[l]
Fe content (%)	19.2	23.5	25.43	27.63	26.43	27.2	10.5
^{54}Mn (dpm/kg Fe)	427	503	361	270	230	525	260
^{22}Na (dpm/kg)	72-108[g,m,n,o]	69-81 (± 2)[h]	80 ± 8[i]	80 ± 8[i]	60 ± 4[j]	111 ± 6[k]	32 ± 4[l]
Solar activity(J)*	min (2.01)	max (1.64)	max (1.52)	max (1.47)	max (1.47)	min (2.34)	max (1.14)

*J is the average GCR flux (E > 1 GeV) over one year previous to the fall (protons/cm^2.s.4π).

a Nordemann et al., (1970)
b McCrosky et al., (1969)
c McCrosky et al., (1971)
d Ballabh et al., (1978)
e Bhandari et al., (1978)
f Bagolia et al., (1977)
g Cressy (1970)
h Rancitelli et al., (1969)
i Bogard et al., (1971)
j Cressy (1971)
k This work
l Wahlen et al., (1972)
m Fireman (1967)
n Tobailem et al., (1967)
o Spannagel and Sonntag (1967)
p Date of collection

d. Spatial variation of GCR fluxes

To explain the excess activities of ^{54}Mn and ^{22}Na we now consider the possibility of an abnormally high GCR flux over the space segment of the Dhajala orbit during the last few years. Ballabh et al. (1978) have computed the orbital elements of Dhajala based on eyewitness accounts of the meteor trail. It was shown that the inclination of the orbit was $28 \pm 4^{\circ}$ to the ecliptic. Their best choice of orbital parameters are: a = 1.8 A.U. e = 0.59, q = 0.74, i = 27.6°, $\omega = 109.1^{\circ}$ and $\Omega = 307.8^{\circ}$ and the orbital period was about 2.5 years. The heliographic latitude and the heliocentric distance as a function of time before collision with the earth, computed on the basis of these orbital parameters are shown in Figure 21. From this figure it appears that the meteoroid spent a considerable fraction of its period off the ecliptic covering 20° N to 38° S heliolatitudes. The aphelion of the meteoroid is in the southern hemisphere and the highest heliographic latitude traversed is about 38°S. It is estimated that the meteoroid spent 80% and 75% of the mean life of ^{54}Mn and ^{22}Na respectively, beyond heliolatitude 15°S (Figure 21). For shorter-lived isotopes like ^{32}P, ^{33}P, ^{51}Cr, ^{7}Be most of the observed activity was produced when the meteoroid was close to the ecliptic in the northern hemisphere. The meteoroid also covered 0.7-2.8 A.U. of heliocentric distance during its orbit. Over the last few years Pioneer 10 and 11 have made direct observations of radial gradient of cosmic ray intensity in space. The results (McKibben et al.,

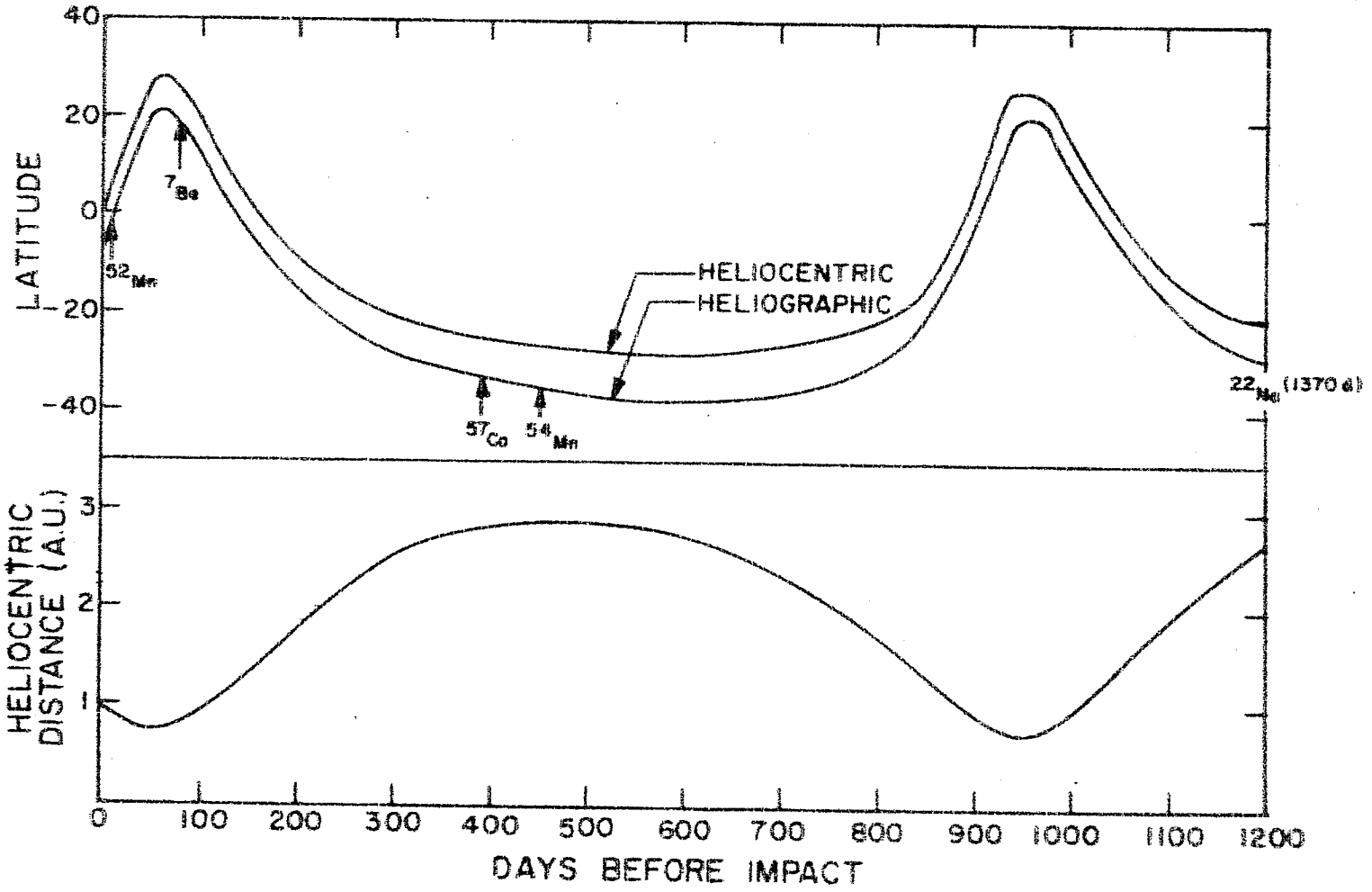

Figure 21. The variation of heliocentric and heliographic latitude, and heliocentric distance with time for the Dhajala chondrite calculated from the orbital parameters given by Ballabh et al. (1978). The mean lives of some of the isotopes are marked by arrows indicating the most important part of the orbital segments for evaluating their activities.

1977) indicate that the gradient (E > 70 MeV) is 1.4 ± 0.2% per A.U. during 1975-76 and about 3.5% during other periods. The aphelion of Dhajala was about 2.8 A.U. and thus this radial gradient can at most contribute 5% to the production of ^{54}Mn and ^{22}Na.

The data on all the radionuclides taken together can be understood if there is a higher flux of GCR at high heliolatitudes during a solar minimum. The measured values of activities in other meteorites except Allende ($i \sim 20^{o}$) are consistent with the ecliptic fluxes determined from Lunar samples (Table 21). The increase in GCR fluxes should, therefore, occur beyond 15^{o} heliolatitude. In view of the exponential build up of the isotopic activity, it is hard to estimate the gradient of GCR fluxes with latitude but a value of + 30% above the ecliptic value may be consistent with the observations of ^{22}Na and ^{54}Mn (Table 22).

Earlier estimates of the cosmic ray gradient perpendicular to the ecliptic are based on neutron monitor data and are confined to $\pm 7^{o}$ (Antonucci and Marocchi, 1976), above and below the solar equatorial plane, as covered by the inclination of the earth's orbit from September to March (Barker and Hatton, 1971; Hashim and Barcovitch, 1972). According to the analysis by Antonucci and Marocchi (1976) of data from 1962 to 1972, the cosmic ray intensity (E > 10 GeV) is higher at higher latitudes at the time of solar maximum, and the intensity minimum is obtained at the solar equatorial plane. The situation is reversed around solar minimum when the cosmic

Table 22

Comparison of the observed and expected activities of ^{22}Na and ^{54}Mn in the Dhajala chondrite

	^{22}Na	^{54}Mn
Mean observed (dpm/kg)	111	144
Expected at ecliptic[a]	82	87
Excess	+ 35%	+ 66%
Effect of solar minimum[b] (1975-1976) at ecliptic	+ 20%	+ 26%
Radial gradient[c]	+ 5%	+ 4%
Residual excess	8%	26%
Required increase in GCR flux at latitude > 15°	11%[e]	45%[e]

a Based on GCR flux J(E > 1 GeV) = 1.7 protons/cm^2.sec (4π).

b Based on observed GCR fluxes since 1965 (Garcia-Munoz et al., (1977) and references therein).

c Mckibben et al., (1977).

d Assuming that the production within ± 15° heliolatitude is the same as at the ecliptic and higher at latitudes > 15°. The irradiation periods in these two zones are based on Figure 20.

e This increase is in addition to the enhancement in the ecliptic during solar minimum.

ray maximum is detected near the solar equatorial plane while minima exist at $\pm 7^{\circ}$ latitude. There is also an asymmetrical component in the gradient across the ecliptic. When the two components are in phase, a gradient of the order of 20 % per A.U. has been deduced by them. The asymmetrical component alone gives a value of 2-8 % per A.U. as deduced by Dorman and Fischer (1966), Barker and Hatton (1971).

With the Dhajala meteorite we are able to cover a larger heliolatitude band because of its higher inclination. Our observations indicate that the situation is significantly different at high heliolatitudes. The flux of GCR is much higher at solar minimum at latitudes exceeding $15-20^{\circ}$S, compared to that at ecliptic. Such an increase in GCR flux is qualitatively expected from sunspot activity and coronal green line intensity which are less at high heliolatitudes, particularly in the south during the solar minimum.

IV.B.5. Measured depth profile of ^{53}Mn activity in cores

In section IV.B.2 production profiles of ^{53}Mn activity were derived by an extension of the Reedy-Arnold method to chondrites and in section IV.B.3 a comparison of the calculations with available data on ^{53}Mn (in spot samples of chondrites) was made. For an accurate evaluation of the depth profiles it is essential to know the preatmospheric size of the meteorite and the depth of the samples studied. In the present section we will discuss the results obtained in the four meteorite-cores in this context.

The equivalent radii of the four meteorites were derived from an analysis of the nuclear tracks and, as discussed in chapter III, they are given below with the adopted exposure ages in brackets:

Madhipura R_o =6.5 cm (15.0 m.y.)

Udaipur R_o = 9 cm (22.0 m.y.)

Bansur R_o = 15 cm (10.0 m.y.)

St. Severin R_o = 20 cm (11.2 m.y.)

It is to be noted that only in rare cases a meteorite can be expected to have a near spherical pre-atmospheric shape. From the available studies, on St. Severin (Cantelaube et al., 1969), Keyes (Lorin, 1975) Bansur, Udaipur (this work) it can be seen that approximating the pre-atmospheric shape by a sphere of equivalent radius is to be done with caution. For example, data from a core taken along the longest axis of an ellipsoidal meteorite (like core 2-4 in Keyes) should be interpreted in terms of sphere whose radius has a value intermediate between the other two axes and closer to the shorter one. To obtain an equivalent radius for a meteorite, a reconstruction of the meteorite from an analysis of track densities at the surface samples is essential. After this is done, the direction of the core will determine the effective radius applicable to the interpretation of data.

The radii values assigned to the four meteorites in this workwere done in the light of the above discussion. The exposure ages adopted for the analysis and the procedure

for getting effective depths of the samples have been discussed before. Table 23 summarises the effective depth and the ^{53}Mn activity of the samples for the four meteorites. The depth profiles of ^{53}Mn activity for the four cases are shown in Figures 22 and 23. The solid lines in the figures show the expected profiles for the corresponding sizes and exposure ages based on the model developed in section IV.B.2.

The figures show that for small size meteorites (Madhipura, Udaipur and Bansur) the measured activity profiles are more or less flat and the maximum variations are 10%, 7% and 12% i.e. $\pm$ 5%, $\pm$ 3.5% and $\pm$ 6% over the mean respectively. There is a tendency for an increase in activity towards the centre of the meteorite (suggested by the dotted curves). For the largest body St. Severin (R_o = 20 cm) the increase from surface to the centre is 43% while for the smaller bodies the increment is 10% or less. These experimental profiles can be compared to the theoretical ones (shown by solid lines in Figures 22 and 23) for Udaipur, Bansur and St. Severin. Madhipura has a size (R_o = 6.5 cm) which is too small for extrapolation from the profiles available in Figure 17. For Udaipur (R_o = 9 cm) and St. Severin (R_o = 20 cm) there is a good agreement in the shape of the experimental and theoretical profiles while for Bansur (R_o = 15 cm) there is no agreement. As far as the absolute magnitude is concerned the deviation from predicted values increases with the size of the meteorite and they are about 5% (Udaipur, 9 cm), 20% (Bansur, 15 cm) and 17% (St. Severin, 20 cm). It was seen in section IV.B.2 that

Table 23

The effective depths and ^{53}Mn activities in the core-samples from four chondrites

Meteorite	Effective radius (cm)	Sample	Depth along core (cm)	Effective depth (cm)	^{53}Mn activity (dpm/kg Fe)
Madhipura	6.5	M-1	0.5	3.5	272 ± 13
		M-2	2.5	5.5	290 ± 17
		M-3	4.3	5.7	275 ± 14
Udaipur	9.0	6-1	0.5	3.7	300 ± 15
		C-2	2.4	4.8	296 ± 15
		C-1	4.3	6.3	314 ± 15
		# 4	~6.1	9.0	317 ± 16
Bansur	15.0	13-1	0.1	2.4	361 ± 19
		13-2	1.3	3.3	351 ± 17
		13-3	2.7	4.3	339 ± 17
		13-4	4.0	5.0	352 ± 18
		14-3	8.6	6.8	357 ± 18
		14-1	10.4	7.0	378 ± 19
St. Séverin	20.0	CB4-1	~0.0	0.4	300 ± 16
		-2	0.2	0.6	313 ± 16
		-10	2.0	2.2	312 ± 17
		-25	9.1	6.0	338 ± 17
		-32	16.1	4.4	351 ± 17
		A-III-10	2.8	4.6	342 ± 17
		-23a	7.5	9.3	401 ± 21
		-25b,c	26.0	16.0	429 ± 22

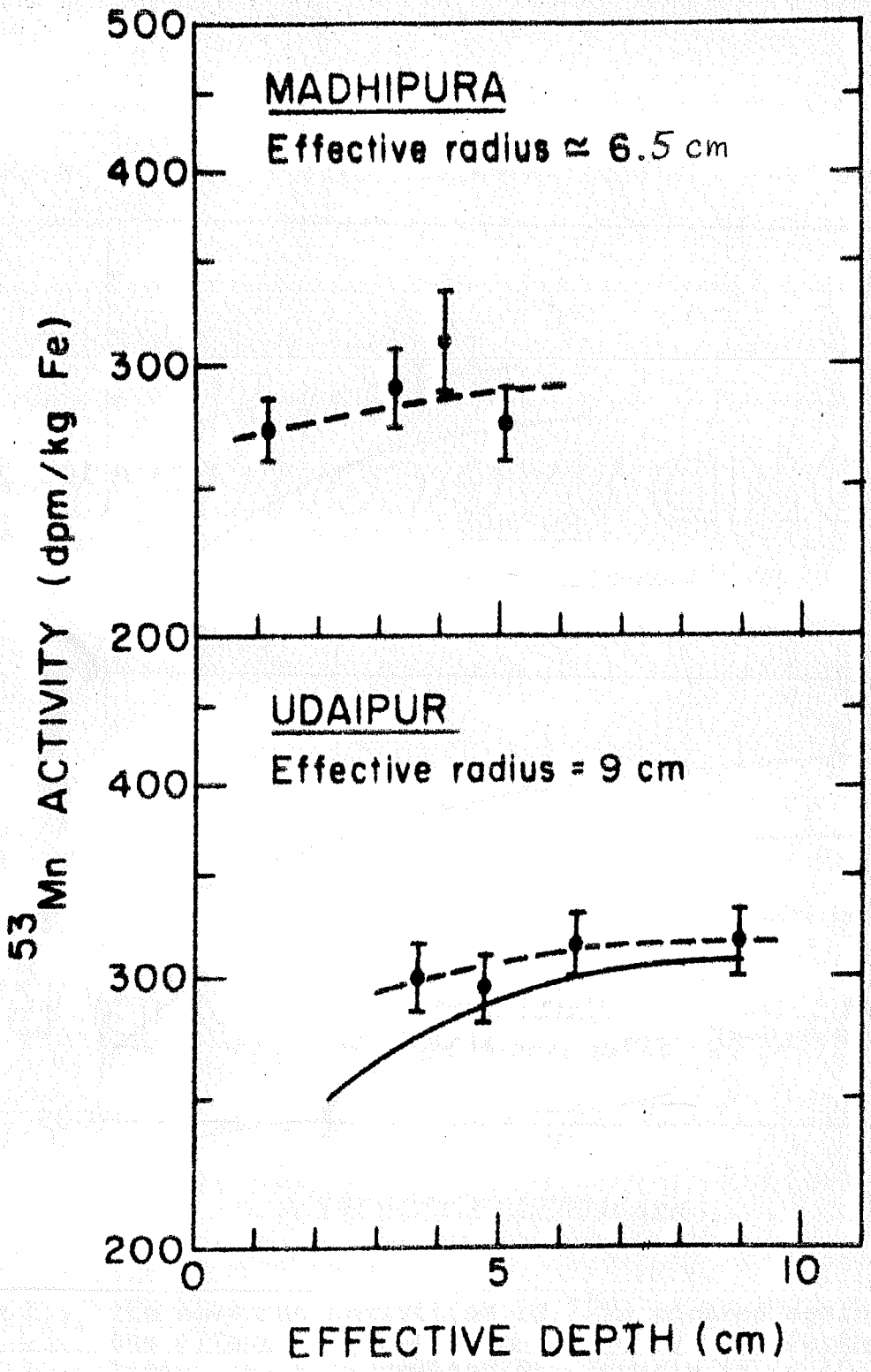

Figure 22. The measured activities of ^{53}Mn plotted against the effective pre-atmospheric shielding depths for Madhipura (R_o= 6.5 cm) and Udaipur (R_o = 9 cm) samples. The dotted lines indicate the best fit experimental profiles. The solid line for Udaipur is the theoretical profile expected from the model discussed in the text.

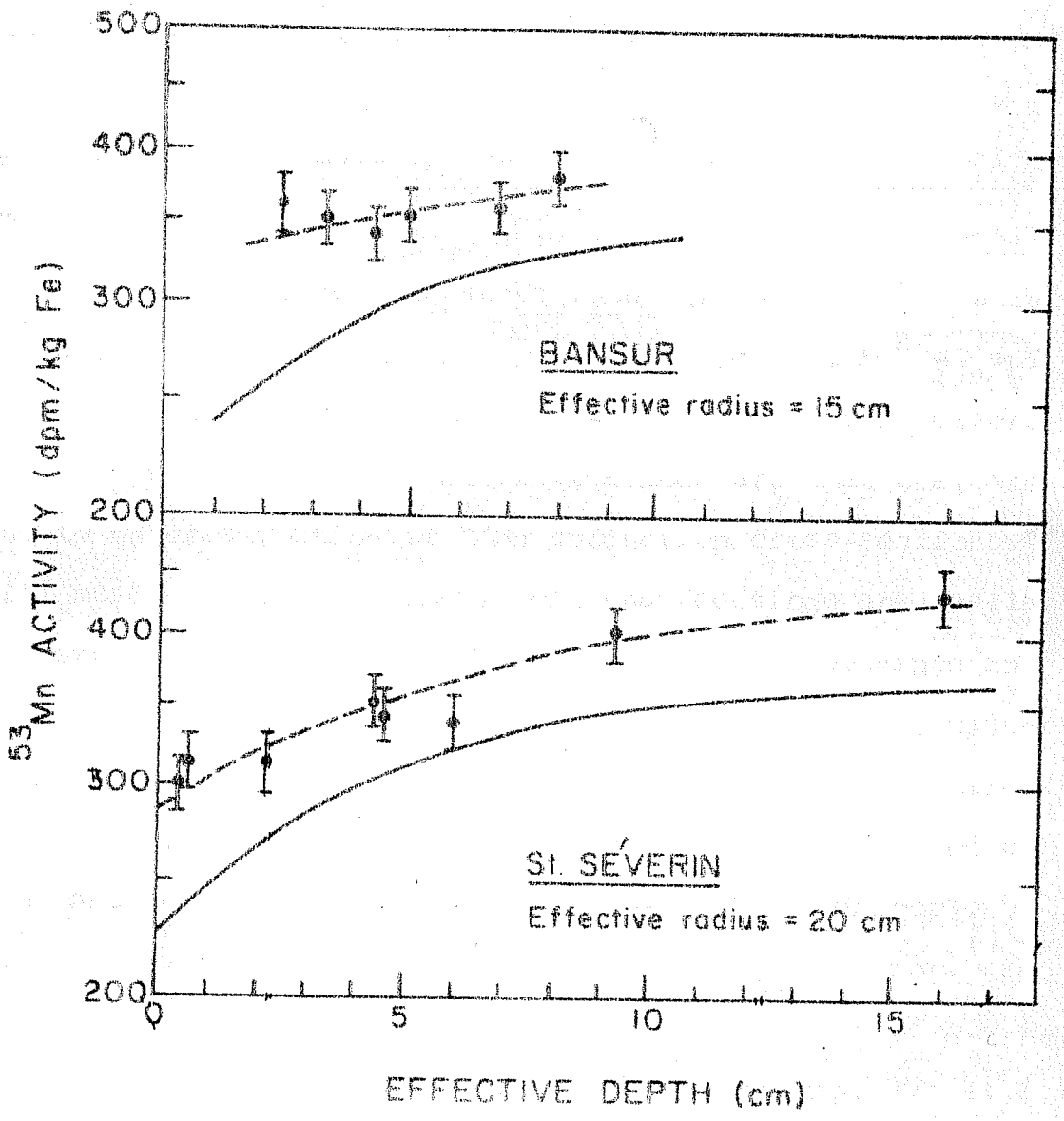

Figure 23. The measured activities of ^{53}Mn plotted against the effective pre-atmospheric shielding depths for Bansur (R_o = 15 cm) and St. Severin (R_o = 20 cm) samples. The dotted lines indicate the best fit experimental profiles. The solid lines are the theoretical profiles expected from the model discussed in the text.

the average discrepancy between the calculated values and the observed data was about 45% for moderate size meteorites ($\gtrsim$ 20 cm). If one increases the shape parameter α for small size bodies, as suggested by analysis of ^{26}Al data, the under-prediction of calculations for small size bodies ($\lesssim$20 cm) will increase to about 45% as in the case of moderate size bodies.

These considerations suggest that with the same set of α values and flux it is not possible to fit both ^{26}Al and ^{53}Mn activities in meteorites. The reason for this discrepancy is still not clear but indications are that they are due to underestimation of ^{53}Mn production cross-sections. Till more confident estimates of cross-sections are available the experimental profiles of ^{53}Mn activity as obtained in this work should be used for analysing activities in case of chondrites of size range (6-20) cm. The observed profiles for this purpose is to be corrected for undersaturation of ^{53}Mn determined from the exposure ages. For Madhipura, Udaipur, Bansur and St. Severin the correction factors are 1.06 (Madhipura, T = 15 m.y.), 1.02 (Udaipur, T = 22 m.y.), 1.18 (Bansur, T = 10 m.y.) and 1.13 (St. Severin, T = 11.2 m.y.) respectively. (Schultz and Signer (1976) gives exposure age of St. Severin as T = 10.8 m.y. If this value is adopted the factor is 1.15.) In the above discussion the half-life of ^{53}Mn is taken as 3.7 m.y. (Honda and Imamura, 1971).

Recently, Englert and Herr (1978 b) have analysed 13 samples from St. Severin core AIII. Three samples from AIII

core were also studied in this work. If we compare the absolute data in our samples taken from nearby locations of samples studied by Englert and Herr (1978 b) there is some discrepancy. Our 3 values are higher by (6-9)%. Though the range (6-9) % lie within the uncertainties, the discrepancy is perhaps due to the difference in ^{53}Mn standards. The 'Koln standard' reported in Englert and Herr (1978 a) gave an 'amplification factor' 2.7% higher compared to Tokyo 'GI' and 'GII' standard. The standard used in the present work was Tokyo Bogou II standard. In the present irradiation, another batch of samples was irradiated with GI standard and gave an 'amplification factor' 4.0% higher than Bogou II standard (Imamura, priv. comm.). It is, therefore, possible that Bogou II standard, used in the present work, differs by about 7% from the koln standard. This difference is in the right direction (i.e. higher amplification factor for Koln standard leading to lower absolute ^{53}Mn activity) to account for the observed discrepancy. This difference can be resolved by intercalibration of the four standards (GI, GII, B-II and Koln standard).

The general shape of the profile obtained by Englert and Herr (1978 b) is in good agreement with the present work. The enhancement found by them in core AIII is about 25% in contrast to our enhancement of 43% from the combined data of cores CB4 and AIII. The reason is that our samples CB4-1 and CB4-2 are from locations closer to the pre-atmospheric surface compared to their sample A-III-6 (pre-atmospheric

depth = 3.6 cm). The shape of the measured depth profile by Englert and Herr (1978 b) agrees excellently with the predicted profile based on the present model and is shown in Figure 23. Based on the experimental data in Figures 22 and 23 and correcting for the exposure ages by factors mentioned before one can construct the production profiles of ^{53}Mn activity for chondrites of various radii. The depth dependence of saturated ^{53}Mn activity for radii 6.5, 9.0, 15.0, 20.0 cm is shown in Figure 24 alongwith the profile for Moon given by Imamura et al. (1974). The figure shows that the saturated activity increases with size initially (5 to 15 cm range) attaining steady value in the moderate size range (15 to 20 cm). The activity for a very large body is 1.5 to 2.5 times lower compared to the smaller sized bodies (5 to 20 cm) due to the effect of geometry. The activity profile for 15 cm size lies a little above that for 20 cm size. This could be due to an underestimation in the assumed exposure age for Bansur (10 m.y.). A remeasurement of rare gas age for Bansur is being done at P.R.L. to settle this point.

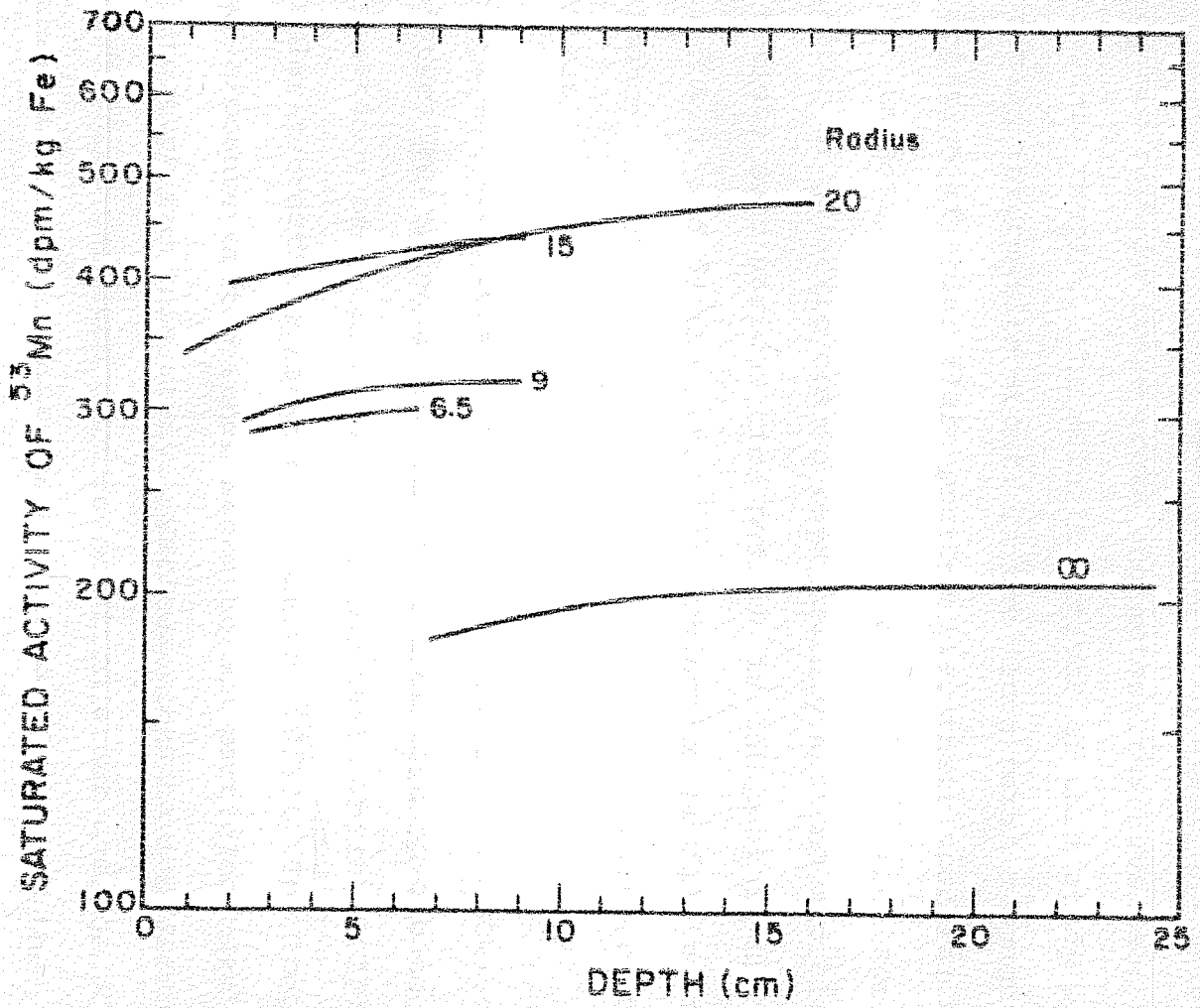

Figure 24. Production profiles of ^{53}Mn in chondrites of radii 6.5, 9.0, 15.0, 20.0 cm. The curve for infinite radius refers to Moon (from Imamura et al., 1974) and is applicable to a very large size chondrite.

Chapter V

Conclusions

Radioactive isotopes produced by solar and galactic cosmic rays in Lunar rocks and meteorites have been studied in this thesis. The main objectives of this study was to obtain information about: 1) the 'long term' average characteristics of solar flare protons i.e. their spectral shape (R_o) and intensity (J), 2), the average intensity and spectral parameter of galactic cosmic rays (mainly protons and alpha particles) over various time periods in the past in the space 1-3 A.U. and 3) the nature of production profile of isotopes induced by GCR particles inside meteorite bodies of different sizes.

The work related to the solar cosmic ray (SCR) characteristics was taken up in view of the continuing debate on the constancy of solar activity in the past (White, 1977) and solar-terrestrial relations (Ulrich, 1975). The long durations of exposure of the Lunar rocks to SCR particles make them ideal detectors for this study. Various rocks having different periods of exposure give information about average SCR characteristics in different windows of time in the past. A simultaneous study of such rocks could then be used to infer the relative variation in these characteristics (J, R_o) over different time periods.

The study of constancy of galactic cosmic ray (GCR) in the past is of considerable importance in Astrophysics. The GCR particles having high energies represent a substantial fraction of the energy density in our galaxy. Any time variation in the GCR intensity will have a considerable bearing on theories of energy production in the galaxy. Cosmogenic radioisotopes of varying half-lives span different windows of time in the past and thereby a relative variation in GCR intensity is detectable by simultaneous study of different radioisotopes. A large group of meteorites has been analysed from this point of view in this work. A drastic variation in GCR intensity has been ruled out by previous studies (Arnold et al. 1961). However, fine scale variation over 10^5-10^8 yr has been suspected from the study of ^{26}Al-^{53}Mn, ^{36}Cl-^{36}Ar, ^{40}K-^{41}K, in meteorites and Lunar samples (Rançitelli et al. 1975; Schaeffer, 1975). The uncertainty in the interpretation of these data stems from the absence of accurate production rates of radioisotopes in meteorites and Lunar samples. A semi-empirical approach is best suited for this purpose. Accurate measurement of radioisotope activity coupled with information on shapes, sizes and shielding depths in meteorite bodies provides the starting point for such an approach.

The main results and conclusions arrived from the work on these three topics are described below.

A. Average SCR parameters in the past

Five Lunar rocks having surface exposure periods, 0.5, 1.0, 1.5 and 3.7 m.y. were studied for cosmogenic radio-

isotope ^{26}Al produced by SCR and GCR. The depth dependent activities are consistent with an average SCR flux

$$J\ (E > 10\ MeV) = 125 \pm 25\ protons/cm^2.sec\ (4\pi)$$

and a spectral parameter

$$R_o = 150\ MV$$

over the last few (2-3) million years.

The data on the five rocks also show that these parameters are mutually consistent within ± 20% (the quoted range on J) over the periods of exposure of the rocks. These results indicate that there has been no major long term (> 10^5 year) change in the emission of energetic particles from the sun over the past 0.5 to about 3 m.y. If particle emission and other radiations are related, these observations rule out any major change in the solar activity over the past few million years. Larger variations in flux over time-scales shorter than about 10^5 yrs are, however, not detectable by the present method.

B. GCR intensity deduced from meteorite studies

i) A model has been developed for calculating the production rates of radioisotopes by a semi-empirical method based on Reedy and Arnold (1972). Data on the activities of ^{26}Al (half-life = 0.72 m.y.) and ^{53}Mn (half-life = 3.7 m.y.) in meteorites, available from literature and this work, have been analysed with the help of this model for detecting

possible GCR variations. The analysis indicates that ^{26}Al activity and ^{53}Mn activity are not mutually consistent with the estimates of production rates. ^{26}Al activities in the meteorites are overpredicted for small size bodies and agree with the production rates for moderate size bodies. For ^{53}Mn, the model prediction agrees with observed activities for small size bodies but deviates significantly (by about -45%) for moderate size bodies. These observations indicate that the production rates of these two isotopes cannot be fitted with the same set of GCR parameters. This misfit was also noted in earlier studies on Lunar rocks by La Jolla group and Battelle group (Kohl, 1977 and Rancitelli et al., 1975). An analysis of meteorites having short exposure ages show that this is not due to a variation in GCR flux over the mean-lives of these two isotopes. The indications are that the cross-sections used for ^{53}Mn production rate calculations are under-estimated.

ii) A relative study of various radioisotopes ranging in half-lives from 5.6 days to 3.7 m.y. in the fresh fall Dhajala shows that (a) the average GCR fluxes over a period of million years are same at heliolatitude upto $40^{o}S$ as near the ecliptic, and (b) during solar minimum the GCR fluxes enhance by about 30% at heliolatitude band $15-40^{o}S$ over and above the 38% observed at the ecliptic due to solar modulation. This implies that during the solar minima the modulation of GCR fluxes is smaller beyond $15^{o}S$, and during the solar maxima, the fluxes are correspondingly less, resulting in the same average intensity.

C. Activity profiles of ^{53}Mn in chondrites

Cosmic ray induced ^{53}Mn activities and nuclear track densities have been measured in samples from cores taken from four chondrites - Madhipura, Udaipur, Bansur and St. Severin. Track density studies establish that these four chondrites had pre-atmospheric shapes equivalent to spheres to radii 6.5, 9, 15 and 20 cm respectively. The track densities in the core-samples are used for determining the shielding depths of the samples. Assuming that these meteorites have received typical cosmic ray irradiation, ^{53}Mn activity profiles in chondrites of four different sizes have been obtained.

The profiles show that for chondrites having effective radius less than 15 cm the increase in activity from near surface region to the centre is small (less than 10%). For St. Severin (20 cm) the increase is about 45% thus indicating that the cascade of secondaries becomes important only for sizes greater than 15 cm.

The important conclusions can be summarised as follows.

1. The solar activity, as evidenced by solar flare protons, has remained constant within $\pm$ 20% over the last (2-3) m.y. and the long-term SCR flux is characterised by

$$J = 125 \pm 25 \text{ protons/cm}^2 \text{ sec } (4\pi)$$

$$R_o = 150 \text{ MV}$$

2. The long-term GCR flux over the last few to about 10 m.y. has not changed significantly as evidenced by ^{26}Al and ^{53}Mn activities in meteorites.

3. The discrepancy between the observed and calculated ^{53}Mn activities in meteorites and Lunar samples is possibly due to an under-estimation of ^{53}Mn production cross-sections (by about 40%) and further studies are necessary to establish this firmly.

4. The GCR flux at high heliolatitudes (> 15°) was significantly high, by about 30%, compared to that near the ecliptic during the solar minimum of 1976.

5. The activity profile of ^{53}Mn is flat (within 10%) for small size (less than 15 cm) chondrites. For larger sizes (20-30 cm) the cascade of secondaries develop significantly and the activity increases with the depth upto the centre by about 40%.

Further scope

In the light of the discussions presented above the following studies should be useful in extending the conclusions and establishing some of the points more firmly.

The results on ^{26}Al activity on Lunar rocks clearly show that no major change (within $\pm$ 20%) in solar activity has taken place over the past (2-3) m.y. Using the radioisotope ^{26}Al (half-life = 0.72 m.y.) one cannot go beyond (2-3) m.y. because of saturation effects. For extending the time-span, the next promising isotope is ^{53}Mn (half-life = 3.7 m.y.). It is produced mainly from iron and the detection method by n-activation is now well-established. The ^{53}Mn activity in the near surface regions of Lunar rocks having surface

exposure ages more than (2-3) m.y. can give information about the relative intensity and spectrum of SCR particles over a larger time-scale. The important point is to establish the surface exposure ages by nuclear tracks and rare-gas studies. The plateau method using tracks described in the present work can be used for this purpose. Recently, Rao et al. (1979) have developed a method for determining surface exposure ages by rare-gas analysis. These two methods can also be used for determining the erosion rate of the rocks which is another crucial parameter in the analysis of radioisotope data. Recently, Kohl et al. (1978) have concluded from ^{53}Mn profiles in three rocks 12002, 14321 and 68815 that SCR flux has remained constant within the past 10 m.y. But the exposure ages used for their calculation are GCR ages and they need not necessarily be the surface exposure ages as discussed before. In fact, the track data of various rocks suggest that on Lunar surface a rock face does not survive for more than about 5 m.y. without chipping or fragmentation. Further studies in tracks, rare-gases and ^{53}Mn activities are necessary to establish the constancy of SCR flux over the time-scale of 5-10 m.y.

Regarding the GCR intensity in the past a drastic variation can be ruled out (Arnold et al. 1961). To detect any finer variation it is now important to establish production rates of ^{26}Al and ^{53}Mn as a function of size (effective radius) of the meteorite and shielding depths of the samples. In the present study the production rates for ^{53}Mn has been

established for chondrites of sizes ranging from 5 to 20 cm. Bhandari et al. (1978, priv. comm.) have recently deduced preatmospheric sizes of several meteorites from analysis of nuclear tracks. In case of about 25 meteorites, the preatmospheric sizes are reliably known. Samples or cores from these meteorites can be analysed for tracks and radioactivities to establish the size and depth dependence of the isotope production. It is especially important to study big meteorites of sizes > 20 cm. The present study has established that the cascade of nuclear active particles becomes important only for bodies > 15 cm. Another interesting aspect would be to follow the development of cascade in bigger bodies and to determine the size range where the production profile reaches its peak. The extent of variation in activity of radioisotopes due to the size and depth dependence in production has to be isolated before any firm statement can be made regarding minor variation in GCR fluxes in the past.

The core-samples from the meteorites studied in this work are also available for destructive analysis to measure the activity of ^{26}Al. A simultaneous measurement of ^{26}Al activity in these meteorites will establish the empirical production rate of ^{26}Al. These two sets of data can then be used for detecting any fine scale variation in GCR intensity independent of model calculations.

REFERENCES

Amin B.S., Lal D., Lorin J.C., Pellas P., Rajan R.S., Tamhane A.S. and Venkatavaradan V.S. (1969) On the flux of low energy particles in the solar system during the last 10 million years. In Meteorite Research, (ed. P.M. Millman), 316-327, D. Reidel Publ. Co.

Antonucci E. and Marocchi D. (1976) Cosmic ray perpendicular gradient during 1962-1972. J. Geophys. Res. 81, 4627-4632.

Apollo 16 Preliminary Science Report (1972). NASA SP-315.

Apollo 17 Preliminary Science Report (1972). NASA SP-330.

Arnold J.R., Honda M. and Lal D. (1961) Record of cosmic ray intensity in the meteorites. J. Geophys. Res. 66, 3519-3531.

Bagolia C., Doshi N., Gupta S.K., Kumar S., Lal D. and Trivedi J.R. (1977) The Dhajala meteorite shower: atmospheric fragmentation and ablation based on cosmic ray track studies. Nuclear track det., 1, 83-92.

Ballabh G.M., Bhatnagar A. and Bhandari N. (1978) The orbit of the Dhajala meteorite. Icarus, 33, 361-367.

Barker M.C. and Hatton C.J. (1971) Evidence for a cosmic ray gradient perpendicular to the solar equatorial plane. Planet. Space Sci. 19, 549-560.

Begemann F., Weber H.W., Vilcsek E. and Hintenberger H. (1976) Rare gases and ^{36}Cl in stony-iron meteorites: cosmogenic elemental production rates, exposure ages, diffusion losses and thermal histories. Geochim. Cosmochim. Acta, 40, 353-368.

Bhandari N. (1969) A selective and versatile low level Beta-, X-, and Gamma-ray detector assembly. Nucl. Instr. Meths., 50, 251-256.

Bhandari N., Goswami J.N., Lal D., Macdougall D. and Tamhane A.S. (1972) A study of the vestigial records of cosmic rays in lunar rocks using a thick section technique. Proc. Ind. Acad. Sci., LXXVI, 1, Sec A. 27-50.

Bhandari N., Bhattacharya S.K. and Padia J.T. (1975) The surface radioactivity of lunar rocks: implications to solar activity in the past. Proc. Lunar Sci. Conf. 6th, 1913-1925.

Bhandari N., Lal D., Trivedi J.R. and Bhatnagar A. (1976 a) The Dhajala meteorite shower. Meteoritics, 11, 137-147.

Bhandari N., Bhattacharya S.K. and Padia J.T. (1976 b) Solar proton fluxes during the last million years. Proc. Lunar Sci. Conf. 7th, 513-523.

Bhandari N., Bhattacharya S.K. and Somayajulu (1978) Cosmogenic radioisotopes in the Dhajala chondrite: Implications to variations of cosmic ray fluxes in the interplanetary space. Earth Planet. Sci. Lett., 40, 194-202.

Bhandari N., Lal D., Arnold J.R., Marti K., Rajan R.S. and Moore C.B. (1978) Atmospheric ablation in meteorites based on cosmic ray tracks. Meteoritics, 13, 391-394.

Bhandari N., Bhattacharya S.K. and Potdar M.B. (1979) Production profiles of radionuclides in chondrites and their solar cycle variation (abstract). In Lunar and Planetary Sci. X, 107-109, The Lunar and Planetary Institute, Houston.

Bhandari N., Prabhakara H.R. and Raman T. (1979) Meteorite record of the cosmic rays during the Maunder Minimum based on ^{39}Ar (abstract). In Lunar and Planetary Sci. X, 110-112, The Lunar and Planetary Institute, Houston.

Bhattacharya S.K., Goswami J.N. and Lal D. (1973) Semi-empirical rates of formation of cosmic ray tracks in spherical objects exposed in space: preatmospheric and postatmospheric depth profiles. J. Geophys. Res. 78, 8356-8363.

Bhattacharya S.K., Goswami J.N., Gupta S.K. and Lal D. (1973) Cosmic ray effects induced in a rock exposed on the moon or in free space: Contrast in patterns for tracks and isotopes. The Moon, 8, 253-286.

Bhattacharya S.K. and Bhandari N. (1975) Effects of exposure conditions on cosmic-ray records in lunar rocks. Proc. Lunar Sci. Conf. 6th, 1901-1912.

Bhattacharya S.K. and Bhandari N. (1976) Modulation of galactic cosmic rays from the study of cosmogenic radioisotopes in meteorites. Proc. Symp. Solar Planet. Phys. 2, 161-169, Ahmedabad, India.

Bhattacharya S.K., Bhandari N. and Perelygin V.P. (1979) Production profile of cosmogenic ^{53}Mn in the Marjalahti pallasite. To appear in J. Geophys. Res.

Bogard D.D., Clark R.S., Keith J.E. and Reynolds M.A. (1971) Noble gases and radionuclides in Lost City and other recently fallen meteorites. J. Geophys. Res. 76, 4076-4083.

Bogard D.D. and Gibson E.K. Jr. (1975) Volatile gases in breccia 68115 (abstract). In Lunar Science VI, 63-65. The Lunar Science Institute, Houston.

Booth N.E., Ledley B., Walker D. and White D.H. (1957) Nuclear cross-sections for 900 MeV protons. Proc. Phys. Soc. (London), 70A, 209-218.

Cameron I.R. and Top Z. (1974) Measurement of ^{26}Al in stone meteorites and its use in the derivation of orbital elements. Geochim. Cosmochim. Acta, 38, 899-909.

Cantelaube Y., Nordemann D., Pellas P. and Tobailem J. (1969) Reconstitution de la meteorite Saint-Severin dans l'espace. In Meteorite Research, (ed. P.M. Millman), 705-713, D. Reidel Publ. Co.

Compton A.H. and Allison S.K. (1968) X-rays in Theory and Experiment. East West Student Edition, D. Van Nostrand Co. Inc.

Cressy P.J. (1964) Cosmogenic radionuclides in stone meteorites. Ph.D. Thesis, Carnegie Inst. of Technology, U.S.A.

Cressy P.J. (1970) Multiparameter analysis of gamma radiation from the Barwell, St. Severin and Tatlith meteorites. Geochim. Cosmochim. Acta, 34, 771-779.

Cressy P.J. (1971) Cosmogenic radionuclides in the Lost City and Ucera meteorites. J. Geophys. Res. 76, 4072-4075.

Cressy P.J. (1975) ^{26}Al in cores of the Keyes chondrite. J. Geophys. Res. 80, 1551-1554.

Cressy P.J. and Bogard D.D. (1976) On the calculation of cosmic ray exposure ages of stone meteorites. Geochim. Cosmochim. Acta, 40, 749-762.

Davis R. Jr. (1972) A progress report on the solar neutrino experiment. Bull. Amer. Phys. Soc. 17, 527-528.

Davis R. Jr. and Evans J.C. (1973) Experimental limits on extra-terrestrial sources of neutrinos. Proc. 13th Int. Conf. Cosmic Rays, 2001-2006.

Dorman L.I. and Fischer S. (1965) Influence of the changes in earth's heliolatitude on the cosmic ray intensity in 1963-1964 and evaluation of the cosmic ray intensity gradient perpendicular to the ecliptic plane. Proc. 9th Int. Conf. Cosmic Rays, 239-242.

Dust S. and Crozaz G. (1977) 68815 revisited. Proc. Lunar Sci. Conf. 8th, 2315-2319.

Ebert K.H. and Wanke H. (1957) Uber die Einwirkung der Hohenstrahlung auf Eisenmeteorite. Z. Naturforsch. 12a, 766-773.

Eddy J.A. (1976) The Maunder minimum. Science 192, 1189-1202.

Eldridge J.S., O'Kelley G.D. and Northcutt K.J. (1973) Radionuclide concentrations in Apollo 16 lunar samples determined by non-destructive gamma-ray spectrometry. Proc. Lunar Sci. Conf. 4th, 2115-2122.

Englert P. and Herr W. (1978 a) A study of exposure ages of chondrites based on spallogenic ^{53}Mn. Geochim. Cosmochim. Acta, 42, 1635-1643.

Englert P. and Herr W. (1978 b) ^{53}Mn exposure ages of chondrites and depth dependent variations of the ^{53}Mn production rate. Meteoritics, 13, 454-458.

Ezer D. and Cameron A.G.W. (1972) Effects of sudden mixing in the solar core on solar neutrinos and ice ages. Nature 240, 180-182.

Finkel R.C. (1972) Depth profiles of galactic cosmic ray produced radionuclides in lunar samples. Ph.D. Thesis, University of California, San Diego, U.S.A.

Finkel R.C., Kohl C.P., Marti K., Martinek B. and Rancitelli L. (1978) The cosmic ray record in the San Juan Capistrano meteorite. Geochim. Cosmochim. Acta, 42, 241-250.

Fireman, E.L. (1967) Radioactivities in meteorites and cosmic-ray variations. Geochim. Cosmochim. Acta, 31, 1691-1700.

Fowler W.A. (1972) What cooks with solar neutrinos? Nature 238, 24-26.

Fritz J.S. and Pietrzyk D.J. (1961) Non-aqueous solvents in anion-exchange separations. Talanta, 8, 143-162.

Garcia-Munoz M., Mason G.M. and Simpson J.A. (1977) The appearances of superfluxes of quiet time cosmic rays. Proc. 15th Int. Conf. Cosmic Rays, 3, 209-211.

Gensho R., Nitoh O., Makino T. and Honda M. (1977) Some long-lived and stable nuclides produced by nuclear reactions. Proc. 2nd Symp. on Origin and Distribution of the elements. Paris. IAGC.

Gopalan G. and Rao M.N. (1976) Rare gases in Bansur, Udaipur and Madhipura chondrites. Meteoritics, 11, 131-136.

Gopalan K., Rao M.N., Suthar K.M. and Venkatesan T.R. (1977) Cosmogenic and radiogenic noble gases in the Dhajala chondrite. Earth Planet. Sci. Lett., 36, 341-346.

Goswami J.N. (1977) Nuclear tracks in extra-terrestrial silicate grains. Ph.D. Thesis, Gujarat University, Ahmedabad, India.

Gupta S.K. and Lal D. (1978) On estimation of mass ablation of meteorites based on studies of cosmic ray tracks. Nuclear Track Det., 2, 37-49.

Hartung J.B., Horz F., Aitken F.K., Gault D.E. and Brownlee D.E. (1973) The development of microcrater populations on lunar rocks. Proc. Lunar Sci. Conf. 4th, 3213-3234.

Hashim A. and Barcovitch M. (1972) A cosmic ray density gradient perpendicular to the ecliptic plane. Planet. Space Sci., 20, 791-801.

Heimann M., Parekh P.P. and Herr W. (1974) A comparative study on ^{26}Al and ^{53}Mn in eighteen chondrites. Geochim. Cosmochim. Acta, 38, 217-234.

Herpers U., Herr W. and Wolfle R. (1969) Evaluation of ^{53}Mn by (n, γ) activation, ^{26}Al and special trace elements in meteorites by γ-coincidence techniques. In Meteorite Research, (ed. P.M. Millman), 387-396, D. Reidel Publ. Co.

Herzog G.F. and Cressy P.J. (1974) Variability of the ^{26}Al production rate in ordinary chondrites. Geochim. Cosmochim. Acta, 38, 1827-1841.

Heymann D. and Anders E. (1967) Meteorites with short cosmic ray exposure ages, as determined from their ^{26}Al content. Geochim. Cosmochim. Acta, 31, 1793-1810.

Heymann D. and Hubner W. (1974) Origin of inert gases in 'Rusty Rock' 66095. Earth Planet. Sci. Lett., 22, 423-426.

Honda M., Umemoto S. and Arnold J.R. (1961) Radioactive species produced by cosmic rays in Bruderheim and other stone meteorites. J. Geophys. Res., 66, 3541-3546.

Honda M. and Imamura M. (1971) Half-life of ^{53}Mn. Phys. Rev. C. 4, 1182-1188.

Imamura M., Matsuda H., Horie K. and Honda M. (1969) Applications of neutron activation method for ^{53}Mn in meteoritic iron. Earth Planet. Sci. Lett., 6, 165-172.

Imamura M., Finkel R.C. and Wahlen M. (1973) Depth profile of ^{53}Mn in the lunar surface. Earth Planet. Sci. Lett., 20, 107-112.

Imamura M., Nishiizumi K., Honda M., Finkel R.C., Arnold J.R. and Kohl C.P. (1974) Depth profiles of ^{53}Mn in lunar rocks and soils. Proc. Lunar Sci. Conf. 5th, 2093-2103.

Kohl C.P. (1975) Galactic cosmic ray produced radioactivity in Lunar and chondritic materials. Ph.D. Thesis, University of California, San Diego, U.S.A.

Kohl C.P., Russ III G.P., Arnold J.R., Nishiizumi K., Imamura M. and Honda M. (1977) ^{53}Mn in lunar cores: Evidence for the time scale of surface gardening (abstract). In Lunar Science VIII, 552-554, The Lunar Science Institute, Houston.

Kohl C.P., Murrell M.T., Russ III G.P. and Arnold J.R. (1978) Evidence for the constancy of the solar cosmic ray flux over the past ten million years: ^{53}Mn and ^{26}Al measurements. Proc. Lunar Planet. Sci. Conf. 9th, 2299-2310.

Kohman T.P. and Bender M.L. (1967) Nuclide production by cosmic rays in meteorites and on the moon. In High Energy Nuclear Reactions in Astrophysics, (ed. B.S.P. Shen), 169-245, Benjamin.

Kolesnikov E.M., Otgonsuren O., Perelygin V.P. and Fisenko A.V. (1977) On the determination of preatmospheric size of Marjalahti meteorite. Meteoritika, 36, 82-86.

Lal D. and Schink D.R. (1960) Low background thin-wall flow counters for measuring beta activity of solids. Rev. Sci. Instrum. 31, 395-398.

Lal D., Lorin J.C., Pellas P., Rajan R.S. and Tamhane A.S. (1969) On the energy spectrum of the iron-group nuclei as deduced from fossil-track studies in meteoritic minerals. In Meteorite Research, (ed. P.M. Millman), 275-285, D. Reidel Publ. Co.

Lal D. and Trivedi J.R. (1977) Observations on the spatial distribution of Dhajala meteorite fragments in the strewn field. Proc. Ind. Acad. Sci., 86A, 393-407.

Lavrukhina A.K. and Ustinova G.K. (1972) Cosmogenic radionuclides in stones and meteorite orbits. Earth Planet. Sci. Lett., 15, 347-360.

Lavrukhina A.K., Ustinova G.K., Ibraev T.A. and Kuznetsova R.I. (1969) Cosmic-Radiation-induced Radioactivity of the Moon and Meteorites and the origin of Meteorites. In Meteorite Research, (ed. P.M. Millman), 227-245.

Lederer C.M., Hollandar J.M. and Perlman I. (1967) Table of isotopes, 6th ed., John Wiley and Sons, Inc.

Lerch P. (1953) Mesure de l'activite β des sources epaisses. Phys. Acta, 26, 663-690.

Libby W.F. (1956) Relations between energy and half-thickness for absorption of beta radiation. Phys. Rev., 103, 1900-1901.

Lorin J.C. (1975) Effets d'irradiation dans les materiaux extra-terrestres. Ph.D. Thesis. The University of Paris, Paris.

Marti K., Shedlovsky J.P., Lindstrom R.M., Arnold J.R. and Bhandari N.G. (1969) Cosmic ray produced radionuclides and rare gases near the surface of St. Severin meteorite. In Meteorite Research, (ed. P.M. Millman), 246-266, D. Reidel Publ. Co.

Mason B. (1962) Meteoritics. John Wiley and Sons. Inc., New York.

Mason B. (1971) Handbook of elemental abundances in meteorites. Gordon and Beach Sci. publ.,New York.

McCrosky R.E., Posen A., Schwartz G. and Tougas C.A. (1969) Preliminary comments on the trajectory, orbit and initial mass of the Allende Meteorite. EOS, Trans. Am. Geophys. Union 50, 458.

McCrosky R.E., Posen A., Schwartz G. and Shao C.Y. (1971) Lost City meteorite - its recovery and a comparison with other fireballs. J. Geophys. Res., 76, 4090-4108.

McKibben R.B., O'Gallagher J.J., Pyle K.R. and Simpson J.A. (1977) Cosmic ray intensity gradients in the outer solar system measured by Pioneer 10 and 11. Proc. 15th Int. Conf. Cosmic Rays, 3, 240-243.

Megrue G.H. (1968) Rare gas chronology of hypersthene achondrites and pallasites. J. Geophys. Res., 73, 2027-2033.

Millard H.T. (1965) Thermal neutron activation: Measurement of cross-section for Manganese-53. Science, 147, 503-504.

Nishiizumi K. (1978) Cosmic-ray produced ^{53}Mn in thirty-one meteorites. Earth Planet. Sci. Lett., 41, 91-100.

Noonan A.F., Fredriksson K., Jarosewich E. and Brenner P. (1976) Mineralogy and bulk, chondrule, size-fraction chemistry of the Dhajala, India, Chondrite, Meteoritics, 11, 340-343.

Nordemann D., Tobailem J. and St.-Genies C.H.L. (1970) La meteorite Saint Severin recherche de la trajectoire atmospherique et de l'orbite. Rapport CEA-R-4045, Centre d'Etudes Nucleaires de Saclay, France.

Oeschger H. and Wahlen M. (1975) Low level counting techniques. Ann. Rev. Nucl. Sci., 25, 423-463.

Opik E.J. (1950) Secular changes of stellar structure and the ice-ages. Royal Astron. Soc., 110, 49-68.

Perron C. (1976) Cross-sections for production of stable and long-lived nuclides by high energy spallation of iron; cosmic ray implications. Phys. Rev. C., 14, 1108-1120.

Pomerantz M.A. (1971) Cosmic-rays. Van Nostrand Reinhold Co. New York.

Potdar M.B. and Bhandari N. (1979) Natural radioactivity of Luna 24 and Apollo 16 soils. To be published in Proc. Ind. Nat. Acad. Sci.

Rajagopalan G. (1969) High sensitivity radiation counting and its applications in Nuclear Physics. Ph.D. Thesis, University of Bombay, Bombay, India.

Rancitelli L.A., Perkins R.W., Cooper J.A., Kaye J.H. and Wogman N.A. (1969) Radionuclide composition of the Allende meteorite from non-destructive gamma-ray spectrometric analysis. Science, 166, 1269-1272.

Rancitelli L.A., Perkins R.W., Felix W.D. and Wogman N.A. (1973) Lunar surface and solar process analysis from cosmogenic radionuclide measurements at the Apollo 16 site (abstract). In Lunar Science IV, 609-611. The Lunar Science Institute, Houston.

Rancitelli L.A., Fruchter J.S., Felix W.D., Perkins R.W. and Wogman N.A. (1975) Cosmogenic isotope production in Apollo deep-core samples. Proc. Lunar Sci. Conf. 6th, 1891-1899.

Rao M.N., Venkatesan T.R., Goswami J.N. and Nautiyal C.M. (1979) Solar cosmic ray produced Neon and Argon isotopes and particle tracks in Apollo 16 soils and rocks and their solar flare exposure ages. In Lunar and Planet. Sci. X, 3, 1004-1006.

Reedy R.C. and Arnold J.R. (1972) Interaction of solar and galactic cosmic-ray particles with the moon. J. Geophys. Res., 77, 537-555.

Reedy R.C. (1977) Solar proton fluxes since 1956. Proc. Lunar Sci. Conf. 8th, 825-839.

Rood R.T. (1972) A mixed-up Sun and solar neutrinos. Nature, 240, 178-180.

Rowe M, and Clark R.S. (1971) Estimation of error in the determination of ^{26}Al in stone meteorites by indirect γ-ray spectrometry. Geochim. Cosmochim. Acta, 35, 727-730.

Rudstam G. (1966) Systematics of spallation yields. Z. Naturforsch. 21a, 1027-1041.

Samworth E.A., Warburton E.K. and Engelbertink G.A.P. (1972) Beta decay of the ^{26}Al ground state. Phys. Rev. C5, 138-142.

Schultz L. and Signer P. (1976) Depth dependence of spallogenic Helium, Neon and Argon in the St. Severin chondrite. Earth Planet. Sci. Lett., 30, 191-199.

Schaeffer O.A. (1975) Constancy of galactic cosmic rays in time and space. Proc. 14th Int. Conf. Cosmic Rays., 11, 3508-3520.

Shedlovsky J.P., Cressy P.J. and Kohman T.P. (1967) Cosmogenic radioactivities in the Peace River and Harleton chondrites. J. Geophys. Res., 72, 5051-5058.

Spannagel G. and Sonntag C. (1967) Cosmic ray produced activities in chondrites. In Radioactive Dating and Methods of Low Level Counting, 231-238, IAEA, Vienna.

Spannagel G. and Heusser G. (1969) Radiation ages of chondrites. In Meteorite Research, (ed. P.M. Millman), 372-386, D. Reidel Publ. Co.

Tamhane S. (1972) Abundance of heavy cosmic ray nuclei from the induced micrometamorphism in meteoritic minerals. Ph.D. Thesis, University of Bombay, Bombay, India.

Tobailem J., David B. and Nordemann D. (1967) Radioactivite induite par le rayonnement cosmique dans la meteorite Saint-Severin. In Radioactive Dating and Methods of Low-Level Counting, 207-213, IAEA, Vienna.

Trivedi B.M.P. and Goel P.S. (1973) Nuclide production rates in stone meteorites and Lunar samples by galactic cosmic radiation. J. Geophys. Res., 78, 4885-4900.

Ulrich R.K. (1975) Solar neutrinos and variations in the solar luminosity, Science, 190, 619-624.

Van Dilla M.A., Arnold J.R. and Anderson E.C. (1960) Spectrometric measurement of natural and cosmic-ray induced radioactivity in meteorites. Geochim. Cosmochim. Acta, 20, 115-121.

Venkatavaradan V.S. (1970) Isotopic changes induced by cosmic rays in interplanetary matter. Ph.D. Thesis, University of Bombay, Bombay, India.

Voshage H. and Hintenberger H. (1963) The cosmic-ray exposure ages of iron meteorites as derived from the isotopic composition of potassium and the production rates of cosmogenic nuclides in the past. In Radioactive Dating, 367-379, IAEA, Vienna.

Wahlen M., Honda M., Imamura M., Fruchter J.S., Finkel R.C., Kohl C.P., Arnold J.R. and Reedy R.C. (1972) Cosmogenic nuclides in football-sized rocks. Proc. Lunar Sci. Conf. 3rd, 2, 1719-1732.

White D.R. (1977) The solar output and its variation. Colorado Univ. Press, Boulder, U.S.A.

Wogman N.A. and Brodzinski R.L. (1973) The development and application of a beta-gamma-gamma multidimensional spectrometer. Nucl. Instr. Meths., 109, 277-283.

Wrigley R.C. (1973) Radionuclides at Descartes in the central highlands. Proc. Lunar Sci. Conf. 4th, 2203-2208.

LIST OF PUBLICATIONS

1. Cosmic ray effects induced in a rock exposed on the moon or in free space: Contrast in patterns for 'tracks' and 'isotopes'.

   S.K. Bhattacharya, J.N. Goswami, S.K. Gupta and D. Lal; Moon, 8, pp 253-286, 1973.

2. Semi-empirical rates of formation of cosmic ray tracks in spherical objects exposed in space: Pre and Post-atmospheric depth profiles.

   S.K. Bhattacharya, J.N. Goswami and D. Lal; J. Geophys. Res., 78, p 7100, 1973.

3. Ancient Solar Wind and Solar Flare Activity.

   S.K. Bhattacharya, K. Gopalan, J.N. Goswami, D. Lal and M.N. Rao, Abstracts of Conference 'Lunar Interactions' held at Wisconsin (Eds. D.R. Criswell and J.W. Freeman), pp 73-75, 1974.

4. Effects of exposure conditions of cosmic ray records in lunar rocks.

   S.K. Bhattacharya and N. Bhandari; Proc. Lunar Sci. Conf. 6th, pp 1901-1912, 1975.

5. Surface radioactivity of lunar rocks:implications to the solar activity in the past.

   N. Bhandari, S.K. Bhattacharya and J.T. Padia; Proc. Lunar Sci. Conf. 6th, pp 1913-1925, 1975.

6. Lunar regolith and gas-rich meteorites:characterisation based on particle tracks and grain-size distributions.

   S.K. Bhattacharya, J.N. Goswami, D. Lal, P.P. Patel and M.N. Rao; Proc. Lunar Sci. Conf. 6th, pp 3509-3526, 1975.

7. Solar proton fluxes during the last million years.

   N. Bhandari, S.K. Bhattacharya and J.T. Padia; Proc. Lunar Sci. Conf. 7th, pp 513-523, 1976.

8. Variation of cosmogenic radioactivity in Dhajala fragments.

   N. Bhandari, S.K. Bhattacharya, S. Krishnaswami and B.L.K. Somayajulu; Meteoritics II, p 250, 1976.

9. Modulation of galactic cosmic rays from the study of cosmogenic radioisotopes in meteorites.

   S.K. Bhattacharya and N. Bhandari; Proc. Symp. Planet. Phys. Vol.2, pp 161-169, Ahmedabad, Jan. 1976.

10. Isotope production in meteorites by galactic cosmic radiation.

    N. Bhandari and S.K. Bhattacharya; Abstracts. Space Sci. Symp. Waltair, Jan. 1978.

11. Cosmogenic isotopes in the Dhajala Chondrite: Implications to variations of cosmic ray fluxes in the interplanetary space.

    N. Bhandari, S.K. Bhattacharya and B.L.K. Somayajulu; Earth Planet. Sci. Lett. 40, p 194, 1978.

12. Ground water models for interpretation of silicon-32 and radiocarbon data.

    S.K. Bhattacharya, S.K. Gupta, R. Hart, D. Lal and V.N. Nijampurkar; Abstract, Symp. on Study and Management of water resources in Arid and Semi-arid regions, p 20, Ahmedabad, April 1978.

13. Production profiles of radionuclides in chondrites and their solar cycle variation.

    N. Bhandari, S.K. Bhattacharya and M.B. Potdar; Lunar and Planet. Sci. (abstracts) X, p 107, 1979

14. Production profile of cosmogenic ^{53}Mn in the Marjalahti Pallasite.

    S.K. Bhattacharya, N. Bhandari and V.P. Perelygin; To appear in J. Geophys. Res. 1979.

15. Depth and size dependence of ^{53}Mn activity in chondrites.

    S.K. Bhattacharya, M. Imamura, N. Sinha and N. Bhandari. Submitted to Meteoritical Society meeting, Heidelberg, 1979.